

Freie Universität Berlin
Fachbereich Geowissenschaften
Institut für Geographische Wissenschaften
Physische Geographie

Masterarbeit
M. Sc. Geographie (Terrestrische Systeme)

Soil Erosion Risk Assessment in the Upper Mefou Subcatchment,
Southern Cameroon Plateau
Application of the RUSLE3D in the humid tropics in the immediate vicinity
of Yaoundé

Fabian Becker

Erstgutachterin: Prof. Dr. Brigitta Schütt
Zweitgutachter: Prof. Dr. Tilman Rost

Berlin, 11. Februar 2015

Acknowledgements

I would like to express my very great appreciation to my supervisor at Freie Universität Berlin, Prof. Dr. Brigitta Schütt, for constructive suggestions, helpful ideas and motivating comments. For co-supervision and various discussions, I am thankful to Prof. Dr. Karl Tilman Rost (Freie Universität Berlin).

During field work in November and December 2012 I met a lot of people from Université de Yaoundé I who helped me and were open for discussion: Rodrigue Aime Feumba, Maurice Olivier Zogning Moffo, Alain Tchamagam Touko, Ruphine Lydie Mbezele Atengana, and Prof. Dr. Nicolas Gabriel Andjica (*Director de Ecole Normale Supérieure*). I would also like to thank the people in the Upper Mefou subcatchment who were open to the field work within the project, especially the chiefs of the villages who made fieldwork more bearable.

I wish to acknowledge the discussions during the “IWM for Upper Mefou Sub-catchment”-workshop at the Higher Teachers Training College in Yaoundé in 2013. Dr. Stefan Thiemann (IWM Expert GmbH, Kempten, Germany) and Anette Stumtner provided assistance during field work and at Freie Universität.

Special thanks should be offered to all colleagues at Freie Universität Berlin. Methodological assistance and patience of Dr. Philipp Hoelzmann and M. Scholz from the Laboratory of Physical Geography were necessary for soil analysis—especially for the preparation of grain size samples.

My special thanks are extended to Norbert Anselm. A comprehensive exchange of ideas and some critical comment helped a lot to process data for the thesis, not to mention some hints which avoided spending hours in R or Latex forums.

To come to an end, I would like to thank Susanne and Heinz-Wilhelm Becker.

The author was financially supported by the German Academic Exchange Service (DAAD, Deutscher Akademischer Austauschdienst) through the university cooperation programme “Welcome to Africa” in the project *Integrated Watershed Management Research and Development Capacity Building (IWM R&D CB)* (2012–2015). The project is headed by Freie Universität Berlin; partners are Kenyatta University, Nairobi, Kenya, University of Yaoundé I, Cameroon, University of Cape Town, South Africa, and United Nations University, Bonn, Germany.

Fabian Becker, Berlin

Contents

List of Figures	VI
List of Tables	VII
List of Acronyms	VIII
Abstract	X
Résumé	XII
1 Introduction	1
2 State of the Art	7
2.1 Soil erosion	7
2.1.1 Erosivity of tropical rainfall	8
2.1.2 Erodibility of tropical soils	11
2.2 Soil erosion modelling	13
2.3 Soil erosion risk	16
3 Study area	19
3.1 Geology and relief	21
3.2 Soils	22
3.3 Climate	23
3.4 Land use and land cover	26
4 Methods and materials	30
4.1 (Revisited) Universal Soil Loss Equation	30
4.1.1 Rainfall erosivity factor (R)	32
4.1.2 Erodibility factor (K)	36
4.1.3 Land cover and management factor (C)	39
4.1.4 Topographic factor (LS)	42
4.2 Net deposition areas	45
4.3 Simulations	46
4.4 Semi-quantitative validation	47

4.5	Statistics and reporting of figures	48
4.6	Computation	49
5	Results	51
5.1	Rainfall erosivity	51
5.2	Soil erodibility	53
5.3	Topographic potential	60
5.4	Cover and crop management factor	63
5.5	Erosion	68
5.5.1	Soil loss	68
5.5.2	Deposition	72
5.5.3	Validation: Reservoir sediment survey	73
5.6	Land use change scenarios	75
6	Discussion	78
6.1	Soil loss	78
6.2	Soil erosion from roads and trails	82
6.3	Erosion determining factors	84
6.3.1	Soil erodibility	84
6.3.2	Cover and crop management factor	92
6.3.3	Rainfall	94
6.3.4	Topographic factor	95
6.4	Validation	98
7	Conclusions	101
	References	108
	Appendix	i

List of Figures

1.1	Location of the Upper Mefou subcatchment	2
2.1	The human and natural spheres of soil erosion	8
2.2	Sediment yield and erodibility in relation to rainfall	9
2.3	Erosion risk and sediment yield in Africa	10
3.1	Altitude ranges of the Upper Mefou subcatchment	20
3.2	Geological sketch map of Cameroon	21
3.3	Climograph of Yaoundé (1960–1990)	24
3.4	Magnitude–frequency analysis of daily rainfall	25
3.5	Forest cover map	26
3.6	Land cover in the rural and periurban parts of the catchment	28
4.1	Flow chart of methodology and objectives	31
5.1	Annual cycle of rainfall erosivity	52
5.2	Infiltration rates of different land use types	55
5.3	Grain size distribution	56
5.4	Parameters determining K in relation to K	58
5.5	Interpolated soil erodibility values	60
5.6	Map of flow accumulation and the LS factor	62
5.7	Linear model of NDVI/DI and ground truth C-values	64
5.8	Validation of modelled C-factor	65
5.9	Map of the cover and crop management factor	67
5.10	Soil loss map	69
5.11	Potential soil loss	71
5.12	Relative soil loss	72
5.13	Erosion/deposition map	73
5.14	Modeled change of soil loss for five land use/cover scenarios	76
6.1	Erosion features on roads and settlement areas	83
6.2	Sensitivity analysis of the erodibility factor K	88
6.3	Comparison of treated and untreated particle size samples	90
6.4	Sensitivity analysis of RUSLE’s input values and factors.	93

List of Tables

3.1	Cropping calendar and rainfall during growing seasons	27
4.1	Database to calculate rainfall erosivity	33
4.2	Tasseled cap coefficients for Landsat 8	41
4.3	R-packages used for data processing and outputs	50
5.1	R-factor values	51
5.2	Monthly mean of daily rainfall erosivity	53
5.3	K-values and input parameter for all samples	57
5.4	Mean values of DEM derivatives using different algorithms and DEMs	61
5.5	Validation of C-factor estimation	65
5.6	Validation of C-factor estimation	66
5.7	Classified soil loss values	70
5.8	Mefou Reservoir sediment survey	74
5.9	Soil loss of land use scenarios	75
6.1	Soil loss in western Africa	79
6.2	Erodibility of African and tropical soils	85
6.3	Influence of selected LS rill-to-interrill parameter on soil loss	97
7.1	Summary: Erosion risk and recommended conservation measures	102
7.2	Methodological view on the factors of the RUSLE3D	105

List of Acronyms

ABAG	Allgemeine Bodenabtragungsgleichung (German for USLE)
ARESED	African Rainfall Erosivity Subregional Empirical Downscaling
ARS	(United States Department of Agriculture) Agricultural Research Service
ASTER	Advanced Spaceborne Thermal Emission and Reflection Radiometer
C	Cover and management factor (USLE)
dBD	dry Bulk Density (of sediments)
D ∞	Deterministic Infinity
D8	Deterministic 8
DEM	Digital Elevation Model
DI	Disturbance Index
DN	Digital Number
ETM+	(Landsat) Enhanced Thematic Mapper Plus
FAO	Food and Agriculture Organization (of the United Nations)
GIS	Geographic Information System
IR	Infrared
IWM	Integrated Watershed Management
K	Soil erodibility (USLE)
KNMI	<i>Koninkrijk Nederlands Meteorologisch Instituut</i>
LS	Slope angle and slope length factor (Topographic factor of the USLE)
LULC	Land Use and Land Cover
LULCC	Land Use and Land Cover Change
MBA	Multilevel B-Spline Approximation
METI	(Japan's) Ministry of Economy, Trade and Industry
MFD	Multiple Flow Direction
MFI	Modified Fournier Index
MNT	Modèle numérique de terrain (Digital Elevation Model)
NASA	(United States) National Aeronautics and Space Administration
NDVI	Normalized Difference Vegetation Index
Nk	Nkolbission (sample identifier)
NSSH	National Soil Survey Handbook (USDA)
OC	Organic Carbon

OFAT	One-factor-at-a-time (sensitivity analysis)
OLI	Operational Land Imager
OM	Organic Matter
P	Soil conservation factor (USLE)
QA	Quality Assessment (band of Landsat 8)
R	(programming language)
R	Rainfall erosivity factor (USLE)
RSAGA	R-System-for-Automated-Geoscientific-Analyses
RUSLE	Revisited Universal Soil Loss Equation
RUSLE3D	three-dimensional enhancement of the RUSLE
SAGA	System for Automated Geoscientific Analyses
SDR	Sediment Delivery Ratio
SEM	Standard Error of the Mean
SI	<i>Le Système International d'Unités</i> , International System of Units
SRTM	Shuttle Radar Topography Mission
SSY	(Area) Specific Sediment Yield
TC	Total Carbon
TCT	Tasseled Cap Transformations
TIC	Total Inorganic Carbon
TOC	Total Organic Carbon
US	United States (of America, USA)
USDA	United States Department of Agriculture
USLE	Universal Soil Loss Equation
USPED	Unit Stream Power Erosion/Deposition
WMO	World Meteorological Organization
WRS	Worldwide Reference System (a global notion system for Landsat data)

Abstract

In the humid tropics of the Southern Cameroon Plateau, the soil erosion risk (by water) is principally low to do a dense natural vegetation cover and a low erodibility of the “pseudo-sandy” soils. But due to deforestation and urban growth, land use is intensified and the soil erosion risk accelerated.

In this context, the objective of the study at hand is firstly to assess the actual and potential soil erosion risk in the Upper Mefou subcatchment in the intermediate vicinity of Yaoundé. Secondly, the future risk is estimated based on four land use intensification scenarios and an assumed forest regrowth. The third objective is to discuss the applicability of a USLE-family model on the Southern Cameroon Plateau.

Soil erosion risk is assessed using a three-dimensional enhancement of the USLE, the RUSLE3D. An algebraic approximation of the USLE nomograph—adapted to tropical soils—is used to estimate soil erodibility (K): Grain size is measured using laser diffraction, organic matter using an CNS-analyser and a carmograph. Permeability is calculated on the basis of field measurements of infiltration rates using a minidisk infiltrometer. A linear model for the daily rainfall–erosivity relationship from southeast Nigeria is applied to calculate the rainfall erosivity factor R. The cover and crop management factor C is modelled on the basis of a linear relationship between the NDVI of a Landsat 8 scene and ground truth values of C. The topographic potential factor LS is calculated on the basis of a SRTM Digital Elevation Model, where upslope contributing area is used instead of the USLE’s slope-length parameter. Deposition areas are masked using an erosion/deposition topographic index based on the unit stream power theory. The model accuracy is tested using the results of a reservoir sedimentation survey of the Mefou Reservoir and a one-factor-at-a-time sensitivity analysis.

(1) In comparison to other studies in the humid tropics of Africa, modelled soil losses are relatively high, but in the same order of magnitude. The validation shows that soil loss is somewhat overestimated. The high values might be explained by the steep relief of the inselbergs, which are pronounced in comparison to the relief Southern Cameroon Plateau. Rainfall is highly erosive, also when field preparation for cassava cultivation is still ongoing. The actual erosion risk is especially high in periurban areas and around the Mefou Reservoir, where short-duration fallowing takes place and land use is more intensive, e. g. maize or manioc monocropping. (2) The simulation of deforestation, land use intensification and an increase in cash crop production is expected to result in a severe increase of soil loss, again especially around Yaoundé and the reservoir, but also in the present rural areas. (3) An

overestimation of soil loss might be attributed to a method inherent overestimation of the silt and fine sand fraction by laser diffraction and a lack of observance of microaggregates in the calculation of soil erodibility. The parameters of the three dimensional topographic factor need to be handled with care, as they are difficult to adapt to local conditions and have a great impact on modelled soil loss. The cover and crop management factor values are relatively reliable when compared with values from literature and field mapping.

In conclusion, the RULSE3D seems to be applicable on the Southern Cameroon Plateau, as factors can be adapted to local conditions and the values of the individual factor and gross soil loss are not out of range. It is recommended to avoid cultivation on the slopes of the inselbergs and to reduce cultivation in the periurban areas and around the Mefou Reservoir. Cultivation should focus on the areas where a land use and land cover change would not affect the erosion risk seriously. As the erosion risk is high where fallowing is short, a watershed management concept and further research should focus on the fallow duration.

Résumé

Dans la zone tropicale humide d'Afrique centrale le risque érosif des sols par l'eau est faible à cause de la couverture végétale dense ainsi que d'agrégation du sol. Des processus comme la déforestation et l'urbanisation rapide et anarchique renforcent le risque érosif. Dans ce contexte la recherche vise premièrement un bilan du risque érosif dans le bassin versant de la Mefou Supérieure à la périphérie de la ville de Yaoundé. En outre, les méthodes adaptées et appliquées sont à évaluer. Pour quantifier le risque érosif, le modèle empirique RUSLE3D — une version tridimensionnelle de l'USLE — a été utilisée. L'érodibilité des sols a été évaluée par une équation adaptée aux sols ferrallitiques du Cameroun. La granulométrie a été mesurée par la diffraction laser et la matière organique par la combustion séchée au laboratoire, tandis que la perméabilité a été mesurée par un infiltromètre disque-mini lors de l'enquête sur le terrain. L'érosivité des pluies a été évaluée grâce à une procédure approximative des précipitations journalières, qui a été adaptée au climat de la zone. Le facteur culture-végétation et gestion a été obtenu grâce à une fonction linéaire de l'indice de végétation par la différence normalisée (NDVI), obtenue du satellite Landsat-8 et de la vérité-terrain. Le facteur de topographie-longueur/inclinaison a été calculé sur la base du modèle numérique de terrain (MNT). L'inclinaison de la pente a été calculée à l'aide d'une méthode SIG normalisée, mais la longueur de la pente a été remplacée par la surface spécifique du bassin aval. Les domaines de la déposition nette sont calculés sur la base d'un indice topographique dérivé du modèle numérique USPED. Une comparaison de la production des sédiments modélisée au bassin versant et les résultats de la relevés de la sédimentation du réservoir ont permis de vérifier les résultats. Il s'est avéré que les résultats de RUSLE3D ont été surestimés, cependant ils restent dans un même ordre de grandeur. En comparaison aux autres études dans les zones tropicales humides, l'érosion est plutôt faible. La granulométrie est un paramètre, qui pourrait être discuté regard des résultats. Le facteur de l'érodibilité est particulièrement sensible à la variabilité de granulométrie; les résultats sont influencés par les méthodes de la préparation des échantillons et la surestimation de la portion limoneuse inhérente à la méthode de diffraction laser. Le risque érosif le plus élevé a été modélisé pour la zone des inselbergs, le territoire autour et au nord du barrage du Mopfou et autour des zones périurbaines de Yaoundé. Les sols sont assez résistants à l'érosion, mais un peu moins résistants que les sols ferrallitiques dans les autres bassins; la pluie est très érosive. Il y a quelques pentes très escarpées où le risque érosif est relativement élevé. Les autres facteurs décisifs sont — entre autres — la culture (des champs) de manioc lors de mois de pluie forte, la réduction

de la mise en jachère, l'utilisation intensive de sol plus vaste dans la zone périurbaine et la monoculture de maïs et de manioc. Le culture sur billons est pratiqué quelquefois en direction de la pente. Quatre scénarios démontrent que les changements dûs à l'utilisation ou à la couverture des sols influencent le risque érosif dans le bassin versant entier, toutefois à des échelles différentes. Il est conseillé d'éviter la culture sur pente des inselbergs et de réduire la cultivation autour du réservoir et de la zone périurbaine. Les méthodes de culture auront besoin d' être adaptées au risque érosif.

1 Introduction

Soil erosion by water—i. e., natural erosion accelerated by human activities—is a major concern in various landscapes around the world; decreased soil fertility, degraded and unusable cultivation areas or completely removed soil layer are drastic consequences. The eroded sediments pollute rivers or wetlands and cause reservoir siltation; the capacity of reservoirs is reduced and the generation of hydroelectricity and water supply are limited. Although the factors controlling the extent of soil erosion by water are not equally distributed around the world, soil erosion might occur everywhere except the areas permanently covered by ice, snow or deserts.

In the humid tropics, soil erosion is expected to be principally low: A dense vegetation and litter cover protects the surface from rainfall impact; due to aggregation, the erodibility of the often well drained soils is relatively low. Nevertheless, intensity and volume of rainfall are very high and soils are particularly located in unfavourable topographic positions.

Two processes which are often observed in the humid tropics are urban growth and deforestation or—more general—land use and land cover changes (DEFRIES et al. 2010, ACHARD et al. 2002 or LAMBIN et al. 2003). Beside various other causes, these processes impact the extent of soil erosion. Urban growth results in an intensification of land use around the cities, a higher portion of large-scale food production and cultivation on steep slopes. Consequently, the soil erosion risk increases. Deforestation and land use and land cover change result in a reduction of the protective plant cover. Thus, the soil is prone to rainfall impact—the low potential risk for soil erosion increases, sometimes considerably.

Southern Cameroon Plateau

Also on the Southern Cameroon Plateau (Figure 1.1d), deforestation, urban growth and land use and land cover change are an issue. According to VAN SOEST (1998), farming, forestry and the situation on the food market are major causes for deforestation in Cameroon. SUNDERLIN et al. (2000) report that the deforestation rate in southern Cameroon—around the city of Yaoundé and in the periphery—is severe in comparison to other African countries. Deforestation is caused by the onset of the economic crisis in 1986, macroeconomic changes, a shift from production of cacao to plantain and population dynamics (SUNDERLIN et al. 2000). MERTENS & LAMBIN (2000) report that the change from forest to non-forest affected 7.6% of the rainforest in southern Cameroon (1976–1991). SIETCHIPING (2003; 2004) reports a

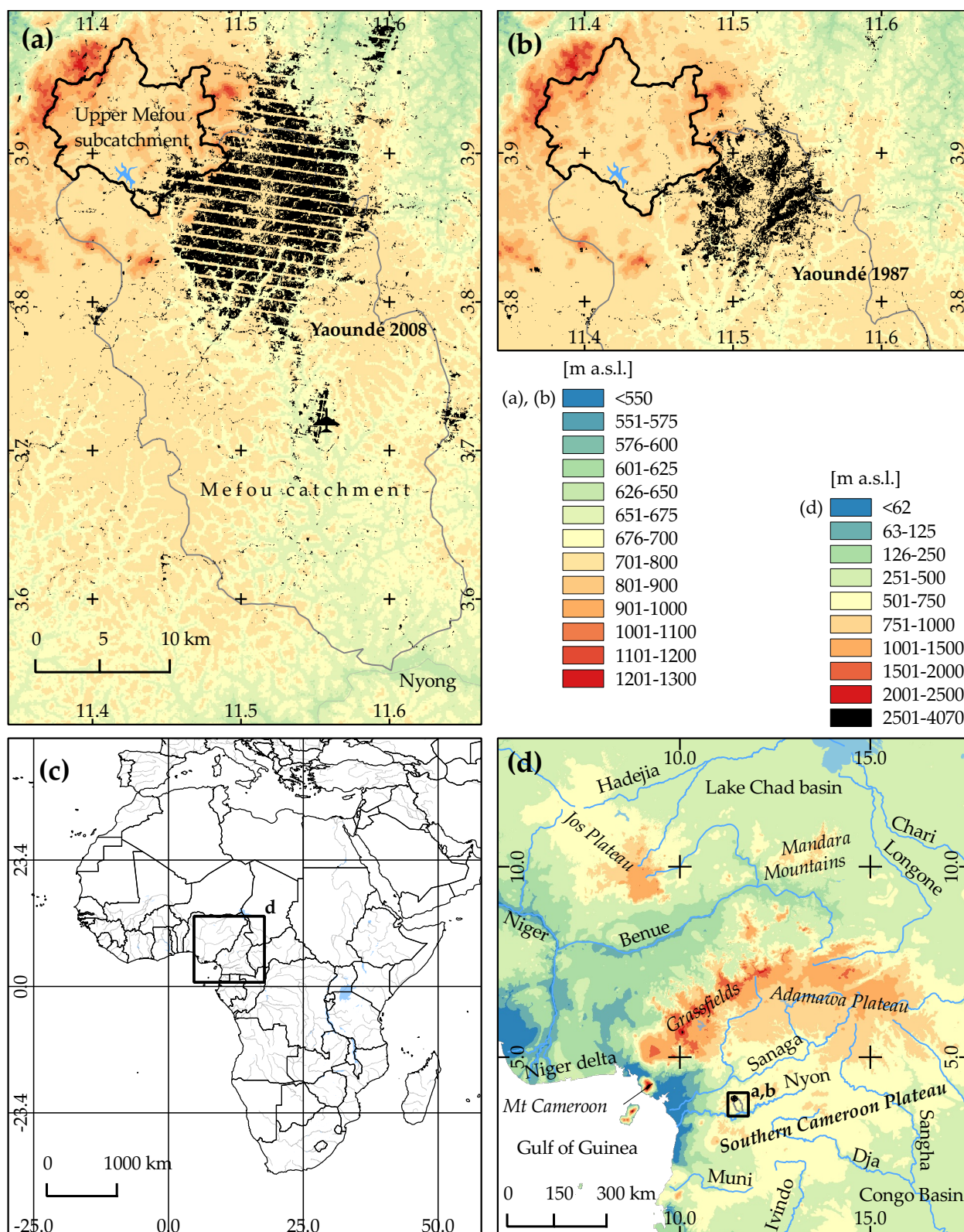


Figure 1.1: Location of the Upper Mefou subcatchment in the boundaries of Cameroon in Africa (d), on the Southern Cameroon Plateau (c), and in the Mefou catchment and the vicinity of Yaoundé (a, b). The urban growth of Yaoundé between 1987 and 2008 is shown in (a) and (b) (Database: INSTITUE GÉOGRAPHIQUE NATIONAL 1956 [a–b], NASA LANDSAT PROGRAM 1987, 2008 [b,a], DISTRIBUTED ACTIVE DATA CENTER & EARTH RESOURCES OBSERVATION SYSTEMS DATA CENTER 1996 [d], CENTERS FOR DISEASE CONTROL AND PREVENTION 2010 [c], NASA AND JAPAN ASTER PROGRAM 2011 [a–b], NATURAL EARTH DATA 2013[a–d])

drastic increase of Yaoundé's population and urban area (for the population development of colonial Yaoundé, cf. FRANQUEVILLE 1979); also for Cameroon's largest city and economic center Duala, a fast growing population is reported (HANNA & HANNA 2009). As stated before, urban growth and deforestation have an influence on soil erosion—the same goes for the Southern Cameroon Plateau.

The study at hand takes up these issues and focuses on the assessment of the actual, potential and future soil erosion risk in the Upper Mefou subcatchment, a catchment located in the intermediate vicinity of periurban Yaoundé (Figure 1.1a,b).

Soil erosion modelling

Soil erosion modelling is a common approach for soil erosion risk assessment, besides field mapping of erosion damages, analysis of sediments and suspended load, exposed-root surveys, factor scoring or participative/expert approaches. In the humid tropics, soil erosion modelling is problematic: Most of the erosion models were developed and calibrated in a different climatic, topographic and geological setting, where cultivation is completely different. Some of the models were applied in the humid tropics, but the databases and validations—especially of empirical models—are not adapted to that region.

In the study at hand, RUSLE3D, a three-dimensional modification of the Revisited Universal Soil Loss Equation (RUSLE), and the topographic deposition routine of USPED (Unit Stream Power Erosion Deposition) will be applied in the Upper Mefou subcatchment. Although there are a lot of restrictions and limitations of the USLE-family models, there are some good reasons to use the RUSLE3D for soil erosion risk assessment in the Upper Mefou subcatchment: *(i)* The application of USLE-family models is discussed for the humid tropics and some authors *successfully* applied the model in western Africa (MILLWARD & MERSEY 1999; ANGIMA et al. 2003 or ROOSE 1977; MATI & VEIHE 2001); *(ii)* thus, the model outputs and the values of input parameters can be compared with other studies and put in context. *(iii)* A number of attempts were made to adapt the input factor to the humid tropics (rainfall erosivity: i. a. SALAKO et al. 1991; BRESCH 1993; YU 1998; SALAKO 2008; SALAKO 2010; DIODATO et al. 2013; erodibility: i. a. ROOSE 1977; VANELSLANDE et al. 1987; ROOSE & SARRAILH 1989; NIL 1993; crop management and cover: i. a. ROOSE 1977; EL-SWAIFY et al. 1982; NIL 1993; NIL et al. 1996); *(iv)* USLE-family models can easily be used for simulations. *(v)* empirical models—like the USLE— are recommended for the catchment scale, whereas conceptual or physical models are recommended for a smaller scale; empirical models are suitable for long term analysis (VOLK et al. 2010); *(vi)* therefore, the erosion risk is well sufficiently assessed with an empirical model. *(vii)* Although the predicted soil loss

values have to be analysed critically, RUSLE3D is suitable as a semi-quantitative tool for risk assessment (VRIELING et al. 2008); *(viii)* the model is suitable within the wider framework of the study, as it is important to use simple, low input models which can easily be implemented in widespread open source software. *(ix)* The easily understandable input parameters are appropriate for capacity building purposes.

Integrated Watershed Management

The study at hand is part of the international research and development project *Enhancing collaborative research and development capacities of German and Sub-Saharan African partners on Integrated Watershed Management (IWM)*. The project focuses on the communication gap between scientists, decision makers and local population with the goal to bridge these gaps. In three partner countries (Cameroon, Kenya and South Africa) joint research of local and German students in so called “living laboratories” is conducted, where awareness raising takes place during field work. In addition, activities in the living laboratories should be used for teaching purposes and stakeholder workshops.

The living laboratory in Cameroon is the Upper Mefou subcatchment, i. e., the headwaters of the Mefou River, a tributary of the Nyong River. The watershed is located in the humid tropics of the South Cameroon Plateau and comprises a periurban part of Yaoundé and a rural part, which is covered with typical Guineo–Congolaise type rainforest and used for shifting cultivation, forestry and cash crop production. One feature of the catchment is the Mefou Reservoir (*Barrage du Mopfou*), which is an important component of the urban water supply of Yaoundé.

Integrated Watershed Management (IWM) is a holistic approach: The management of all resources in a watershed is included, both biophysical resources (water, soil, biomass) and human resources, which include the sociocultural, economic, political and institutional considerations in a watershed (EASTER & HUFSCHMIDT 1985). IWM is a research and a management approach. Besides scientists, also non-governmental organizations, (local) administration and stakeholders participate (FÖRCH & SCHÜTT 2005). The IWM-process includes a planning and an implementation step, i. e. the formation and design of activities and the installation, operation, maintenance and evaluation of measures (EASTER & HUFSCHMIDT 1985). The role of scientists is not at least the collection and analysis of basis information and the identification of key problems. A watershed is the spatial basis of IWM. It is a topographic defined land area, which drains to one point of a stream (FFOLIOTT 2011). The concept is therefore based on natural boundaries. Administrative boundaries are nevertheless important, due to the fact that different institutional settings may exist in a watershed that

is located in different administrative units (EASTER & HUFSCHMIDT 1985). The interaction between upland and downstream areas is an important part of IWM. As a watershed is not a container, off-site effects should not be ignored. The IWM-approach and soil erosion studies are methodological linked. The watershed is a functional unit with physical relationships, which are also important for soil erosion, as it is the case for upstream–downstream linkages (DIXON & EASTER 1991). Various studies combine erosion assessment and IWM, such as HOARE (1991) in Thailand, BRIONES (1991) in a Philippine watershed or BECK et al. (2004) in Ethiopia. Soil erosion is appraised to be one of the major biophysical aspects in a watershed and linked to human disturbance (HAMILTON & PEARCE 1991). Erosion is one of the “challenges faced” in IWM (GREGERSEN et al. 2007: p. 6).

During an initial implementation workshop of the IWM-project in Cameroon and during a stakeholder workshop in the Upper Mefou subcatchment in November 2013 (BECKER et al. 2013) the problem of soil erosion was addressed, not least because of the potential siltation of the Mefou Reservoir and an impact on the quality of the water supply for Yaoundé.

Objectives

As one of the tasks of IWM is to “develop a rapid diagnostic methodology to assess the condition of watersheds and to formulate and evaluate possible course of actions” (EASTER & HUFSCHMIDT 1985: p. 2), the objectives of the study on hand are:

1. to assess the soil erosion risk in the study area,
2. to evaluate the possible impacts of land use and land cover changes on the soil erosion risk and
3. to evaluate the applied methods to find out if they are suitable for the context of the study catchment.

Objective 1 includes the evaluation of the erosion determining factors as they are included in the RUSLE3D-model: Rainfall erosivity, soil erodibility, topographic potential of erosion, land cover and crop management and conservation measures. The topographic potential of deposition are calculated separately—based on a topographic erosion/deposition index derived from USPED (MITASOVA et al. 1996; HOFIERKA et al. 2009).

In various studies, soil erosion risk assessment includes the calculation of the **actual** and long term soil erosion risk—often with a USLE approach—and the **future** soil erosion risk (cf. PRASUHN et al. 2013). Therefore, Objective 2 comprises the development of potential land use and land cover change scenarios and the assessment of the expected effect on soil erosion. In addition to actual and future soil loss, **potential** soil loss is calculated, which covers in a broadly sense the natural sphere of soil erosion (the physical parameters rainfall, relief,

soils), but not the human activities (land use and land cover, soil conservation measures). As the term *risk* includes the “exposure to . . . the possibility of . . . unwelcome circumstances” (Oxford English Dictionary), soil erosion is not only estimated, but assessed in comparison with tolerable soil loss. As the USLE-family models are not developed for the characteristic of the study region, different approaches are used to calculate the input parameters of the RUSLE3D to show the problematic of the adaption of an approach to other conditions. The main aim of Objective 3 is therefore to consider the applicability of the RUSLE3D on the Southern Cameroon Plateau.

Objective 3 should also be pursued by comparing the values of all input factors of RUSLE3D with the results of other studies in a similar context. This should firstly give information on the plausibility of the modelled erosion values (fit-to-reality) and simultaneously allow to estimate if values are high or low. In addition the model results will be evaluated by comparing soil erosion values and sediment yield data obtained by a reservoir sedimentation survey. A sensitivity analysis of the USLE-input parameters will be conducted to show the weighting of the input factors of the model (and a potential delicateness of errors).

2 State of the Art

2.1 Soil erosion

Erosion is a function of various parameters and controlled by the energy force of rainfall (erosivity) and the relief, the resistability of soil particles to detachment and transport (erodibility) and the protective function of vegetation cover and soil conservation measures (MORGAN 2009; Figure 2.1). Eroded soil is deposited in the catchment on fields, on foot slopes, in floodplains, in channels or other sinks and depressions (FRYIRS 2013). The sediment not stored in the catchment is the sediment yield (Figure 2.1). Topography and rainfall erosivity are mainly natural forces. The erodibility of a soil is first and foremost a natural characteristic but is also influenced by human impact such as fertilization or overuse. (Ground) cover is either natural or, as it is often the case, influenced by human land use.

The energy of the forces varies between different landscapes around the world. Erosivity and erodibility in the humid tropics are quite different from the temperate or more dry regions; they are determined by different parameters. Therefore, the extent of soil erosion is specific.

In tropical Africa, rainfall erosivity has the lowest variability between different places (factor: 14–20, NILL 1997). Also the soil loss variability when applying different soil conservation measures is relatively low. The maximal factor is 1 representing a lack of conservation measures; the minimal factor is 1/25 (hillslope terracing). Both, erodibility and topography vary on a wide scale in the tropics. Some soils have a 580-times higher erodibility value (determined with the USLE) than the least erodible soils. The impact of topography can be very low on flat, short slopes and up to 640 times higher on steep, long slopes (NILL 1997). This variability is not specific for the tropics, as in a lot of other regions, both flat and steep slopes are located. According to NILL (1997), the crop cover was the highest relative distance between low and high values. For example, he reports an USLE-C-factor of 0.0002 for “dense tropical forest or 100% mulch cover” and a value of 0.58 for plowed upland rice. Land use and land cover differs within small catchments, where soil erodibility and especially rainfall erosivity are relatively constant.

For most of the Southern Cameroon Plateau a “medium” (NATURAL RESOURCES CONSERVATION SERVICE 1998) soil loss amount is expected (Figure 2.3a). The annual sediment yields in the region is estimated at 20–200 t ha⁻¹ (WALLING & WEBB 1996). In comparison to the Guinea savanna in the north and the Equatorial Forest in the south (especially in the Congo basin), the sediment yield is relatively high (Figure 2.3b).

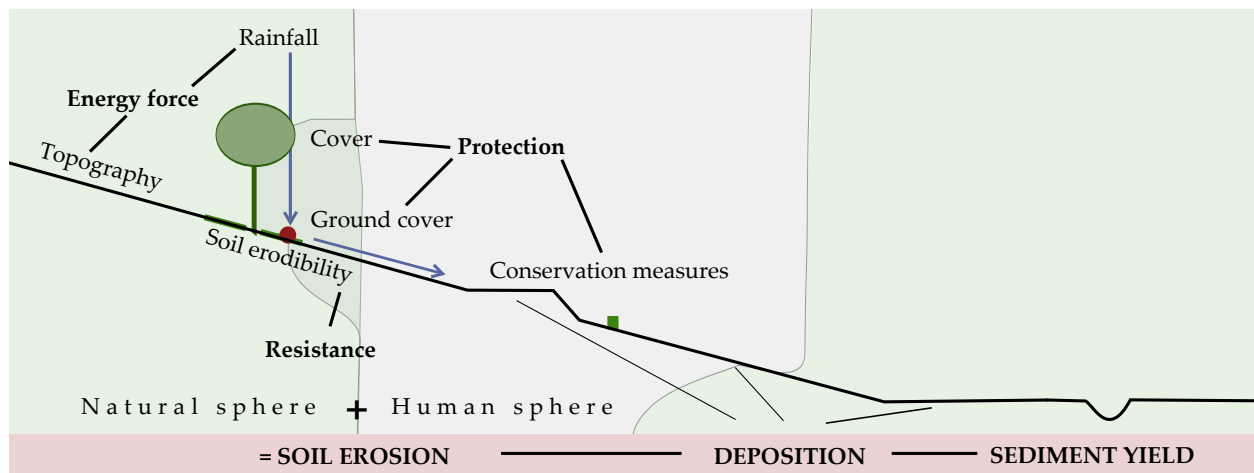


Figure 2.1: The human and natural sphere of soil erosion.

Rainfall erosivity is relatively high in the humid tropics, whereas soil erodibility is expected to be low (Figure 2.2, cf. AMBASSA-KIKI & NIL 1999). Supposing a natural vegetation cover, sediment yield is low in the humid tropics (Figure 2.2, cf. LANGBEIN & SCHUMM 1958); due to land use and deforestation, the natural vegetation cover on the Southern Cameroon Plateau is disturbed and sediment yields might be much higher. Although the Southern Cameroon Plateau is characterized by a moderate relief, the relief in the Upper Mefou subcatchment is relatively high and steep; the Yaoundé massif is the highest massif on the Plateau (OLIVRY 1986).

2.1.1 Erosivity of tropical rainfall

Rainfall erosivity in the tropics—and especially in the humid tropics—is characterized by high amounts and high intensities and therefore a high kinetic energy (VRIELING et al. 2010). In comparison to the other forces and parameters of soil loss, the erosive force is the strongest in the humid tropics (AMBASSA-KIKI & NIL 1999; VRIELING et al. 2010). Erosivity per rainfall amount is lower in the semi-arid tropics than in the humid tropics (NIL 1998). Besides the high annual rainfall totals (more than 10 000 mm at Mount Cameroon), the drop-size distribution of tropical rains is often reported to be one reason for the high kinetic energy of storms. The energy of tropical large drops is higher due to a higher terminal velocity (VAN DIJK et al. 2002). In addition, larger drops occur more often during high intensity storms (SALAKO et al. 1995).

The positive effect of wind on erosivity of tropical storm is often reported (ARNOLDUS 1980; NIL 1997), but not true for all locations (SALAKO et al. 1995). This emphasizes the high variability of erosivity within the tropics.

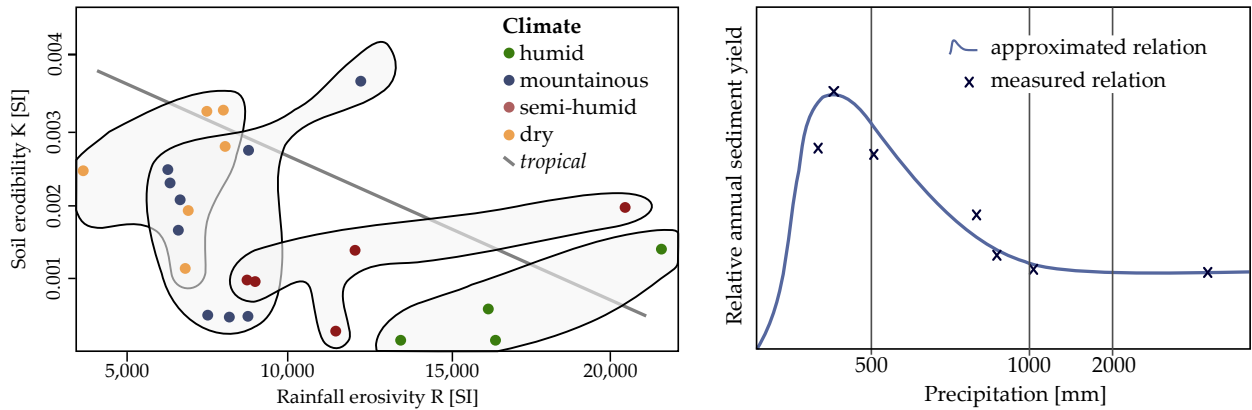


Figure 2.2: (a) Soil erodibility in relation to rainfall erosivity and precipitation regime (ROOSE & SARRAILH 1989, dots, and NILL 1998, line) and (b) sediment yield as a function of precipitation obtained from reservoir data from the US (LANGBEIN & SCHUMM 1958); both USLE-factors in metric units (see Section 4.1). In LANGBEIN & SCHUMM (1958)'s relation, the variation in annual sediment yield with precipitation is traced to a change in natural vegetation cover. The annual precipitation at Nkolbisson, close to the Upper Mefou subcatchment, totals ca. 1600 mm, what corresponds to an roughly approximated rainfall erosivity R-value of 12100–13400 (ROOSE 1977).

55% of the rainfall events are short and characterized by an early intensity peak; 45% of the rainfall events are long, but intensities are low (SALAKO et al. 1995; cf. OBI & SALAKO 1995). Both types have a high erosivity, one because of intensity, one because of volume (SALAKO et al. 1995).

The spatial distribution of erosivity within tropical West and Central Africa varies with altitude, distance to coast and latitude. In the west, heavy rainstorms are more pronounced than in the East (DIODATO et al. 2013). The highest erosivity values in Africa were found on the western coasts of West and Central Africa (VRIELING et al. 2010), what might be explained by wind systems. Erosivity per rainfall amount is generally higher at the coasts, whereas it is lower in the inland and even lower in the highlands, because mean drop sizes and intensities are lower in highlands (NILL 1997). For Cameroon, NILL (1997) reports a rainfall–erosivity ratio of 10:124 for coastal stations, 10:111 for inland stations and 10:82 for highland stations.

Erosivity of tropical rains in the USLE

In the USLE and its revision (WISCHMEIER & SMITH 1978; RENARD et al. 1997) rainfall erosivity is the product of the kinetic energy (E) of a storm and the maximal 30-minute-intensity (I_{30}) (WISCHMEIER & SMITH 1958). LAL (1976) investigated rainfall and soil loss near Ibadan, Nigeria, and concludes that this relationship underestimates erosivity of tropical rain. The slope of the regression between kinetic energy and rainfall amount is steeper in

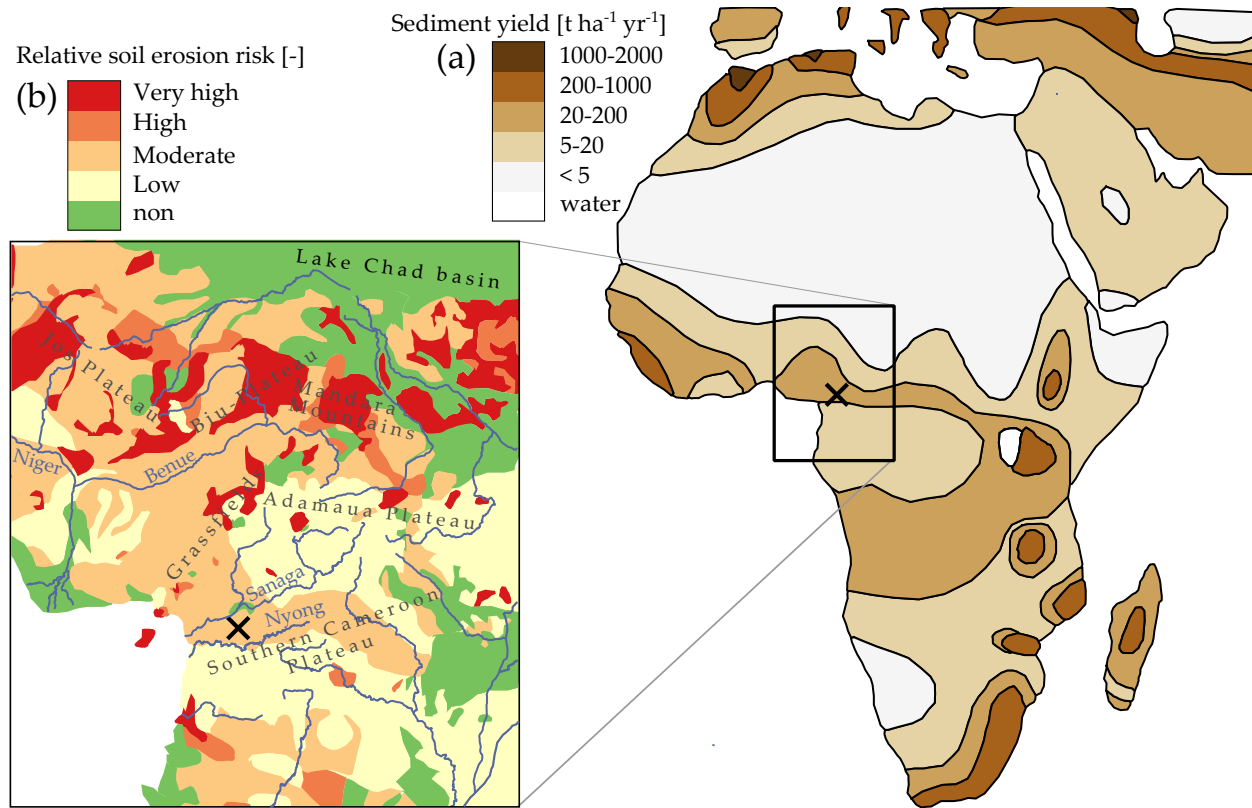


Figure 2.3: Sediment yield of African basins (a) and erosion risk in Cameroon and its vicinity (b). The 'x' marks the study area. Projections/datums as in the original figures (Database: WALLING & WEBB 1996; NATURAL RESOURCES CONSERVATION SERVICE 1998; NATURAL EARTH DATA 2013).

Nigeria than in the central USA, where WISCHMEIER & SMITH (1958)'s index was developed. Thus, LAL (1976) proposes to calculate erosivity as the product of storm rainfall volume (A) and the peak of the storm (maximal 7.5-minutes-intensity). The importance of peak intensities is reaffirmed by OBI & NGWU (1988); they measured better correlations between soil loss and $A \times I_{7.5}$ than between soil loss and $E \times I_{30}$; SALAKO (2010) got better results when using $E \times I_{15}$ instead of $E \times I_{30}$.

In the study at hand, rainfall erosivity will be calculated using a regional regression for the approach originally used in the USLE due to a lack of high resolution rainfall data. As (SALAKO et al. 1995) formulated felicitously, the lack of sufficient data to calculate erosivity indices is a characteristic of rainfall erosivity in the humid tropics (of West and Central Africa). Also regressions based on other kinetic energy approaches than WISCHMEIER & SMITH (1958)'s equation are tested.

2.1.2 Erodibility of tropical soils

One of the most important and most widely discussed factors determining erosion is the concept of *erodibility*. Following the definition of MORGAN (2009: p. 50) erodibility is the “resistance of the soil to both detachment and transport”. Three assumptions are met as a common understanding of the concept: First, soil erodibility is valid for all water erosion processes; second, soil erodibility is a function of a limited number of measurable soil properties; third, soil erodibility is constant for a specific period of time (BRYAN et al. 1989). Although topography and location parameters (e. g. slope) or the degree of physical stress (e. g. tillage) influence soil erodibility, soil properties are deemed primary important (BRYAN et al. 1989; BRYAN 2000; MORGAN 2009). These properties are texture, shear strength, infiltration capacity and organic and chemical components (binding agents). Sand and clay are more resistant to detachment and transport than silt; sand because more kinetic energy of overland flow is necessary to transport particles, clay because they are bound in complexes. Soils with a content of the silt fraction between 40 and 60% are most erodible (MORGAN 2009).

Apparent particles but coarse sand are often aggregated. Aggregates are either formed by physical stress or by binding agents (BRYAN 2000). Macroaggregates are less susceptible to detachment and transport. Soil organic matter is the strongest binding agent in most soils. While humic acids, microbial debris, polysaccharides or mucilages stabilized microaggregates (< 250 µm), plant debris, roots, hyphae, plant nuclei bind macroaggregates (> 250 µm) (EDWARDS & BREMNER 1967; OADES & WATERS 1991; BRYAN 2000). The type of organic material is also important for its influence on erodibility, as litter and large plant remains do not influence aggregate stability (MORGAN 2009). Also clay—depending on the mineralogy of the clay minerals—is a binding agent (clay flocs); the sodium adsorption ratio is responsible for differences in aggregate stability. The third type of binding agents are polyvalent metals (EDWARDS & BREMNER 1967), often in a complex with clay and organic matter. For tropical soils, they are more important than organic bonds (OADES & WATERS 1991). IGWE et al. (1995) show that soil samples treated with sodium dithionite-citrate-bicarbonate to dissolve ferric oxides and aluminium oxides have higher clay contents; MBAGWU & SCHWERTMANN (2006) gained similar results and measured an only slightly higher clay content after the removing of organic matter with hydrogen peroxide. However, BARTHÈS et al. (2008) measured a dissolution of water-stable aggregates correlated to organic matter content, but concluded that the correlation with sesquioxides for tropical soils is much higher and the relationship between organic matter content and aggregates depends on these sesquioxides. Besides aggregate stability, also the size of aggregates, their shape and

their size homogeneity is of importance. Macro- or microaggregates are bound by different agents, which are characterized by a different susceptibility to dissolution. Size homogeneity of aggregates affects pore volume and therefore infiltration capacity of soils. Infiltration capacity determines erodibility due to the fact that high infiltration capacity limits the proportion of overland flow (MORGAN 2009). Shear strength expresses the resistance of a soil to the energy of flowing water (and gravitation). Together with the surface roughness, which both depend on soil texture, pore volume, shear strength and infiltration capacity are the main hydrological parameters of soil erodibility. Antecedent water content is as much relevant: Overland flow is more probable on a wet soil; wet aggregates are less stable and surface sealing might appear (BRYAN 2000; MORGAN 2009). Taking these parameters into account, it seems to be evident that erodibility is very variable in space and time.

As it is mentioned by EL-SWAIFY et al. (1982) and NILL (1998) the variability of the erodibility of tropical soils is extraordinary high; soils of the same order have different soil erodibility. The values range from 0.06 to 0.48 (EL-SWAIFY et al. 1982) or from 0.0006 to 0.35 with a mean of 0.08 $\text{ton acre h } 100^{-1} \text{ acre}^{-1} \text{ ft}^{-1} \text{ tonf}^{-1} \text{ in}^{-1}$ (NILL 1998). In general, the erodibility of tropical soils is classified as low due to a high content of weathering-resistant sand (high infiltration capacity) organometallic complexes and Kaolinite as a binding agent. The silt fraction is often weathered.

Erodibility estimation

To be included in a soil erosion model, erodibility has to be measured or approximated; either by measuring soil loss under controlled conditions or by an index taking various soil properties into consideration (BRYAN 1968; MORGAN 2009). One index is Middleton's dispersion index, which is the ratio of the fraction of non-dispersed silt and clay and the fraction of dispersed silt and clay. Other early indices are based on the clay ratio (Bouyoucos' index), the amount, size and stability of aggregates (Gerdel's index), organic matter (Peele et al.'s index) or a complex interaction of grain size, permeability, absorption and dispersion (Bayer's index; for an overview of the history of indices and formulas BRYAN 1968; MORGAN 2009). In the USLE, erodibility is expressed by the K-factor, which is based on a unit plot database. A nomograph was developed to estimate the K-factor based on organic matter content, grain size, permeability and soil structure. Due to the fact that the database of the nomograph is only valid for some parts of the US, the application of the K-factor for tropical conditions is under discussion. ROOSE & SARRAILH (1989) found a good correlation between nomograph approximations and measured K values, while others voiced criticism and found lower correlations. Among others, ROTH et al. (1974) developed a nomograph which is well

adapted to tropical conditions, taking aluminium and ferric oxide as well as silicon dioxide into account. NILL (1993) developed a scheme to convert nomograph values into tropical K-values. This scheme is used in the study at hand.

2.2 Soil erosion modelling

As models in general, erosion models are simplified depicted realities of a specific part of the landscape (BORK & SCHRÖDER 1996). Using parameters, factors, their constellation and interaction, erosion models are a representation of real erosion processes. Soil erosion models are an academic and land stewardship approach to cope with soil erosion. Among other approaches—e. g. measurement, mapping and sediment sampling—soil erosion models have been developed within the last one hundred years. Especially after the *Dust Bowl* in the United States (1934–1940), attempts were made to focus on erosion models for soil conservation. As the number of models is huge and a lot of reviews and state-of-the-art descriptions exist (BORK & SCHRÖDER 1996; MERRITT et al. 2003; MORGAN & NEARING 2010; BORRELLI 2011; SCHMENGLER 2011) only a general view of different types of models is given in the following.

Models are either empirical, physical or conceptual. Empirical models are based on empirical measurements on plots or in catchments. The results are used to calculate regressions between different parameters. The problem of these models is that values measured at one location are difficult to use in other climates, land use schemes, soils and topographic conditions. Physical models in contrast are based on the principal laws of physics. Often physical models require more input than empirical models. Conceptual models are based on flows and storage in a catchment; they only generally describe the processes in a catchment (MERRITT et al. 2003). All these types of models can be both, deterministic or stochastic. Deterministic models are based on a defined input value of a parameter, whereas stochastic models are based on probability distributions of the input parameters. The temporal representation of models includes temporally static input parameters or time-depended input parameters. Erosion models are event-based or continuous. Continuous models in turn can be based on mean values over a specific time period or represent the variability of processes over a longer period (BORK & SCHRÖDER 1996). The spatial representation of erosion models ranges from plot scale to basin scale (cf. RENSCHLER & HARBOR 2002). This is especially important due to the fact that the contribution of different types of erosion (interrill, rill or gully erosion) to total soil loss depends on scale (EVANS & BRAZIER 2005). Also the proportion of erosion and deposition varies with scale. On a small hillslope, deposition and sediment storage is much

smaller than in a catchment (DE VENTE et al. 2008). Thus, hillslope erosion models exist as well as field, small catchment and catchment scale models (MERRITT et al. 2003). The input parameters vary over the area of investigation when applying distributed models. Input parameters are constant over the entire area in lumped models. The spacial discretization depends on whether models are based on homogeneous compartments of the landscape (subcatchments, hydrological response units), homogeneous portions of a slope in the direction of flow or regular portions of the landscape (grid cells; BORK & SCHRÖDER 1996). Functional relationships—especially important concerning the flow direction of water—are considered in the first two approaches, but less integrated in the latter one.

The USLE-family

An empirical, deterministic and continuous erosion model is the Universal Soil Loss Equation (USLE). The USLE and its modifications are one of the most used erosion models world wide. The USLE was developed in the United States in the late 1950s. First applications took place in the early 1960s in the Midwest (RENARD et al. 1991); the first version is published in the USDA Agricultural Handbook 282. A second version of the Handbook was published in 1978 (USDA Agricultural Handbook 537, WISCHMEIER & SMITH 1978) and is the standard reference to the model. A revisited USLE (RUSLE) was first published in 1991 and is described in the USDA Agricultural Handbook 703 (RENARD et al. 1997). Further developments are implemented in a more computerized version (RUSLE2, FOSTER et al. 2000; USDA AGRICULTURAL RESEARCH SERVICE 2013). A 3-dimensional version of the RUSLE was developed for GIS applications and convergent flow on catchment scale (RUSLE3D) and erosion and deposition modelling (USPED, MITASOVA et al. 1996). Other models were developed on the basis of the USLE, e. g. the sediment delivery model MUSLE (WILLIAMS 1977) or the USLE-M (KINNELL & RISSE 1998), which explicitly includes runoff.

The original USLE is based on a huge database of values from a bare standard “Wischmeier”-plot with a length of 72.6 ft (22.13 m), a wide of 6 ft (1.83 m) and a slope of 9%, where soil loss is a linear function of erosivity and erodibility (cf. WISCHMEIER & SMITH 1978).

The results can be used to calculate soil loss on plots different from the standard plot. Factors are used to get the soil loss for other land cover, topography or conservation measures. The procedures to calculate the factors are described in the USLE manual (WISCHMEIER & SMITH 1978).

The Revisited USLE includes some major improvements; all factors are calculated differently. A new rainfall–erosivity term was adapted which is based on a larger data set than the term used in the USLE. In addition, snow is included in the RUSLE (RENARD et al. 1991; BORK

& SCHRÖDER 1996). The parameter of the slope length was modified and is now calculated as a ratio of rill to interrill-erosion. While in the USLE C- and K-values are calculated on the temporal basis of crop stages, they are calculated for half month intervals in the RUSLE. In addition, the C-factor in the RUSLE is based on several subfactors and is a function of mulch or ground cover, crop residues, roots and a subsurface cover (RENARD et al. 1991). The USLE's C-factor is based on the weighted average soil loss ratio of a plot with the land cover under investigation and the standard plot. A critical slope length for conservation measures is newly integrated in the RUSLE's P-factor (cf. BORK & SCHRÖDER 1996). In the RUSLE3D and the USPED model, slope length is replaced by upslope area, which takes convergent flow into account. In addition, the Unit Stream Power Theory (MOORE & BURCH 1986b) is used in the USPED model to calculate erosion and deposition (MITASOVA et al. 1996). The USLE assumes erosion on the entire plot/catchment.

USLE limitations

Although the USLE-family models received wide attention and are applied frequently, there is a great deal of criticism. Some of the points commented are improved in the revisited version(s), but are nonetheless important to consider:

- the equation is based on mean values over a longer period. Thus, event-based erosion is not calculated with the USLE (MERRITT et al. 2003), although single events contribute to a high proportion to total soil loss.
- Although gully erosion or mass movements are largely responsible for total soil loss, they are not calculated with the USLE (MERRITT et al. 2003).
- In the USLE—and most of its modifications and revisions but the USLE-M (KINNELL & RISSE 1998)—runoff is not considered explicitly.
- The calculation of rainfall erosivity is based on a limited database; only drop size measurements from 1943 in Washington, D. C., and velocity measurements from 1949 were included (BORK & SCHRÖDER 1996);
- soil erodibility as in the USLE is only valid for silt contents less than 70%, which makes it difficult to apply the equation in loess soils. In addition, the erodibility increases with increasing aggregate sizes, which is contrary to the actual process (BORK & SCHRÖDER 1996);
- as it is shown by DIKAU (1986), the equation is very sensitive to slope length and inaccuracies are very good correlated to slope length variations;

- the database of the USLE and the RUSLE is only valid for the USA and applications in areas with different climatic or soil characteristics are prone to errors. This is especially important when applying the USLE in the humid tropics.

The criticism that deposition is not considered (i. a. MERRITT et al. 2003) in the calculation can be avoided using USPED or RUSLE2. Also other problems are solved in the revisited version, such as a lack in the temporal variability of C-factors.

Especially the lack of applicability of the USLE to other regions than the original study areas is often invoked (e. g. MERRITT et al. 2003; BORK & SCHRÖDER 1996). Nevertheless, various attempts were made to adapt the USLE to other conditions. One example is the AGAB (*Allgemeine Bodenabtragsgleichung*), a German version of the USLE developed for the state of Bavaria and Europe (SCHWERTMANN et al. 1990). Other authors try to adapt single USLE-factors to their regions of interest; NILI (1993) reports equations to calculate a tropical erodibility factor, ROOSE (i. a. 1977), EL-SWAIFY et al. (1982), and NILI et al. (1996) present cover-and-management factor values for tropical cultivation systems and various authors tried to calculate rainfall erosivity values for other climates, which are even suitable for a limited database (e. g. ROOSE 1977; RENARD & FREIMUND 1994; SALAKO 2006; DIODATO et al. 2013 for [West] African conditions).

In the study at hand, the RUSLE3D model will be used, whereas erodibility, erosivity and cover-factors were calculated based on regional adaptations for the study region. Deposition is considered applying an erosion/deposition index.

2.3 Soil erosion risk

Soil erosion risk assessment is done in various regions, on different scales and temporal frameworks, with different goals and methods.

Two methodological approaches can broadly be distinguished: Expert-based methods and erosion modelling (VAN DER KNIJFF et al. 2000; VRIELING et al. 2006; KARYDAS et al. 2009). USLE-family models are common models used for risk assessment, either the original USLE (VAN DER KNIJFF et al. 2000; VAN ROMPAEY et al. 2001; SABBI & SALVATI 2014), the revisited version (RUSLE; BOELLSTORFF & BENITO 2005; TERRANOVA et al. 2009) or other USLE-based models (e. g. ABAGflux; VOLK et al. 2010).

Although these kinds of models give quantitative results, the term *erosion risk* is—except of some authors (cf. KARYDAS et al. 2009; BORRELLI et al. 2014)—understood qualitatively. The quantitative results are classified or used for a relative comparison of the risk within a study area (VAN DER KNIJFF et al. 2000; VRIELING et al. 2008; NEKHAY et al. 2009). Expert-based

methods generally only give relative results (e. g. LE BISSONNAIS et al. 2002; BOU KHEIR et al. 2006; VRIELING et al. 2006). The results of an erosion risk assessment is consistently a relative risk map of “hotspots” or priority areas, which show the spatial distribution of the erosion risk (NIGEL & RUGHOOPUTH 2010; VOLK et al. 2010). The goal of this risk mapping is risk management and erosion control—i. e. planning and implementation of soil conservation measurements (VRIELING et al. 2006)—, the identification of priority areas (NIGEL & RUGHOOPUTH 2010) or policy development and decision-making (LE BISSONNAIS et al. 2002; BOELLSTORFF & BENITO 2005; MUTEKANGA et al. 2010).

Concerning these goals, the spatial scale of erosion risk assessment is important. On the European and national scale, policy development (set-aside scenarios or agricultural support planning) is important, the planning of conservation measures is important on local scale. Especially the risk assessment on continental scale emphasize the relative character of erosion risk, as it is difficult to model exact values on that scale (VRIELING et al. 2008). The areas of erosion risk studies range from small municipalities (KARYDAS et al. 2009) to national territories (LE BISSONNAIS et al. 2002; SABBI & SALVATI 2014) or even the European Union (VAN DER KNIJFF et al. 2000) on the level of political hierarchies and from small watersheds (VRIELING et al. 2006; BORRELLI & SCHÜTT 2014) to large river basins (ZHANG et al. 2010). Other studies assess erosion risk of regions or islands (BOELLSTORFF & BENITO 2005; BOU KHEIR et al. 2006 or NIGEL & RUGHOOPUTH 2010).

Soil erosion risk is often seen as the interaction of different factors, which are either specific for an area or human-induced. Therefore, there are other terms related to erosion risk. NIGEL & RUGHOOPUTH (2010) define erosion risk as the interaction of erosion susceptibility (of the topography) and sensitivity (of the land cover) in combination with rainfall erosivity. Other authors use susceptibility more or less synonym to risk (BORRELLI & SCHÜTT 2014) or as an inherent character of a landscape (soil, topography, climate; GIORDANO n. d.). The inherent susceptibility is expressed in many studies by the potential erosion of an area—or a “worst case scenario” (RENSCHLER et al. 1999)—whereas the present land use and land cover determines the *actual* (or current) erosion risk (MUTEKANGA et al. 2010; ZHANG et al. 2010; SABBI & SALVATI 2014). This distinction is used by some authors to give erosion risk a temporal dimension: The change of land use and land cover is used to calculate either historical (MUTEKANGA et al. 2010) or future erosion risk (PRASUHN et al. 2013). Also the possible reduction of soil erosion risk is estimated (KARYDAS et al. 2009) or the erosion risk of environmental changes is evaluated (ZHANG et al. 2010).

Risk is interpreted in most studies as a relative term of assessed erosion in a study. Only some authors set erosion risk in context to the economic or ecological consequences of soil loss

(e. g. costs of erosion or tolerable soil loss); e. g. RENSCHLER et al. (1999) and BOELLSTORFF & BENTO (2005) or GIORDANO (n. d.) can be mentioned here. As risk is seen as a relative value, the results are not always validated, an exception being LE BISSONNAIS et al. (2002) or BORRELLI et al. (2014).

3 Study area

The Upper Mefou subcatchment is located in the Région du Centre (Central province) in the Republic of Cameroon. The country belongs either to the West African or to the Central African subregion of the continent—depending on definition. While the small southeastern part of the catchment is located in the Département du Mfoundi (Mfoundi division), a larger portion is within the boundaries of Lekié division. The catchment is located in four *arrondissements* (subdivisions): Yaoundé VII, Yaoundé II, Lobo and Okola. Most of the villages are located in Okola. Beyond this administrative structure, there is also a system of heritage chiefdoms (traditional authorities, French: *chefferies traditionnelles*). The villages of the catchment are organized in this system and its different hierarchies, which comprises a *chef de troisième degré* (chief of a village) and a *chef de groupement* and a *chef supérieur*. Their role is important concerning land ownership and land use (for the northwest of Cameroon: DIDUK 1992).

Within the framework of the Integrated Watershed Management project a bridge in Nkolbisson ($3^{\circ} 52' 20.6''$ N, $11^{\circ} 27' 02.2''$ E) marks the outlet of the project's catchment. The outlet is located between the confluence of the Mefou River and the Afeumev/Afémé River and the mouth of the Abiergue River to the Mefou. The catchment area of the Upper Mefou is 97 km^2 ; the altitude ranges from 701 m at the outlet to 1225 m a. s. l. at the highest point in the Yaoundé massif (Odou summit).

The Mefou River is a right tributary of the Nyong, which forms one of the major river basins in Cameroon and drains to the Bight of Bonny (Gulf of Guinea). The confluence is located 10 km east of Mbalmayo (river-kilometre 345). The catchment area of the Mefou is about 840 km^2 (OLIVRY 1986). The northwestern divide of the Upper Mefou subcatchment is also the major Nyong–Sanaga divide.

Upper Mefou discharge-data are not available at the moment, as it is the case for data of the Mefou Reservoir. A gauge close to the outlet is out of operation and in a dilapidated condition. Discharge was recorded in the past (LEFÈVRE 1966), but data are not available at the present. Discharge of the Mefou is recorded at Etoa (235 km^2 , 672 m a. s. l., observation period: 1966–1977) and Nsimalen (425 km^2 , 650 m a. s. l., 1962–1977). The mean annual discharge of the Mefou at Etoa is 3.3 and $6.1 \text{ m}^3 \text{ s}^{-1}$ at Nsimalen; the unit discharge is 14.1 and $14.4 \text{ l s}^{-1} \text{ km}^{-1}$ respectively (OLIVRY 1979; OLIVRY 1986). Highest mean discharges were recorded in October ($7.7 \text{ m}^3 \text{ s}^{-1}$) and lowest in February ($1.47 \text{ m}^3 \text{ s}^{-1}$; Mefou at Etoa; OLIVRY 1979).

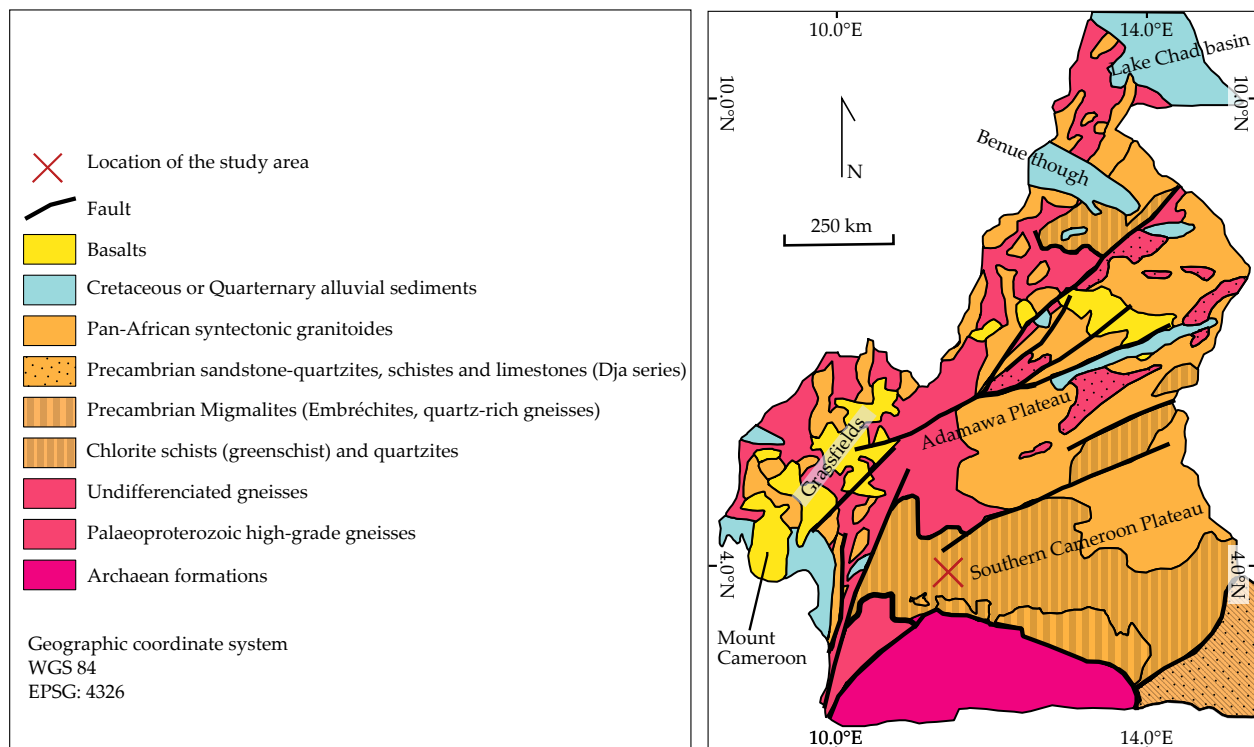


Figure 3.2: Geological sketch map of Cameroon (Source: CHAMPETIER DE RIBES et al. 1956; NZENTI et al. 1988, modified).

3.1 Geology and relief

The Upper Mefou subcatchment is located in the Pan-African North-Equatorial fold belt (PANEFB; NZENTI et al. 2010). The PANEFB is divided in a northern, a central and a southern domain (NZENTI et al. 2010). The southern domain is structured in the orogenic Mbalmay and Yaoundé series of the Precambrian basement and the Archaean formations of the Congo Craton (NZENTI et al. 1988; NGNOTUÉ et al. 2000). As it is shown in Figure 3.2 the study area is located in the neoproterozoic Pan-African metasediments of the Yaoundé series, a tectonic nappe overthrusting the Congo Craton (CHAMPETIER DE RIBES et al. 1956; NZENTI et al. 1988). The Yaoundé series consists of medium to high-grade garnet-bearing micaschists and gneisses (Yaoundé gneiss), metasediments of a Neoproterozoic greywack-shale sedimentary sequence, which recrystallised during a single tectonic event (620 ± 10 Ma; NGNOTUÉ et al. 2000). The layers of the Yaoundé series crop out on the inselbergs in the study area (cf. NZENTI et al. 1988).

The relief of the Upper Mefou subcatchment is characterized by two distinct units: the lowlands corresponding to the peneplains of the Southern Cameroon Plateau (MARTIN 1967) and the inselbergs. Both belong to the Yaoundé massif. The inselbergs are located in the

central part of the catchment, in the west and in the north(west); also in the east and in the outer south inselbergs are part of the study catchment (Figure 3.1). The inselbergs are of the Bornhardt type with very steep slopes, which are most pronounced in the northwest (Ekongo and Mbikal; see Figure 3.1). They originate from fluviomorphological selection following a dislocation line (EISENBERG 2009). Although pedimentation is expected for most parts of the Southern Cameroon Plateau, it is not the main geomorphological process in the catchment, as the terrain is undulating and therefore not typical (AHNERT 2009). Instead, hillslope pedimentation dominates the slopes of the inselbergs and valley floor pedimentation in the valleys (EMBRECHTS & DE DAPPER 1990).

The hillslope pediments were formed during the more dry phases in the Quarternary, while the valley floor pediments were formed during more humid phases. The pediments at the hillfootes are underlain by a Paleogene surface. At the summits of the inselbergs, the relief is Cretaceous (EMBRECHTS & DE DAPPER 1990). The surface of the lowlands is undulating: the valleys of the river were cut in the older pediment surface during an arid phase; slope retreat and lateral erosion forma relatively plat valley bottom (EISENBERG 2009). *Demi-oranges* hills are abundant in the lowlands of the catchment (Figure 3.1).

3.2 Soils

The soils in the study area are mainly Ferralsols, which are typical for the humid tropics. The development of these soils is a product of high temperature, water availability and a relative morphological stability, which allows a long duration of soil formation (>100 000 yrs). Under these conditions, weathering is efficient. The weathering products are quartz and sesquioxides. In addition, Ferralsols are well drained, which favors hydrolysis and desilification (DECKERS et al. 1998). Silicic acid react with hydroxides to form Kaolinit, a low cation-exchange capacity clay mineral. As Fe-hydroxides are mesostable and Fe-oxides are more stable, a relative enrichment of Fe-oxides is observed, what explains the red colour of the soils (rubefication). The low cation-exchange capacity of the soils results in a low fertility, because the soil is not able to bind nutrients. The clay content of Ferralsols is relatively low due to high weathering of minerals (DECKERS et al. 1998). The texture of Ferralsols is dominated by aggregation and the forming of “pseudo-sand” or “pseudo-sand” (EMBRECHTS & SYS 1988), product of the interaction of positively charged sesquioxides and negatively charged Kaolinite (cf. BLUME et al. 2010). The permeability of the Ferralsols is high due to the high porosity. A typical horizon sequence of a Ferralsol in the study (in French often *sols rouges* or *sols jaunes*) includes a thin humic A horizon, a ferric Bo horizon and a saprolite layer (MALA 1993). The

ferric Bo horizon is often divided in a subhorizon with the abundance of micro-aggregates, a second, more dense and sometimes plinthitic subhorizon and a third subhorizon with Fe-oxide nodules. The subsequent saprolite layer is divided in the alloterite (structure of the parent material disappeared) and the isalterite, where the structure of the parent material is preserved (MALA 1993). The regional pattern of soil on a typical hill in the area of the Upper Mefou subcatchment is characterized by topography. While in the valley floors hydromorphic soil dominate (BACHELIER 1959), the soil on the slopes are Typical Ferralsols. The summits of the hills are covered with soils with large blocky oxid nodules and no dense Bo horizon (MALA 1993). On some footslopes, more yellowish Ferralsols are located; in the thalweges, the soils are yellowish to reddish (MALA 1993). The difference in the soil colour might be explained by the ratio of goethite to hematite (KÄMPF & SCHWERTMANN 1983). The ratio is a function of ferrithydrate availability, soil organic matter content (Fe is fixed in Fe–humus complexes), soil temperature (dehydration and the decomposition of soil organic matter at higher temperatures), water availability and pH. Higher soil organic matter content favors goethite, whereas higher soil temperature and higher or very low pH favors hematite (KÄMPF & SCHWERTMANN 1983; DECKERS et al. 1998; CORNELL & SCHWERTMANN 2006). Especially in the wet-and-dry humid tropics, the water availability in different topographical positions is decisive (TARDY & NAHON 1985): the yellowish goethite is mainly dominant downslope.

3.3 Climate

According to the Köppen–Geiger classification, the climate of the Upper Mefou subcatchment is a tropical wet-and-dry equatorial Savanna climate with a dry winter (Aw; KOTTEK et al. 2006; PEEL et al. 2007). Depending on the observation period, the catchment is located on the border to the tropical monsoon climate (Am; RUBEL & KOTTEK 2010). The mean annual temperature is higher than 18 °C (23.5 °C). The precipitation of the driest month (January) totals 22 mm, mean annual rainfall totals 1628 ± 240 mm (standard reference period, 1960–1990, Yaoundé meteorological station, PETERSON & VOSE 1997, see 4.1).

Minimal annual precipitation was measured in 1963 (1280 mm) and a maximal precipitation in 1966 (2126 mm). The lowest monthly mean temperature is 22.3 °C (July), the highest 25.0 °C (February). A lowest monthly mean temperature measured in the observation period is 21.4 (January 1987), the highest 26.1 °C (February 1978). January is the driest month, mean precipitation totals only 22 mm; the wettest month is October with a mean total precipitation of 297 mm. There is a second minimum in July (80 mm) and a second maximum

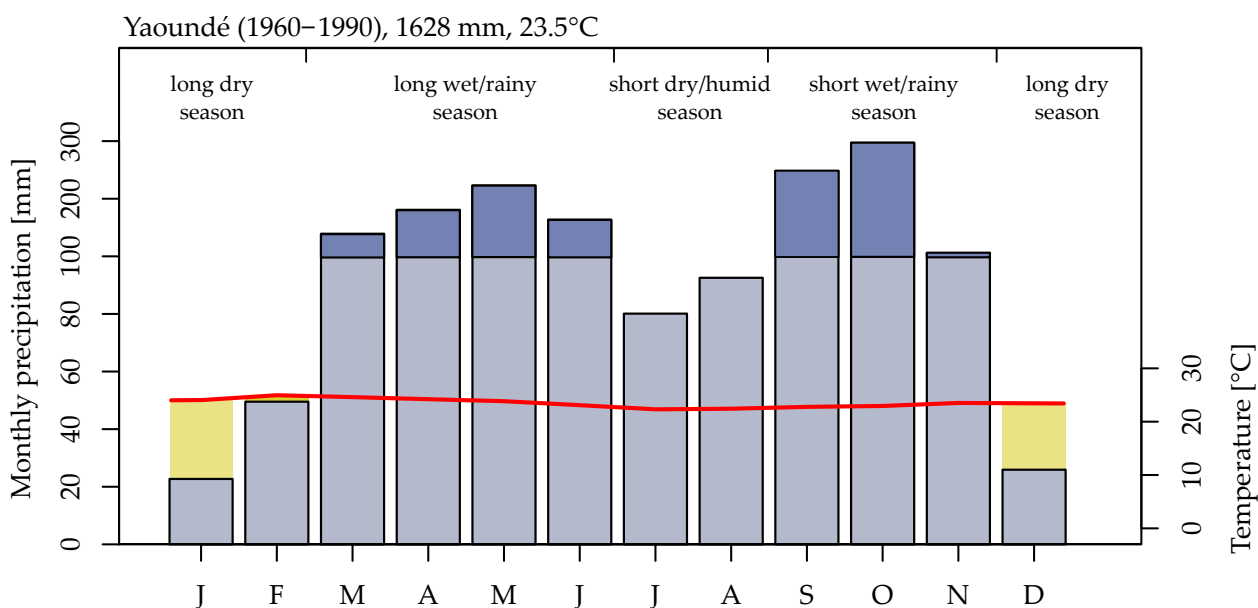


Figure 3.3: Mean monthly precipitation (primary y-axis, blue bars) and mean monthly temperature (secondary y-axis, red line) of the Yaoundé meteorological station (1960–1990). Note the Walter–Lieth-scaling of the y-axis (Database: PETERSON & VOSE 1997).

in May (223 mm; Figure 3.3). Thus, the annual distribution of rainfall is bimodal. The long rainy season is from March to June, followed by a short dry season (July and August), a second, short rainy season in September and October and the long dry season from November to January. Rainfall totals 706 mm (43% of annual rainfall) in the long and 544 mm (33%) in the short rainy season; nevertheless, the rainfall intensity is higher in the short rainy season (mean monthly rainfall in the short rainy season is 272 mm and 177 mm in the long rainy season). In the long dry season rainfall totals 204 mm (51 mm month⁻¹); in the short, but more wet, dry season rainfall totals 173 mm (87 mm month⁻¹). In 16% of the years in the observation period, January was without rain, February in 3% of the years and December in 13% of the years. All other months—also July and August in the short dry season—always received some rain.

36% of the days are rainy (Nkolbisson meteorological station, 1956–1980; COMITE INTERAFRICAIN D’ETUDES HYDRAULIQUES & OFFICE DE LA RECHERCHE SCIENTIFIQUE ET TECHNIQUE OUTRE-MER SERVICE HDROLOGIQUE n. d., COMITE INTERAFRICAIN D’ETUDES HYDRAULIQUES et al. 1990); 31% of the days in the observation period received more than 1 mm and 12% of the days more than 12.7 mm (an erosivity threshold, cf. ANGULO-MARTÍNEZ & BEGUERÍA 2009) and 1% of the days heavy rainfall ($P_d \geq 50$ mm). The magnitude–frequency analysis of daily rainfall in the observation period shows that the recurrence interval of heavy rain is 122 days; the recurrence interval of rainfall exceeding

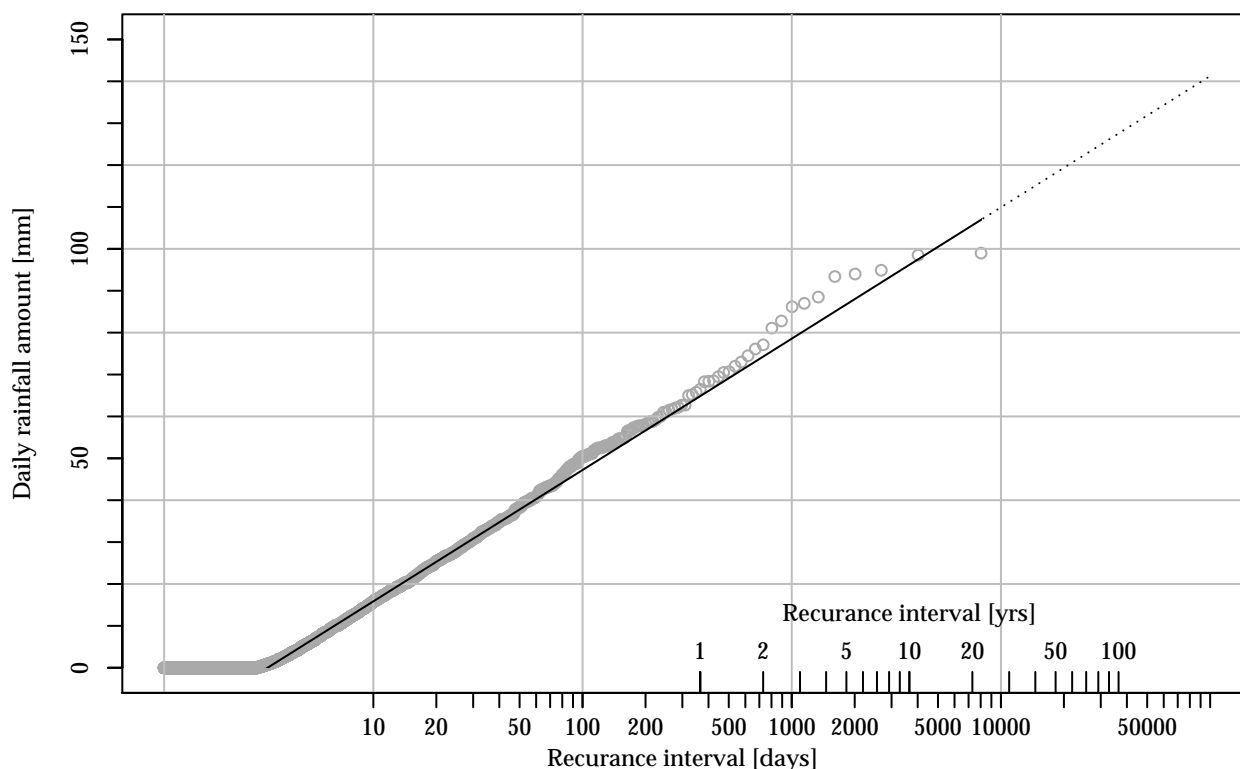


Figure 3.4: Magnitude–frequency analysis of daily rainfall (AHNERT 1982; Nkolbisson meteorological station (1954–1980; database: COMITE INTERAFRICAIN D’ETUDES HYDRAULIQUES & OFFICE DE LA RECHERCHE SCIENTIFIQUE ET TECHNIQUE OUTRE-MER SERVICE HDROLOGIQUE n. d., COMITE INTERAFRICAIN D’ETUDES HYDRAULIQUES et al. 1990).

12.7 mm is 8 days. The Magnitue–Frequency Index (GFI; AHNERT 2009) for Nkolbisson is $GFI=(64.2;95.6)$. Thus, daily rainfall of 64.2 mm or more is expected once a year, daily rainfall exceeding 95.6 mm every 10 years.

The climatic pattern of the Upper Mefou subcatchment is dominated by the movement of the Innetropical Convergence Zone (ITCZ) (GOUDIE 1996). When the ITCZ is at it’s southernmost position in January, the climate of the Southern Cameroon Plateau is dominated by northeasterly dry continental trade winds (Harmattan). This winds blow hot and dry air from the Sahara desert in the direction of the Gulf of Guinea. Monthly precipitation is at it’s minimum. With a change of solar radiation (tilt of Earth axis), the ITCZ moves in northward direction. The influence of the Hamattan decreases and humid monsoonal winds from southwest grow on influence. In the first rainy season the area of low pressure of the ITCZ crosses the Southern Cameroon Plateau: Due to convergence, rainfall (mostly as thunderstorms) increases. During the short dry season, the ITZC is at it’s northernmost position at the tropic of cancer. Monsoonal winds from the Gulf of Guinea bring some rain.

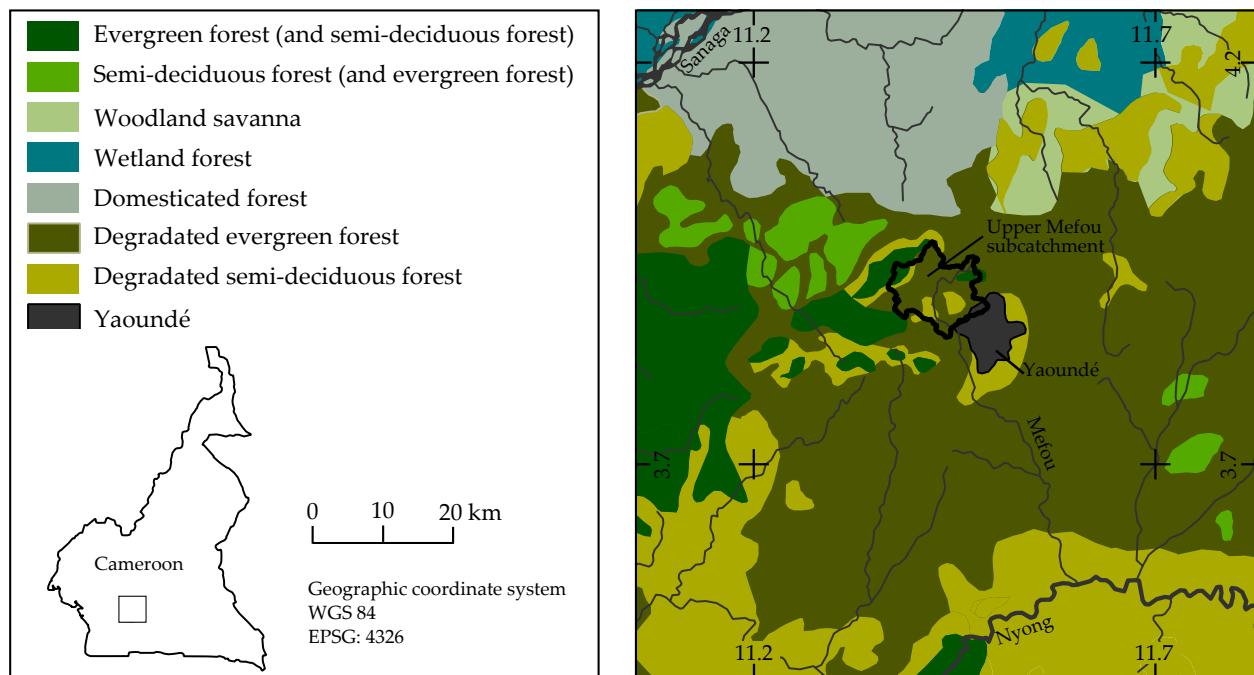


Figure 3.5: Forest cover map of the vicinity of the Upper Mefou subcatchment highlighting its position in a transition zone between woodland savanna (Caper) and degraded semi-deciduous (Citrus) or evergreen forest (Olive) (Database: SANTOIR & VILLIERS 1995; CENTERS FOR DISEASE CONTROL AND PREVENTION 2010; NATURAL EARTH DATA 2013).

The short rainy season starts when Central Cameroon is again crossed by the southwards movement of the ITCZ (GOUDIE 1996).

3.4 Land use and land cover

The Upper Mefou subcatchment is located in the transition zone between the woodland savanna of the Guineo–Soudanian type and semi-deciduous and evergreen forests of the Guineo–Congolaise type (SANTOIR & VILLIERS 1995). The major part of the catchment is classified as degraded evergreen (Atlantic Nigerian–Cameroonian–Gabonese type) humid forest.

In the high altitudes of the catchment, there is a primary forest whereas in the lowlands, the forest is degraded. Some parts of the catchment are also covered with a mixture of evergreen and semi-deciduous forest. West of the catchment there is a mosaic of primary and degraded evergreen and semi-deciduous forests (Figure 3.5). South and east of the catchment one can mainly find degraded evergreen forest, while far south, the vegetation consists mainly of semi-deciduous trees. Savanna woodland adjacent directly north of the catchment. The

lowlands around the Sanaga river are covered with floodplain forests or domesticated forests (SANTOIR & VILLIERS 1995).

The forest in the study area is used for hunter and gatherers activities and for splash-and-burn agriculture. Food crops are produced on relatively small plots, which are typical for agriculture in southern and central Cameroon (YEMEFACK et al. 2006). Cultivated patches are merged with primary and secondary forest as well as bush, fallows and plantations to a land cover mosaic. 13 to 15 patches per square kilometre are not seldom for the area (YEMEFACK et al. 2006). The most important crops are cassava (local name: *mbon*, binomial name: *Manihot esculenta*), maize (*fon*, *Zea mays*), groundnut (*owondo*, *Arachis hypogea*), sweet potato (*mebouda*, *Ipomoea batatas*) and tannia (*mekaba*, *Xanthosoma sagittifolium*) (local names according to MUTSAERS et al. 1981).

Monocropping of maize or cassava are the most frequent forms of cropping, while various forms of multiple mixed intercropping can be found (in order of abundance; own mapping, Nov/Dec 2012):

- Maize–cassava(–groundnut)
- Cassava–maize
- Cassava–sweet potato(–tannia)
- Maize–beans(–Sweet potato)
- Groundnut–maize–cassava
- Sweet potato–maize

Taro (*atu*, *Colocasia esculenta*), okra (*bitetam*, *Hibiscus esculentus*), bitterleaf (*ndoleh*, *Vernonia spp.*), chili pepper (*ondondo*, *Capsicum frutescens*), tomato (*ngoro*, *Lycopersicon esculentum*) and fruit or oil trees like African oil palm (*biton*, *Elaeis guineensis*), papaya (*fofo*, *Carica papaya*), mango (*Mangifera spp.*) or plantain (*ekon*, *Musa Plantain*) are also intercropped. The main-plants are mostly maize or cassava. Groundnut, cassava and maize

Table 3.1: Cropping calendar and rainfall during growing seasons. Timing and duration of work steps according to farmer’s information, own observations and NOUNAMO & YEMAFACK (2000). An asterisk (*) marks a month in which only cassava is planted. Mean rainfall of months in Nkolbisson (1956–1980; COMITE INTERAFRICAIN D’ETUDES HYDRAULIQUES & OFFICE DE LA RECHERCHE SCIENTIFIQUE ET TECHNIQUE OUTRE-MER SERVICE HDROLOGIQUE n. d., COMITE INTERAFRICAIN D’ETUDES HYDRAULIQUES et al. 1990).

	Clearing	Felling/burning	Planting	Harvest
1 st growing season	Dec/Jan 22 mm	Jan/Feb 35 mm	Mar/Apr/(May*) 179 mm (211 mm)	Jul 49 mm
2 nd growing season	Jun/Jul 99 mm	Jul/Aug 59 mm	Aug/Sep(/Oct*) 151 mm (307 mm)	Nov/Dec 75 mm

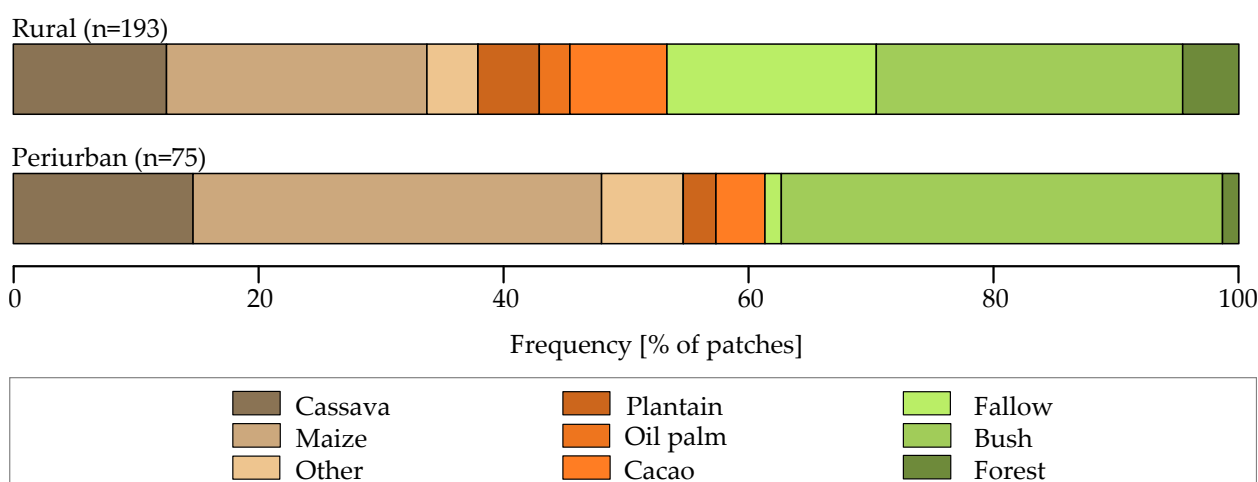


Figure 3.6: Land cover in the rural (division Lekié) and periurban parts of the catchment (subdivisions Yaoundé II and VII). Note the low frequency of fallows and the higher extent of cropping areas in the periurban part. Percentage of patches does not allow a statement about area proportions. Cropping areas in the periurban parts tend to be bigger than in the rural areas, where bush and forest patches are bigger (Source: own observations, Nov/Dec 2012).

are often grown on ridges, cassava also on small mounds. It is assumed that on mounds and ridges, yields are higher (HOWELER et al. 1993). Ridges are either contour parallel or not. Accordingly to the two distinct rainy seasons, there are also two growing seasons. Clearing for the 1st growing seasons “essep” starts during the long dry period in December and January. Felling and burning begins in January and is normally finished until the end of February. Planting and seeding of the most crops takes place in March and April. In the Upper Mefou subcatchment, cassava is planted also in May, the month in the long wet season receiving most rain (211 mm). Also when the other crops are planted, rainfall is relatively high (Table 3.1). The crops of the first growing season are regularly harvested in July. The second growing season “oyon” starts in June or July, felling and burning takes place during July and August, planting in August and September and harvesting in November or December. Again, cassava is planted somewhat later, in October.

In the traditional shifting cultivation system, after one year of cultivation, fallowing starts. The typical plant succession of a fallow duration of 15–25 years (forest fallow) is crops and weeds, grasses and herbs, woody herb, shrubs and trees (bush fallow) succeeded by forest (NOUNAMO & YEMAFACK 2000). Nevertheless, in the Upper Mefou subcatchment, the fallow period is often shorter. According to farmers, fallow duration is 1 to 15 years in the rural parts of the catchments, while in the dense settled periurban parts and around the Mefou Reservoir, the fallow period is much shorter (1–6 yrs). Fields are often not cultivated for one year, but for up to 4 years. The rotation intensity (RUTHENBERG & MACARTHUR 1980) is

therefore relatively high: In the rural parts, traditional shifting cultivation is still practiced; in the periurban parts, land use has often changed to semi-permanent cultivation (60% of the farmers) or even stationary cultivation with fallowing (20%). Only 20% of the farmers practice shifting cultivation (personal communication with farmers in Nov/Dec 2012). This shift is not uncommon in central or southern Cameroon. BROWN (2004) reports that in a village in the vicinity of Yaoundé, two-thirds of the households do not practice forest fallow (>15 yrs), whereas it is practiced by three-quarters of the households in remote villages. In another study, which also covers the Mefou catchment, the shortening of fallowing (3–5 yrs) in the more populated areas is observed for a long time (MUTSAERS et al. 1981). A shortening of the fallow period is explained by population pressure, a growing preference to fields close to the villages and the expansion of cash crops (NOUNAMO & YEMAFACK 2000; BROWN 2004). As it is shown in Figure 3.6, fallowing is more common in the less populated rural areas of the Mefou catchment than in the dense populated (periurban) areas. Also the cropping intensity is higher close to Yaoundé, whereas cash crop production (cacao, coffee) is more common around the villages.

4 Methods and materials

The study on hand focuses on three main objectives: The assessment of the actual and potential soil erosion risk in the Upper Mefou catchment using the RULSE3D and an erosion/deposition index, the simulation of the impact of future land use scenarios on the erosion risk and the evaluation of the applied methods in a humid tropical catchment. The evaluation includes a semi-quantitative validation of the erosion model results—a reservoir sediment survey—and a discussion of the values: comparison with values from literature and a sensitivity analysis. The main work flow is depicted in Figure 4.1.

4.1 (Revisited) Universal Soil Loss Equation

The main focus of the study at hand is erosion modeling. During field work in November and December 2012, soil samples were collected, land use was taken down and sediments in the Mefou Reservoir were observed. In addition, some non-structured interviews were conducted with the help of a local interpreter.

Erosion is modeled using the RUSLE3D, a three-dimensional enhancement of the RUSLE for the catchment scale. The RULSE3D is principally based on the USLE, but the topographic factor LS is replaced by a modified LS-factor, which can easily be computed in a GIS environment and is suitable for a catchment-scale application of the USLE/RUSLE.

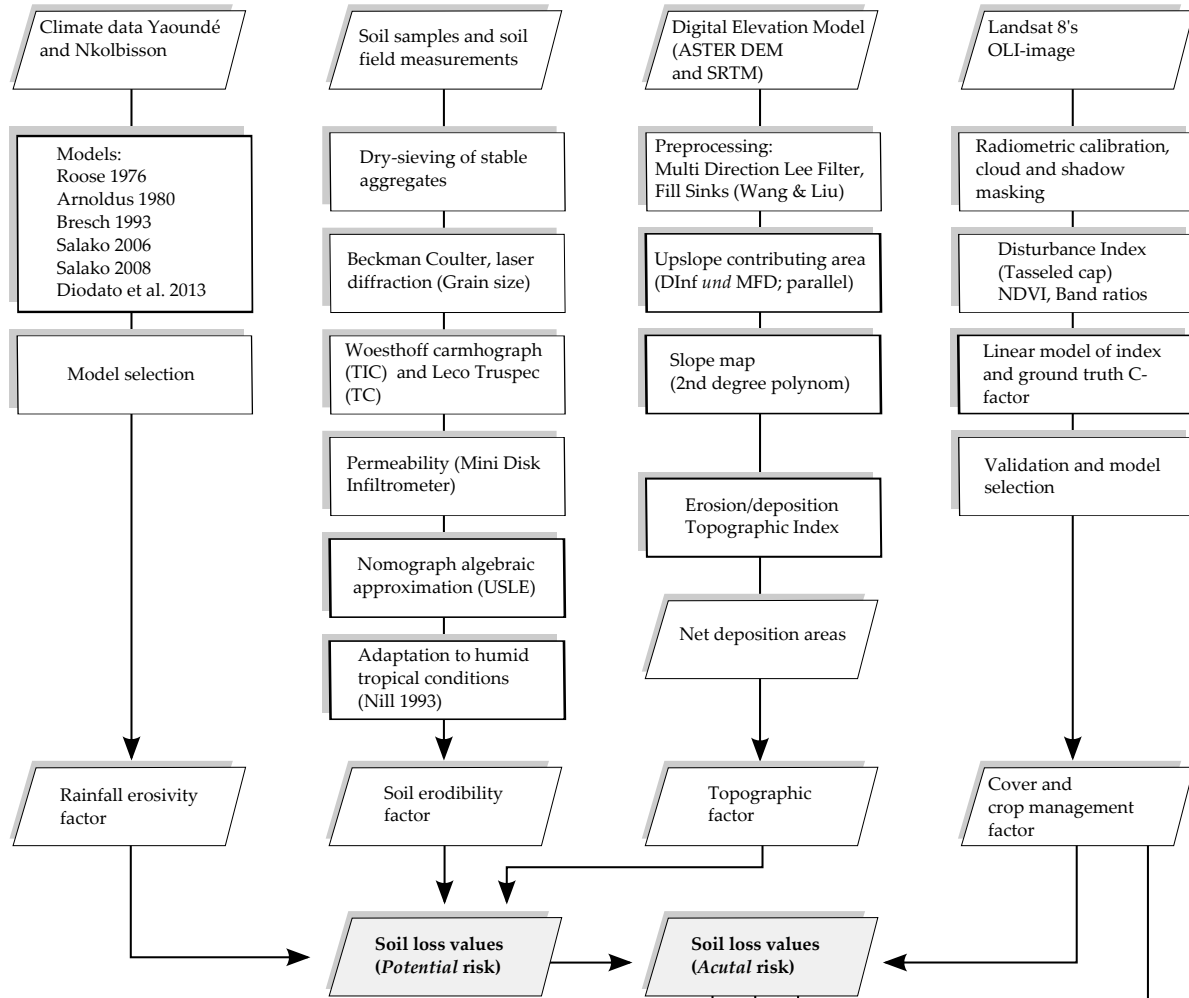
In the original unit-plot-based USLE, soil loss (E_0) is a function of rainfall erosivity and soil erodibility (WISCHMEIER & SMITH 1978):

$$E_0 = K \times R \quad (4.1)$$

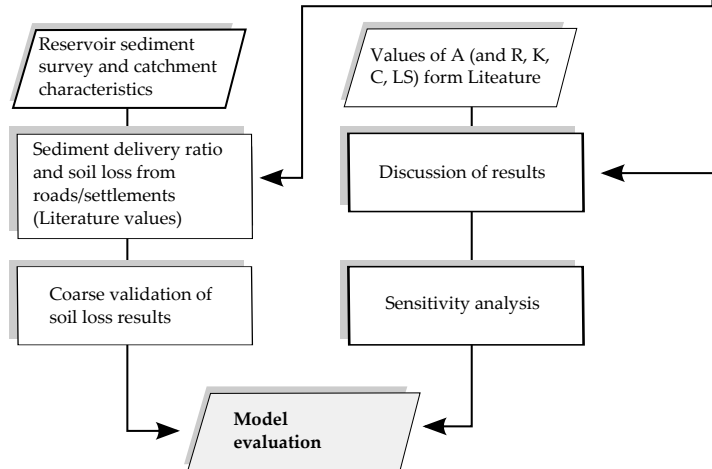
where K is a measure of soil erodibility in $\text{ton acre h } 100^{-1} \text{ acre}^{-1} \text{ ft}^{-1} \text{ tonf}^{-1} \text{ in}^{-1}$ and R is a measure of the rainfall erosivity in $100 \text{ ft ton-force in ac}^{-1} \text{ h}^{-1} \text{ yr}^{-1}$. If the area under considerations deviates from the unit plot, Equation 4.1 has to be adjusted. Soil loss is then calculated by multiplying E_0 with ratios of the deviation of parameters different from the unit plot (WISCHMEIER & SMITH 1978).

$$E = E_0 \times LS \times C \times P \quad (4.2)$$

Objective 1 Assessment of the actual and potential soil erosion risk in the Upper Mefou subcatchment



Objective 3 Suitability of methods (for the humid tropics)



Objective 2 Erosive impact of future land use

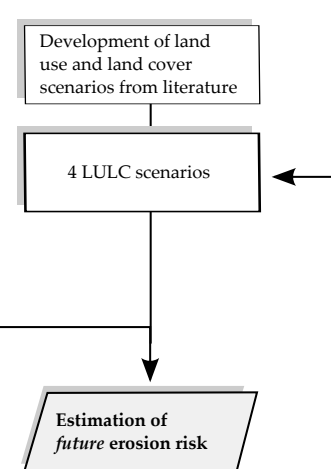


Figure 4.1: Flow chart of objectives, methods and materials. Parallelograms show input/output, rectangles measurements (tiny contours) or main calculations (bold contours); expected main results are depicted with filled parallelograms.

where LS is a topographic factor, C a cover and crop management factor and P a soil conservation factor. The principles of determining K , R and the adjustment factors are described in the following sections.

4.1.1 Rainfall erosivity factor (R)

As in the original version of the USLE, rainfall erosivity is expressed by the product of the total storm energy (E) times the maximum thirty minutes intensity (I_{30}) in the RUSLE, where E is a function of the rainstorm intensity I . The calculation of I and therefore the R-factor requires the availability of high resolution pluviographic data. In the Upper Mefou subcatchment and its vicinity, such data is not available. The rain gauge data from the station at Nkolbisson covers a period of 20 complete years of daily data (8458 days, Table 4.1). The station at Yaoundé covers a time series of 71 complete years of monthly data (1030 month, Table 4.1). Thus, the R-factor values of the Upper Mefou subcatchment have to be estimated using a validated regression.

In the following, a set of approaches to approximate the R-factor is presented. These models are more or less specific for Cameroon, the humid tropics or at least West Africa. An additional overview of methods for R-estimations can be found in BORRELLI (2011) and a specific overview for Africa in RENARD & FREIMUND (1994).

Using the equation, special attention has to be paid to the units used. Some equations are originally in US customary units (hundreds of foot tonforce inch acre⁻¹ hour⁻¹ year⁻¹) and some in metric (SI) units (Megajoule millimetre hectare⁻¹ hour⁻¹ year⁻¹). Also there are good reasons to use the US system (RENARD & FREIMUND 1994), in the thesis on hand metric units are used. To convert results of an equation in US-units, a conversion factor of $\kappa_R = 17.02$ is used (FOSTER et al. 1981).

Roose's rough approximation

One of the oldest and simplest approximation of the R-factor is the well established equation of ROOSE (1977):

$$R = P_a \cdot (0.5 \pm \delta) \cdot \kappa_R \quad (4.3)$$

where P_a is the total annual precipitation, $\delta = 0.05$ is a 5%-error and $\kappa_R = 17.02$ is the conversion factor.

Table 4.1: Description of the rainfall stations and the data set used to calculate rainfall erosivity. Data from Yaoundé were download from the Koninkrijk Nederlands Meterologisch Instituut (KNMI) Climate Explorer (climexp.knmi.nl).

	Yaoundé	Nkolbisson
Coordinates	3.90° N, 11.50° E	3.87° N, 11.46° E
Altitude	753 m a.s.l.	740 m a.s.l.
Resolution	monthly	daily, monthly
Time span	1889–1996	1954–1980
Years (complete)	108 (71)	27 (20)
Month	1030	314
Days	–	8458
Major gaps	04/1895–12/1908 01/1913–12/1926	06/1962–12/1963
Data set	PETERSON & VOSE (1997)*	COMITE INTERAFRICAIN D’ETUDES HYDRAULIQUES & OFFICE DE LA RECHERCHE SCIENTIFIQUE ET TECHNIQUE OUTRE-MER SERVICE HDROLOGIQUE (n. d.) COMITE INTERAFRICAIN D’ETUDES HYDRAULIQUES et al. (1990)
WMO station code	64950	–

* Global Historical Climatology Network *prcp* from *v2.prcp* in *v2.temperature.inv*

The equation is based on a data set of 20 rainfall recording stations in West and Central Africa. It is not valid for coastal areas, mountainous regions and the transition zone between unimodal and bimodal rainfall distributions (RENARD & FREIMUND 1994).

Modified Fournier Index

A second widespread erosivity index is Fournier’s index (FOURNIER 1960).

$$FI = P_{mw}^2 \cdot P_a^{-1} \quad (4.4)$$

where FI is Fournier’s Index, P_{mw} is the amount of rainfall in the wettest month in a year in millimetres and P_a is the total annual rainfall in millimetres.

The index is often criticized due to it’s low reflection of erosivity (MORGAN 2009). The contribution of other months than the wettest to erosion is underestimated by the index. Therefore, ARNOLDUS (1980) developed a new index, the Modified Fournier Index. This index considers the rainfall of all months. Here, the increase of the rainfall in a month other

than the wettest causes an increase of the erosivity value.

$$MFI = \sum_{i=1}^{12} (P_m^2 \cdot P_a^{-1}) \quad (4.5)$$

where MFI is the Modified Fournier Index, P_m is the amount of rainfall in a month m in millimetre and P_a is the total annual rainfall in millimetre.

To use the MFI in the RUSLE, the values have to be transformed into R-values. One transformation is modeled by RENARD & FREIMUND (1994), which is based on the relationship between MFI and measured R-values. ARNOLDUS (1980) used a similar relationship for Africa. He found out that the correlation between FI and R at 14 not further described stations in West Africa is relatively low ($r = 0.36$). The regression between the MFI and R is in contrast much better ($r = 0.83$) for the same stations.

$$R = 5.44 \cdot MFI - 416 \quad (4.6)$$

A rainfall–R relationship for Cameroon

BRESCH (1993) calculated a relationship between annual rainfall amounts and erosivity for Cameroon. This regression is based on 18 stations in the semi-humid to humid parts of West Africa and Central Africa where rainfall totals 700–4000 mm a⁻¹ (3–14 years; $r^2 = 0.91$).

$$R = (11 + 0.012 \cdot P_a)^2 \quad (4.7)$$

Salako’s model

A more spatially specific model to estimate the R-factor of the RUSLE was developed by SALAKO (2006). He uses long term pluviograph data from Ibadan and Onne (Port-Harcourt), both in Nigeria, to calculate the R-factor according to the procedures described in WISCHMEIER & SMITH (1978) or BROWN & FOSTER (1987). These erosivity values are used to model the regression for daily and monthly data (SALAKO 2006):

$$R = a \cdot P^b \quad (4.8)$$

where P is the rainfall amount in millimetre and a and b are site specific empirical model parameters.

For the humid forests in southern Nigeria a and b were calculated using the Port-Harcourt database covering a period of 18 years or 2106 days and a mean annual rainfall averaging 2417 mm (SALAKO 2008; SALAKO 2010) using Wischmeier's storm erosivity index:

$$R_i = 0.130 \cdot P_a^{1.070}, \quad R_i = \sum_{n=1}^{365,366} (0.113 \cdot P_d^{1.205}) \quad (4.8a,b)$$

where R_i is the annual erosivity of a year i , P_a is the annual rainfall amount and P_d is the daily rainfall amount.

Values for a or b using the Brown–Foster Index are 0.223 or 2.057 for daily data and 0.302 or 1.462 for annual rainfall data (SALAKO 2010). The coefficient of determination (r^2) of all regressions is 0.97–0.98 (SALAKO 2008; SALAKO 2010).

African Rainfall Erosivity Subregional Empirical Downscaling

African Rainfall Erosivity Subregional Empirical Downscaling (ARESED, DIODATO et al. 2013) is based on high resolution erosivity calculations over a long time span for several locations in Africa. The information is interpolated and relationships between latitude, longitude and elevation are used to represent the spacial variability of rainfall over Africa. The horizontal spacial variability is a function of the seasonal migration of the Intertropical Convergence Zone (latitude) and the higher energy load of heavy rainfall events in western Africa (LAL 1985). A weighted geographical scale factor (η) is developed by DIODATO et al. (2013) to incorporate the variability in ARESED:

$$\eta = H \cdot Z \quad (4.9)$$

where H is a horizontal component and Z is a vertical component;

$$H = a \cdot \varphi - b \cdot \lambda^3 + \gamma \quad (4.10)$$

where φ is the latitude in decimal degree south, λ is the longitude of the study area in decimal degree east, $a = 0.01$ and $b = 0.00003$ are scale parameters and $\gamma = 10$ is a shift parameter;

$$Z = 1 - \Delta \cdot E \quad (4.11)$$

where E is the elevation of the study area in metre above sea level and $\Delta = 0.001$ is an elevation scale parameter.

The RUSLE's rainfall erosivity factor (R) is (DIODATO et al. 2013):

$$R_{ARESED} = \eta \cdot \phi \cdot P_{85} \cdot c \quad (4.12)$$

where P_{85} is the 85%-percentile of the monthly precipitation data in millimetre, $\phi = 1$ is a regional scaling operator and $c = 1.271$ is a shape parameter (RENARD & FREIMUND 1994).

4.1.2 Erodibility factor (K)

An erodibility nomograph (WISCHMEIER et al. 1971) is the most widely used tool to approximate the erodibility factor K . In the USLE, erodibility is a function of grain size, organic matter, soil structure and permeability. As presented in the RUSLE Handbook (RÖMKENS et al. 1997), the nomograph can be replaced by an algebraic approximation of the K factor (WISCHMEIER & SMITH 1978) if the silt fraction does not exceed 70%.

$$K_{alg} = \frac{2.1 \cdot 10^{-4} \cdot 12 - OM \cdot ((mS + mU) \cdot mU)^{1.14} + 3.25 \cdot s - 2 + 2.5 \cdot p - 3}{100} \quad (4.13)$$

where K_{alg} is the approximated erodibility of the RUSLE K -factor nomograph in US customary units (ton acre h 100^{-1} acre $^{-1}$ ft $^{-1}$ tonf $^{-1}$ in $^{-1}$), OM is the content of organic matter in percent, mS is the fraction modified sand in percent (0.100–2.000 mm, or very coarse sand to fine sand following the USDA size separates in percent; SOIL SURVEY DIVISION STAFF 1993), mU is the fraction modified silt in percent (0.002–0.100 mm, or very fine sand and silt following the USDA size separates; SOIL SURVEY DIVISION STAFF 1993), s is the structure class and p is the permeability class.

The values can be converted to SI units using a conversion factor of $\kappa_k = 7.59^{-1}$.

As an application of the K -factor for relatively clay-rich, aggregated tropical soils is under discussion (EL-SWAIFY et al. 1982; see Section 2.1) many approximations are used to better represent the erodibility of these soils. In the study at hand, NILL (1993)'s approximation for tropical soils is used, which has been tested in Cameroon for soils similar to the soil in the Upper Mefou subcatchment.

$$K_{trop} = a \cdot K_{alg} + b \quad (4.14)$$

where K_{trop} is an erodibility factor adapted to tropical conditions, K_{alg} is the K -factor approximated as described in Equation 4.13 and a and b are soil specific parameters.

NILL (1993) classified tropical soils from Cameroon and Nigeria into three groups with specific parameters. A soil is classified into one group where the following equations give the highest value:

$$X_1 = 1.118 \cdot U + 90.5 \cdot BD + 0.416 \cdot OM + 13.4 \cdot pH + 0.724 \cdot AGG - 100.6 \quad (4.15a)$$

$$X_2 = 1.700 \cdot U + 134.7 \cdot BD + 1.395 \cdot OM + 7.577 \cdot pH + 0.478 \cdot AGG - 114.4 \quad (4.15b)$$

$$X_3 = 1.343 \cdot U + 114.2 \cdot BD + 1.617 \cdot OM + 7.816 \cdot pH + 0.378 \cdot AGG - 90.5 \quad (4.15c)$$

where X_1 , X_2 and X_3 are the different groups, U is the fraction silt in percent, BD is the bulk density in a depth of 5–10 cm in gramm per cubiccentimeter, OM is the content organic matter in percent and AGG is the content of dry-sieved 0.630–0.200 mm aggregates in percent.

Bulk density was not measured for the soils in the Upper Mefou subcatchment during field work. Therefore, mean empirical values from NILL's study are used here (BD is 0.87 for X_1 and X_3 and 1.06 for X_2). The same applies to pH (pH is 5.3 for X_1 , 5.1 for X_2 and 5.0 for X_3).

The soil specific parameter a is 2.3 for group 1, 1.1 for group 2 and 0.03 for group 3; parameter b is 0.12 for group 1, 0 for group 2 and 0.006 for group 3 (NILL et al. 1996).

Grain size analysis

Modified silt and modified sand content are analysed by sieving and laser diffraction using a Beckman Coulter LS 13320 PIDS. The method is based on the assumption that the angle of laser diffraction of a particle decreases with increasing particle size. 117 detectors record the diffraction at a specific angle. Thus, the fraction of particle volume for each detector and it's mean grain size can be calculated based on the Fraunhofer theory and the Mie theory. The sample are sieved to the <1 mm fraction and 2 g of each sample pretreated several times with hydrogen peroxide (30% H_2O_2) to dissolve all organic material (GRAY et al. 2010). As the samples have a relatively high content of organic material and fine grain fractions, dissolution is slow. To fasten up the process and to ensure that all organic material is dissolved, the samples are put in a tempered shaking water bath. Water is separated from the samples by centrifugation to reinforce concentration levels of hydrogen peroxide. When no reaction is visible any more, the samples are divided and particle size is measured with the Beckman Coulter. Two measurement runs are done per sample. The Beckman Coulter itself measures threefold; altogether a sixfold determination is done: mean values are used for

further calculations. Additionally, three samples are also measured without pretreatment to verify the effect of non-removed organic material on grain size distributions.

Organic matter content

The organic matter content (OM) of 47 samples is analyzed by measuring total inorganic carbon (TIC) and total carbon (TC):

$$OM = f \cdot TOC = f \cdot (TC - TIC) \quad (4.16)$$

where TOC is the total organic carbon content in percent and f is a conversion factor.

The “van Bemmelen factor” ($f = 1.724$) is often used for conversion, which traces back to Sprengel 1826 (PRIBYL 2010). A review of PRIBYL (2010) shows that this factor is often misused and lines of evidence in its calculation are not comprehensible. So in the study on hand, a more reliable factor $f = 2$ (PRIBYL 2010) will be used, based on the assumption that organic material consists of 50% organic carbon.

Total organic carbon is calculated as the difference between total carbon and inorganic carbon. Total inorganic carbon is measured using a Carmhograph C-16 (co. H. Woesthoff Messtechnik). The fundamental operational principle is digestion in phosphoric acid (H_3PO_4) at a temperature being approximately $70^\circ C$, the transfer of the released carbon dioxide in diluted sodium hydroxide and measurement of electrical conductivity differences of treated and untreated sodium hydroxide. The conductivity difference of standards with a known TIC content are used for a linear model of TIC values and conductivity differences (Appendix, p. iii). A LECO Truspec CHN–elemental analyzer is used to measure TC. The apparatus combusts the sample in a stream of oxygen at $950^\circ C$ and uses an IR-detector to calculate the content of TC from the CO_2 concentration. Various standards are used for calibration.

Permeability

To calculate hydrological conductivity a Mini Disk infiltrometer (*Decagon Devices, Inc.*) was used during field work. The volume of water infiltrating in the soil is measured at a specific interval and a defined suction rate. As the suction rate is the a function of porosity, the selection of an adequate rate is texture-dependent. Because the soils in the study area have sandy texture, a suction rate of 2 is chosen (DECAGON DEVICES 2012). The time interval is adapted to the total duration of measurement. Up to 5 minutes, the level of the water column is taken down every 0.5 minutes. In slow infiltrating soils, the level is taken down every 2.5 minutes or every 5 minutes after 5 minutes.

Hydraulic conductivity (k) is determined following the method of ZHANG (1997):

$$k = \frac{C_t}{A_k} \quad (4.17)$$

where C_t is the slope of the graph of cumulative infiltration at the time t against the square root of time (\sqrt{t}) and A_k is a soil specific parameter:

$$A_k = \frac{11.65 \cdot (n^{0.1} - 1) \cdot \exp(z \cdot (n - 1.9) \cdot \alpha \cdot h_0)}{(\alpha \cdot r_0)^{0.91}} \quad (4.18)$$

where α and nk are the van-Genuchten parameters (VAN GENUCHTEN 1980), h_0 is the suction rate and $r_0 = 2.25$ cm the radius of the mini disk; z is 2.92 for $n \geq 1.9$ and 7.5 for $n_G < 1.9$.

The van-Genuchten parameters are taken from CARSEL & PARRISH (1988: p. 759). C_t is determined by a quadratic regression (2nd degree polynomial regression; DECAGON DEVICES 2012).

$$I_t = C_t \cdot \sqrt{t}^2 + b \cdot \sqrt{t} \quad (4.19)$$

where b is a model parameter and I_t is the cumulative infiltration at time t .

The quadratic regression is solved with the function `nls` of the *stats*-package in R (R CORE TEAM 2013).

4.1.3 Land cover and management factor (C)

A Landsat 8 image is used to calculate the land cover and management factor (C). The image is preprocessed and spectral information of pixels with well known C-factor information from ground-truthing is used to calculate a linear model of spectral information and the C-factor. The relationship calculated from the sampled point is then used to predict C-factor values for the entire image; the predicted values are validated with a second set of ground-truth information.

Landsat 8 image

Landsat 8 is a medium-resolution satellite system and part of the Landsat continuity mission (30 m resolution). Observations of the sensor *Operational Land Imager* (OLI) are similar to those of the previous sensor (ETM+). The bands of Landsat 8 are somewhat more narrow than the bands of ETM+; two additional are added: a shorter blue wavelength band and a second short infrared band for cirrus detection. Landsat 8 has 11 bands including

two thermal bands and a panchromatic band (15 m resolution). Wavelength information is given below if necessary; descriptions of the system can be found in IRONS et al. (2012) for the announcement of Landsat 8 and ROY et al. (2014) for details. The Landsat 8 scene *LC81850572014137LGN00* (WRS-path 185, WRS-row 57) used here was acquired on May 5th 2014 and is clipped to the extent of the study area.

Landsat 8 preprocessing

Radiometric calibration of the Landsat 8 scene is done separately for each band. Due to the fact that the raw scenes as provided by the USGS and available via the Earth Explorer consist of quantized and calibrated scaled digital numbers (DN), the values at first have to be converted to top-of-the-atmosphere reflectance (US GEOLOGICAL SURVEY 2013):

$$\rho\lambda = \frac{M_\rho \cdot DN + S_\rho}{\sin \theta_{SE}} \quad (4.20)$$

where $\rho\lambda$ is the top-of-the-atmosphere planetary reflectance, M_ρ is a band-specific multiplicative rescaling factor, S_ρ is a band-specific additive rescaling factor, DN is the digital number and θ_{SE} is the local sun elevation angle in degree.

The rescaling factors and the sun elevation angle for the specific Landsat scene are given in the meta data of the scene. All bands instead of temperature bands and the Quality Assessment (QA) band are calibrated.

The 16-bit information of the QA band is used to detect clouds in the image; Bits 14 and 15 can be translated to a confidence that the condition “cloudy” is fulfilled (00 is no cloud, 01 is a low confidence of clouds, 10 is a medium confidence of clouds and 11 is a high confidence of clouds). In the study on hand, only high confidence of clouds are used to mask the clouds. Cloud shadows are masked using the normalized ratio of the short wavelength Coastal/Aerosol Band 1 (B_1) to Band 2 (B_2) (YALE CENTER FOR EARTH OBSERVATION 2013):

$$ACI = \frac{B_1 - B_2}{B_1 + B_2} \quad (4.21)$$

Shadows have relatively high values. A non-shadow–shadow threshold is defined by a visual interpretation of a true colour displayed Landsat scene.

Transformations, ratios and indices

Normalized Difference Vegetation Index (NDVI) values are often used to model C-factor values (DE JONG 1994; ERENCIN 2000). The NDVI is the normalized ratio of the red to the

Table 4.2: Coefficient for the Tasseled Cap transformations of Landsat 8 reflectance as used in Equation 4.24 (BAIG et al. 2014)

Transformation i	Coefficients ν_x for Landsat 8 band B_x					
	Band 2	Band 3	Band 4	Band 5	Band 6	Band 7
Greenness	-0.2941	-0.2430	40.5424	0.7276	0.0713	-0.1608
Brightness	0.3029	0.2786	0.4733	0.5599	0.5080	0.1872
Wetness	0.1511	0.1973	0.3283	0.3407	-0.7117	-0.4559

near infrared band (TUCKER 1979):

$$NDVI = \frac{B_5 - B_4}{B_5 + B_4} \quad (4.22)$$

where B_5 is Landsat 8's band 5 (near infrared: 0.845–0.885 mm) and B_4 is band 4 (red: 0.630–0.680 mm).

Another index is HEALEY et al. (2005)'s forest Disturbance Index (DI). The Index is a linear combination of the Tasseled Cap transformations *Brightness*, *Greenness* and *Wetness* (KAUTH & THOMAS 1976). The assumption that a cleared forest has a high brightness and a low greenness and a dense forest a high greenness and a low brightness (HEALEY et al. 2005) fits to the presumptions of the C-factor. The DI is calculated by combining normalized Tasseled Cap values (HEALEY et al. 2005):

$$DI = \frac{Br - Br_\mu}{Br_\sigma} - \frac{G - G_\mu}{G_\sigma} + \frac{W - W_\mu}{W_\sigma} \quad (4.23)$$

where Br is Brightness, G Greenness and W Wetness as defined below, Br_μ , G_μ and W_μ are the mean and Br_σ , G_σ and W_σ are the standard deviations of Brightness, Greenness and Wetness of forest pixels (see below).

The Tasseled Cap transformations (TCT) of Landsat 8 bands are calculated as follows (cf. BAIG et al. 2014):

$$TCT = \sum_{i=1}^3 \left(\sum_{x=2}^7 \nu_{x,i} \cdot B_x \right) \quad (4.24)$$

where B_x is the reflectance of the Landsat 8 bands 2 ... 7 and $\nu_{x,i}$ is the corresponding coefficient for one of the three transformations (Table 4.2).

A third group of values used for the linear modelling of the C-factor is a simple band ratio. Therefore, within a loop, the ratio of all bands from band 2 to band 7 are calculated. Kendall's Tau coefficient (KENDALL 1938) is used to measure the correlation between the band ratios

and the C-factor values of the training data set (see below). The ratio with the highest correlation coefficient will be chosen for further analysis.

Linear models

General linear models are calculated to test the relationship between the C-factor from a training data set with well known C-values and the indices and ratios.

The training dataset contains a total number of 69 ground-truth point samples, of which 37 are classified as *dense forest* and 32 as *bare ground* (C-factors 0.002 and 1.000; cf. EL-SWAIFY et al. 1982). These samples are visually interpreted Google Earth views, which are drawn using the OpenLayers Plugin (KALBERER & WALKER 2014) in QGIS 2.0.1 *Dufour* (QGIS DEVELOPMENT TEAM 2013). A validation data set is generated the same way; the sample points of both are shown in the Appendix (p. v). The validation data set consists of 28 points classified as *dense forest* and 25 as *bare ground*.

Linear models are calculated using the *Fitting Linear Model* function in R (R CORE TEAM 2012). A visual interpretation of residual vs fitted values, a Scale–Location plot, a Normal Q–Q plot, a plot of the square root of the model residuals against the fitted values and a plot of Cook’s distance against leverage are used to test the model assumptions. In the case the models do not meet the assumptions of normal distribution of the residuals and homoscedasticity, the response variable *C-factor* is Box–Cox transformed (BOX & COX 1964). For predicting the C-factors of the entire grid, the values will be transformed again if $-1 \geq \lambda < 0.5$. Otherwise, no re-transformation is necessary (THOME 2005). The prediction of C is based on the regression equation given by the linear model.

The estimated C-factor grid is reclassified in a last step. C-factor values below 0 and above 1 are not possible by definition, so all values less than 0.002 are set to 0.002 (*dense forest*) and all values above 1 to 1.000 (*bare ground*).

4.1.4 Topographic factor (LS)

The dimensionless topographic factor (LS) of the RUSLE3D is calculated using the approach of MITASOVA et al. (1996). In contradiction to the original version of the USLE (WISCHMEIER & SMITH 1978), this approach is based on upslope contributing area instead of slope length. Upslope contributing area is defined as flow accumulation per unit contour width (MITASOVA et al. 1996)—i. e., the length of the uphill pathes of converging flow (DESMET & GOVERS 1997). In a grid-based algorithm, a unit contour width equals the resolution of the DEM. The original USLE’s LS-factor is the ratio of soil loss from the area under investigation to the standard plot from a length of 22.13 m and a slope of 9% (WISCHMEIER & SMITH 1978).

LS is here a function of slope length and slope angle:

$$LS = \left(\frac{\lambda}{\lambda_0} \right)^m (65.41 \sin^2 \beta + 4.56 \sin \beta + 0.065) \quad (4.25)$$

where β is the slope angle in percent rise over run, λ is the slope length in feet, $\lambda_0 = 72.6 \text{ ft} = 22.1 \text{ m}$ is the length of the standard plot and m is a dimensionless parameter, which in itself depends on the slope angle and is 0.5 for a slope angle of 5.0% or more, 0.4 for slopes of 3.5% to 4.5%, 0.3 for slopes of 1.0% to 3.0% and 0.2 for slopes of less than 1.0%.

MITASOVA et al. (1996) modified the equation based on the unit stream power theory (MOORE & BURCH 1986a) to incorporate flow convergence and replaced λ by A_{cont} to calculate the modified LS -factor of a grid cell r :

$$LS_r = (m + 1) \left(\frac{A_{cont}}{\lambda_0} \right)^m \left(\frac{\sin \beta}{\beta_0} \right)^n \quad (4.26)$$

where $\beta_0 = 9\% = 5.14^\circ$ is the slope of the standard plot, $\lambda_0 = 22.13 \text{ m}$ is the slope length of the standard plot, A_{cont} is the upslope contributing area in metre and $m = 0.1$ and $n = 1.3$ are dimensionless parameters, adapted to a high vegetation cover and the absence of a rill network during field work (cf. MITASOVA et al. 1996; HOFFMANN et al. 2013).

An ASTER Global Digital Elevation Model V002 (30 m resolution; NASA AND JAPAN ASTER PROGRAM 2011) and a SRTM DEM (90 m resolution; UNITED STATES GEOLOGICAL SURVEY (USGS) 2012) are used to calculate upslope contributing area and slope in RSAGA (BRENNING 2008) an interface between the statistic software R (R CORE TEAM 2013) and SAGA GIS (System for Automated Geoscientific Analyses; BÖHNER et al. 2006; CONRAD 2006).

DEM preprocessing

A Multi Direction Lee Filter, an enhanced version of Lee's Sigma Filter (LEE 1983), is applied in a first step to reduce speckled noise and outliers of the DEMs. The advantage of this algorithm is that noise is detected and reduced without reducing the terrain information; narrow valleys, linear information and slopes will be preserved (LEE 1983). The original Sigma Filter is based on the assumptions that noise of an image follows a Gaussian distribution and is not correlated to the neighbouring pixel values. The filter algorithm relies on local statistics; values exceeding the prior local variances are not included in the posterior means of the filtered image (LEE 1983). In SAGA GIS, a Multi Direction Lee Filter is implemented which applies a Sigma Filter on the directional neighbourhood with minimum variance (LEE

et al. 1998). The 16 possible neighbourhoods are shown in SELIGE et al. (2006). For estimated relative and absolute noise as well as for weighting, RSAGA defaults are used.

In a second step, sinks are filled in the filtered DEM to avoid flow to artificial depressions in the DEM. For a better representation of the stream network in the Mefou subcatchment, a stream grid, which is based on rasterized stream lines from a topographic map (1:50 000; INSTITUE GÉOGRAPHIQUE NATIONAL 1956), is burned into the DEM ($\epsilon = 1.5$ m).

The fill algorithm used here is the technique developed by WANG & LIU (2006), which uses spill elevation and low-cost paths to fill depressions. Spill elevation is defined as the minimum elevation which is necessary to compute a depressionless grid. The technique starts at a border cell of a grid and progressively tests if the flow of each grid cell is connected to the border. If not, the value of the cell will be raised to spill elevation. A least-cost search is applied to find the flow direction of each grid cell (WANG & LIU 2006). The Wang-and-Liu-algorithm implemented in RSAGA slightly modifies the spill elevation using a minimum slope of each grid cell (0.01°) to avoid areas without flow.

Computation of LS

The preprocessed DEMs are used to calculate the two input variables of MITASOVA et al.’s LS-factor.

A slope grid is calculated according to the method of ZEVENBERGEN & THORNE (1987), which is based on the 2nd degree polynomial adjustment. This method is recommended by GARCIA RODRIGUEZ & GIMENEZ SUAREZ (2012) among others to be used in USLE-family erosion models.

Flow accumulation (or: catchment area, upslope area) is calculated using both Multiple Flow Direction (MFD; FREEMAN 1991; QUINN et al. 1991 and Deterministic infinity (D_∞ ; TARBOTON 1997). The results are used to evaluate the influence of algorithm selection on the LS-factor. Algorithms based on single flow, e. g. Deterministic 8 (D8) (O’CALLAGHAN & MARK 1984) or Rho8 (FAIRFIELD & LEYMARIE 1991), are not used due to their limited representation of real flow patterns and the overrating of grid cells with slightly higher elevation (SEIBERT & MCGLYNN 2007). This is especially important when working with filled DEM, where the spill elevations of neighboring grid cells have low differences.

As D8 and Rho8, D_∞ is principally based on a single flow direction. But in contrast to the first mentioned algorithms, flow direction is not considered to be from one center of a grid cell to another center, but defined as the “steepest downward slope on planar triangular facets on a block-centered grid” (TARBOTON 1997). The flow direction can be everything between

0 and 2π , considering that $0, \pi/2, \pi$ and $3\pi/2$ are the cardinals and $\pi/4, 3\pi/4, 5\pi/4$ or $7\pi/4$ are the diagonals of a rectangle drawn between the centers of the eight neighboring cells.

The flow accumulation to the i th downhill grid cell is calculated as a proportion of flow between two downslope pixels. The proportion is the proximity of the flow direction angle to the direction angle of the grid cell center (TARBOTON 1997):

$$A_i = \frac{\alpha_2}{(\alpha_2 + \alpha_1)} \cdot A_{i-1} \quad (4.27)$$

where A_i is flow accumulation of the i th downhill grid cell, A is the flow accumulation of the upslope grid cell, α_1 and α_2 are the angle between the flow direction and the verticals of the triangular facets in flow direction.

Thus, flow dispersion to two of eight neighboring pixels is possible (for a detailed description of the procedure see TARBOTON 1997).

The MFD-algorithm is based on the principal that the outflow of an uphill cell is distributed to all of the eight neighboring downhill cells with lower elevation (FREEMAN 1991). The proportion distributed to each cell is a function of the slope angle between an uphill and a downhill cell ($\tan \beta$) and the effective contour length of the flow direction (L_i), which depends on whether the flow direction is cardinal or diagonal. The amount of flow accumulation in the i th downhill cell (A_i) is (QUINN et al. 1991):

$$A_i = \frac{(\tan \beta_i \cdot L_i)}{\sum_{k=1}^8 (\tan \beta_k \cdot L_i)} \cdot A_{i-1} \quad (4.28)$$

Computation in SAGA GIS starts at the grid cell with the highest value and is done parallelly downwards (SAGA module: *Catchment Area [Parallel]*).

Using the output grid of both algorithms, upslope contributing area (A_{cont}) is calculated by dividing the grid values with the grid cell size. LS is then computed as described in Equation 4.26.

4.2 Net deposition areas

Both USLE, and RUSLE/RUSLE3D calculate only net erosion—also on areas experiencing net deposition. To avoid the problem of an overestimation of total soil loss, deposition areas are identified using a topographic erosion/deposition index, which is based on the transport capacity limited Unit Stream Power Erosion Deposition (USPED) model (MITASOVA et al.

1996; MITAS & MITASOVA 1998):

$$ED = d(T \cdot \cos \psi) / dx + d(T \cdot \sin \psi) / dy \quad (4.29)$$

where ED is erosion or deposition, $T = A$ is the soil loss modeled with the RUSLE3D and ψ is the terrain aspect.

The derivatives are calculated with a slope algorithm in a GIS (MITASOVA & MITAS 1999; HOFIERKA et al. 2009). Rainfall erosivity, soil erodibility and cover/crop management, T can be replaced by the topographic factor of the RUSLE3D to consider only the topographic potential (HOFIERKA et al. 2009):

$$ED_{LS} = d(1.4 \cdot L \times S \cdot \cos \psi) / dx + d(1.4 \cdot L \times S \cdot \sin \psi) / dy \quad (4.30)$$

Here, $L \times S$ is calculated with the parameters used in MITASOVA et al. (1996):

$$L \times S = \left(\frac{A_{cont}}{22.13 \text{ m}} \right)^{0.4} \times \left(\frac{\sin \beta}{5.16^\circ} \right)^{1.3} \quad (4.31)$$

4.3 Simulations

For managing purposes in the context of IWM—or more specific water management—the simulation of the effect of future land use and land cover changes (LULCC) on the environment is a well known tool (DEKKERS & KOOMEN 2007; HEATHCOTE 2009). Based on modeled soil loss and the NDVI-approximated C-factor, the effect of five LULCC-scenarios on soil losses is simulated in the thesis on hand. Maps will be drawn which highlight areas of high expected impact. A change of the C-factor corresponding to the LULCC is used as simulation input. All other values and factors (R, K, LS, P) are kept constant (cf. NEARING et al. 2005; TERRANOVA et al. 2009); possible changes of soil erodibility as a result of a changed cover or soil conservation strategies are not taken into consideration.

Scenario 1: Mixed-cropping extensification In Scenario 1, it is assumed that—possibly driven by a higher demand for food for a growing population in rural or periurban areas—food production in the area is expected to increase by forest clearance or a cultivation of bush or fallows. The expansion of mixed-forest systems and the associated deforestation is described—at least as an ongoing process—by IMBERNON & BRANTHOMME (2001) and LAMBIN et al. (2003) for tropical rainforests in central Cameroon. In addition, SUNDERLIN et al. (2000) (cf. SAYER et al. 2012) note that the intensification of food crops is a strategy to

cope with an economic crisis. As it is described in Section 3.4, field covers a higher proportion of the land around dense settled areas. The scenario is implemented in a soil erosion model by a change of the C-factor from 0.001–0.01 to 0.23 (**Scenario 1a**) and from 0.01–0.10 to 0.23 (**Scenario 1b**). C-factors 0.001–0.01 are typical for dense forest, well established dense bush and natural savanna-like vegetation. Values from 0.001 to 0.01 are typical values for forests in the area (ROOSE 1977; EL-SWAIFY et al. 1982; NILL et al. 1996); a C-value of 0.23 is typical for mixed cropping systems in the area of Yaoundé (NILL et al. 1996). The range from 0.01 to 0.10 covers spars bush and short time fallows (NILL et al. 1996).

Scenario 2: Mono-cropping intensification The second scenario takes account of the intensification of cropping, i. e. mixed-cropping systems will change to cassava or maize mono-cropping. Thus, C-factor inputs for erosion modelling are changed from 0.18–0.28 to 0.36 (EL-SWAIFY et al. 1982; NILL et al. 1996). As in Scenario 2, the intensification might be caused by economical problems (SUNDERLIN et al. 2000; SAYER et al. 2012) and the general trend to more intensive crop production for the food supply of Yaoundé (cf. KOTTO-SAME et al. 1997).

Scenario 3: More cash crops In addition to an intensification of food production, also the production of cash crops might increase. In Scenario 3 it is therefore assumed that forest or dense shrub is converted to plantations—either to coffee, cacao or palm oil plantations for cash food production or to plantains for food production. C-factors are accordingly changed from 0.001–0.01 to 0.06 (EL-SWAIFY et al. 1982; NILL et al. 1996) to simulate the extensification of cash crop production.

Scenario 4: Forest regrowth The last scenario simulates the erosional impact of reforestation measures; C-factors from 0.18 to 0.41 (mixed-cropping systems or monocropping) are converted to 0.01 (forest/bush).

4.4 Semi-quantitative validation

Validation approaches of soil erosion models include field mapping of erosion features, remote sensing, erosion plots, radioactive isotopes such as Cs-137, measurement of river sediment load and reservoir siltation measurements (cf. BORRELLI 2011). Due to the fact that most of the methods are too time consuming and/or too expensive for the scale of the study at hand, a reservoir sedimentation study is applied to validate the erosion model, which was encouraged by the release of the Mefou Reservoir during field work in 2012.

The reservoir sedimentation study is based on two main input variables namely sediment volume and trap efficiency (VERSTRAETEN & POESEN 2002). The sediment volume is estimated by the following equation:

$$\text{sediment volume} = \text{reservoir surface area} \times \text{thickness} \times \text{bulk density} \quad (4.32)$$

Reservoir surface area is calculated with a Geographical Information System, sediment thickness was measured during field work and is averaged for calculation and typical values of sediment bulk density are taken from the literature.

Sediment mass has to be set in relation to the operation time of the reservoir, the catchment area and the trap efficiency of the reservoir (cf. VERSTRAETEN & POESEN 2002):

$$SSY_r = \text{sediment mass} \times 1/\text{catchment area} \times \text{trap efficiency} \quad (4.33)$$

where SSY_r is the area specific sediment yield in the reservoir.

Trap efficiency is approximated using the Brown curve (BROWN 1943) as used in MORRIS (1998) and VERSTRAETEN & POESEN (2000), which is more easy to apply for metric units without conversion. In the Brown curve, trap efficiency is a function of the catchment–capacity ratio.

To validate the model, SSY_r is compared with the area specific sediment yield of the catchment (SSY_c), which is calculated as a function of the proportion of erosion from slopes and settlements/roads (empirical values from literature), the modelled gross erosion (E) and the sediment delivery ratio (SDR), also taken from literature.

SDR expresses the percentage of erosion which is not stored in the catchment in wetlands, floodplains, on fields, in bufferstripes, in topographical depression or on foodslopes.

$$SSY_c = SDR \times A \times \text{proportion of field erosion} \quad (4.34)$$

Due to the fact that values from literature are not site specific, a set of normal distributed values is used for sediment bulk density, SDR and the proportion of erosion from fields (means and standard deviation are the means and standard deviation of all literature values used).

4.5 Statistics and reporting of figures

Mean, standard deviation, range, quartiles, maximum, minimum and ranges are reported as described in statistics textbooks (BAHRENBURG et al. 2010). Means are always reported plus/minus their standard deviation ($\bar{x} \pm s$). The standard error of the mean (SEM) is

calculated by dividing the standard deviation of a sample by the square root of the sample size. Outliers are eliminated applying the procedure descriptive in BAHRENBURG et al. (2010): A value i is not used for further calculation or descriptive statistics if the value does not fit in the range of the mean of the sample without the proposed outlier plus/minus the fourfold standard deviation of the sample's mean. Due to the fact that there is no standard procedure to describe significant figures, an approach based on the SEM is used here: A figure of a mean is considered to be significant if the same figure of the mean's SEM is non-zero. For some indices or values, is common to report two digits (e.g. NDVI). In this case—although the first/second digit is not significant—two digits are reported, but the last significant figure is emphasized with an underscore (e.g. a mean NDVI-value 0.52 is reported as 0.52 if SEM=0.11). A figure of measured values is only significant if the correction of a value by its error obtained from the measurement of a standard sample would not completely change the information of that figure.

Test statistics are used to test for difference of sample means. A *t-test* is used if the two samples are normally distributed and the variances are homogeneous; a *Wilcoxon-rank-sum-test* (WILCOXON 1945; MANN & WHITNEY 1947) is used if the two samples are not normally distributed, but variances are homogeneous. (Other cases didn't appear.) To test for normal distribution, a *Shapiro-Wilk test* (SHAPIRO & WILK 1965) is used; homogeneity of variances is tested using a *Levene Test* (LEVENE 1960) for non-normal distributed values and a *F-test of Equality of Variances* for normal distributed values (CORNILLON et al. 2012). The computation of the RUSLE3D is completely done in R; for the scripts of the model see the DVD-appendix.

4.6 Computation

All statistics are computed using R (R CORE TEAM 2013). Except of the Levene test (`levene.test`), all statistics and tests are part of the base version of R. Default setting as proposed in R are kept. Image processing, handling and analysis is done in R. A list of packages is given in Table 4.3. Maps are prepared with QGIS 2.0.1 *Dafur* (QGIS DEVELOPMENT TEAM 2013). Plots are drawn in R (Table 4.3). Other Figures as well as maps are finally drawn in *Inkscape* 0.48.4 (ALBERT et al. 2013).

Table 4.3: Packages used in R (R CORE TEAM 2013) for data processing and graphical or tabular output.

Package	Description	Reference
landsat	preprocessing of landsat imagery (image-based radiometric correction)	GOSLEE 2011
raster	reading, writing, manipulation and analysis of grid based data	HIJMANS 2013
rgeos	vector geometry (shapefiles)	BIVAND & RUNDEL 2013
shapefiles	handling of shapefiles	STABLER 2013
sp	handling geospatial data in R	PEBESMA & BIVAND 2005; BIVAND et al. 2013b
rgdal	handling of geospatial data	BIVAND et al. 2013a
stringr	handling of strings (manipulation of Beckman Coulter data)	WICKHAM 2012
RSAGA	SAGA GIS interface for R	BRENNING 2008
car	Levene test	
plotrix	making nice plots using R	LEMON 2006
xtable	export of data frames from R to LaTeX	DAHL 2014

5 Results

5.1 Rainfall erosivity

Rainfall erosivity in the Upper Mefou subcatchment is estimated using different approaches and data sets. In Table 5.1 the mean annual R-values of Nkolbisson and Yaoundé are shown. The R-values differ clearly. For Nkolbisson, the highest R-value ($15\,658 \text{ MJ mm ha}^{-1} \text{ h}^{-1} \text{ yr}^{-1}$) is calculated using the approximation of BRESCH (1993); the lowest value ($10\,015 \text{ MJ mm ha}^{-1} \text{ h}^{-1} \text{ yr}^{-1}$) is calculated using the daily regression for Nigeria (SALAKO 2008). The value range of ROOSE (1977) is 12 259–14 983. The data of the climate station in Yaoundé are quite similar to those of the station in Nkolbisson, with one exception: While the mean annual R-value using the approach of DIODATO et al. (2013) is 10 033 for Nkolbisson, the R-value for Yaoundé is 13 766.

The standard error of the mean (SEM) of the Yaoundé-values is much smaller, due to the fact that a large data set is used for the calculation. Also the SEMs of the models differ. For the approach based on the Modified Fournier Index and BRESCH’s regression, the error is relatively high, while the error is clearly smaller when applying the approaches of ROOSE (1977) or SALAKO (2008). Due to a higher variability in the daily data set, the error using the SALAKO (2006)-approach is higher than the regression based on annual data.

For further calculations—either the seasonal fluctuation of rainfall erosivity or soil loss—the Foster–Brown-based daily erosivity model of SALAKO (2008) will be used for two reasons: Firstly, models based on daily data sets are more reliable (see Section 6.3.3; ANGULO-

Table 5.1: R-factor values calculated on the basis of different algorithms (* rainfall kinetic energy EL_{30} acc. to WISCHMEIER & SMITH 1978, † EL_{30} acc. to BROWN & FOSTER 1987)

Algorithm/Author	R-values [$\text{MJ mm ha}^{-1} \text{ h}^{-1} \text{ yr}^{-1}$]	
	Yaoundé	Nkolbisson
P_a , ROOSE 1977	12 178–14 884	12 259–14 983
MFI , ARNOLDUS 1980	11 729	12 626
P_a , BRESCH 1993	15 528	
$ARESED$, DIODATO et al. 2013	13 766	10 033
P_a , SALAKO 2006*	14 469	14 111
P_a , SALAKO 2008†	13 999	14 610
P_d , SALAKO 2006*	–	10 015
P_d , SALAKO 2008†	–	12 579

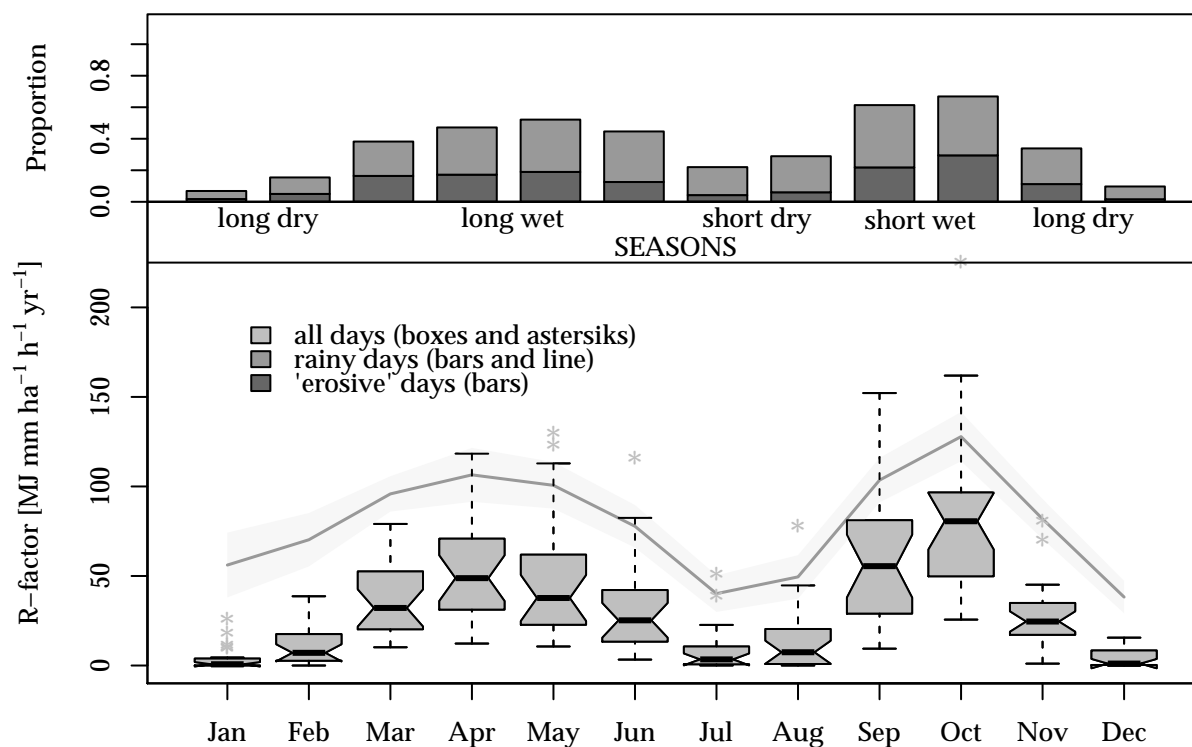


Figure 5.1: Annual cycle of rainfall erosivity calculated using the approach of SALAKO 2010 on the basis of daily values from Nkolbisson. The upper plot shows the percentage of rainy days and days with rainfall totals >12.7 mm (WISCHMEIER & SMITH 1978), the lower plot shows daily rainfall erosivity of each month in the years 1952–1980; boxes include dry days, while lines (mean) and shades (standard error of the mean) include only rainy days.

MARTÍNEZ & BEGUERÍA 2009) and allow the calculation of seasonal erosivity; secondly, these R-values fit very well to the wide range of the ROOSE-approach, what is not true for all approaches.

The seasonal variation of the R-values is shown in Figure 5.1. The barplot shows the frequency of rainy days ($P_d > 0.1$ mm) and *erosive* days ($P_d > 12.7$ mm; cf. ANGULO-MARTÍNEZ & BEGUERÍA 2009); the boxplots show the mean daily R-values in each month. The line indicates the seasonal variability of the R-factor of rainy days. December, January and February in the long dry season and July and August in the short dry season are the months with the lowest mean daily R-values.

In March to June and September and October mean daily R-values are much higher. The dispersion of mean daily R-values varies with the month. There are some years with high mean daily R-values in the wet seasons, but also months with low values. Variability is much smaller in the dry seasons, especially in January. The highest mean daily R-value is calculated for October. In the short wet season, the proportion of rainy days is around

Table 5.2: Monthly mean of daily rainfall erosivity [MJ mm ha⁻¹ h⁻¹ yr⁻¹]

	Jan	Feb	Mar	Apr	May	Jun	Jul	Aug	Sep	Oct	Nov	Dec	Mean
Rainy day	2.4	3.7	5.4	5.9	4.9	3.6	1.6	2.0	5.4	7.4	4.1	1.5	4.12±1.15
Erosive day	7.3	7.2	7.4	10.2	8.8	9.2	6.9	7.9	9.7	9.7	8.2	7.7	8.27±1.79

three third (September: 61%, October: 67%); in January, only 7% of the days are rainy, in December only 10% are rainy. R-values of rainy days are higher in the short than in the long rainy season, as it is the case for mean daily R-values of all days. Erosive days are the most frequent in Mai (19%) September (22%) and October (29%), whereas they are seldom in January (2%), December (2%) and July (4%). In the long rainy season—except of June—and the short rainy season, more than one third of the rainy days are erosive days. In October, 44% of the rainy days are erosive days. Although January is the month with smallest proportion of rainy days and low mean daily R-values, the R-values on rainy days are relatively high (Table 5.2). Months with a high mean erosivity and a high proportion of rainy or erosive days have also a higher erosivity of the rainy days. Erosive days of these month are considerably less pronounced more erosive. Erosivity of erosive days in the long dry season is not clearly less than in some months of the long wet season (Table 5.2).

5.2 Soil erodibility

Organic matter

The measured organic matter content of 46 samples ranges from 1.6% to 9.4% with a mean of 5.2 ± 1.8 pp. The highest OM values are measured on a fallow, a forest with intergrowing oil palms, on a cacao plantation and on a mixed plantain–palm plantation (samples Nk13, NK26, Nk22 and Nk7). In contrast, samples with low OM values (<3%) are from maize–groundnut fields (Nk35), from mix-cropping fields with cassava as main plant and sweet potato or Macabo as second plants (Nk11 and Nk36) or from a recent cassava fallow (Nk28). A t-test¹ of equal means shows that plantations and forest/bush have a significantly higher mean organic matter content than fields; mean %OM of fields is 4.2, while the mean of plantations is 6.5 and the mean of forests is 6.6. The means of other combinations of land use types (fallow, field, forest and plantation) are not significantly different; the mean %OM of fallows is 5.4. The samples with a low OM content were collected around the Mefou Reservoir or in the urban parts of the Upper Mefou subcatchment.

¹deviance of %OM from normal distribution is rejected using a Shapiro–Wilk test ($W=0.98$, $p>0.1$); homogeneity of variances is confirmed with a F-test ($F_{3-14,4-5}=0.3889-1.7446$, $p>0.38$)

Permeability

Range and dispersion of permeability is very wide. The minimum value is ca. $0.016 \cdot 10^{-3} \text{ cm s}^{-1}$, measured in a forest with palms on a sandy loam. The maximum value of $3.290 \cdot 10^{-3} \text{ cm s}^{-1}$ is measured on a tomato field (Nk3: sandy loam). The mean permeability value is $0.5 \pm 0.6 \cdot 10^{-3} \text{ cm s}^{-1}$. For the use in the RUSLE, the values are classified in six permeability classes according to the National Soil Survey Handbook (NSSH) No. 430 (USDA 1983; RÖMKENS et al. 1997). The majority of soils under investigation are classified as moderate, moderate to rapid or slow to moderate infiltrating. Two soils are classified as rapidly infiltrating, while five soils, mainly covered with semi-natural vegetation or plantations, are classified as very slow infiltrating. As it is shown in Figure 5.2, conductivity of a soil is a function of land use and land cover.

Forest and bush soils have the lowest conductivity, while conductivity is higher on plantations and fallows. The highest values are measured at fields, where the dispersion of the values is very high; both relatively low values and high values are measured. The mean permeability of fields and forests or of fields and plantations differ significantly (Wilcoxon rank-sum test, $W=70$ or $W=95$, $p<0.05$)². The means of fields and fallows and fields, forests and plantations and forests and plantations do not significantly differ ($W=12-19$, $p>0.05$). On five fields with ridge tillage, infiltration was tested on the ridges and on the pathes between the ridge. Conductivity values are up to ten times higher on ridges at three sides. In contrast, on two ridges conductivity is up to twice lower in comparison with the intermediate path. The mean conductivity on ridges is $0.66 \cdot 10^{-3} \text{ cm s}^{-1}$, whereas the mean conductivity on the intermediate paths is $0.32 \cdot 10^{-3} \text{ cm s}^{-1}$. In relation to the high dispersion of the conductivity values ($\bar{x} = 0.5 \pm 0.6 \cdot 10^{-3} \text{ cm s}^{-1}$) and the range of values as shown in Figure 5.2, neither values on ridges ($0.3-1.27 \pm 0.6 \cdot 10^{-3} \text{ cm s}^{-1}$) nor values on intermedia pathes ($0.03-0.66 \pm 0.6 \cdot 10^{-3} \text{ cm s}^{-1}$) are—except of one value—extraordinary high or extraordinary low.

Grain size

The grain size of 38 samples is measured using laser diffraction. Except of a few samples, all grain size distributions have a similar shape. Sample Nk26 shows differences between the first and the second run, but mean values seem to be similar to the other results. Three

²Conductivity values differ significantly from normal distribution (Shapiro–Wilk test, $W=0.643$, $p<0.05$); the permeability- variances of the land use and land cover types are homogeneous (Levene's Test for Homogeneity of Variance, $F_{3,29}=1.07$, $p>0.05$). Thus, the Wilcoxon test is applied here

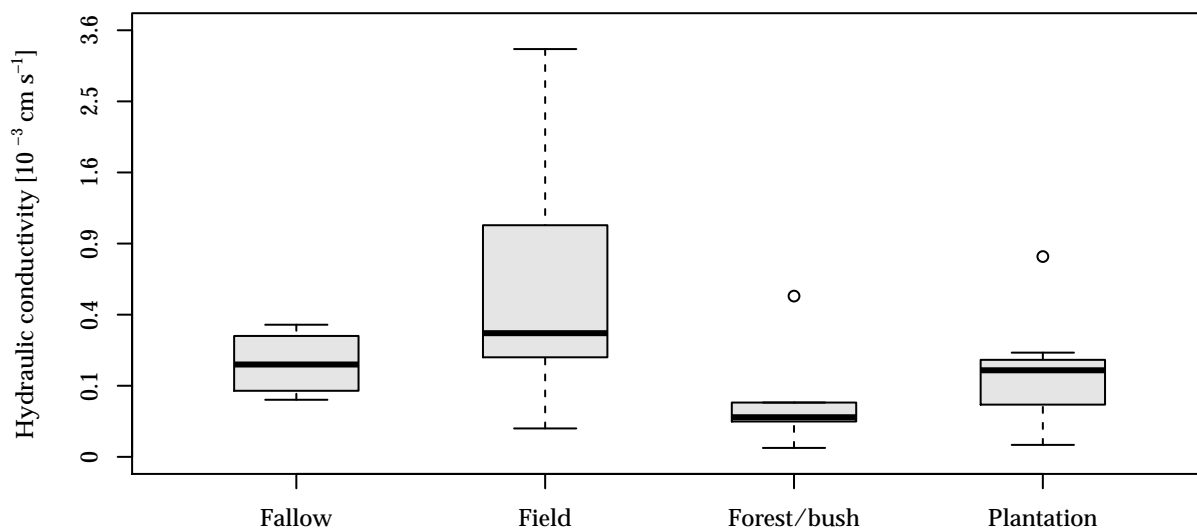


Figure 5.2: Infiltration rates on different land use types. Note the non-linear scaling of the y-axis.

samples (Nk8, Nk18, Nk10F) have an extraordinary high content of fine silt (2–20 μm). The mean grain size distribution and the dispersion of sizes are shown in Figure 5.3.

An average sample contains 11% clay, 22% silt and 67% sand, whereas the most frequent grain size separate is medium sand (21%), followed by fine sand (19%) and coarse sand (18%).

The variability between the samples is relatively low in the clay fraction and the coarse silt to fine sand fractions, while in the fine silt fraction and especially in the medium and coarse sand fraction, the deviation is high (Figure 5.3, grey shadow). Descriptive grain size statistics are calculated for the mean grain size of all samples following the approach of FOLK & WARD (1957). The mean grain size (M_z) is 0.235 mm, physically described as the fine sand separate; the inclusive graphical standard deviation of the grain size distribution is 0.265 mm. $D_{10} = 2.000$ mm, $D_{50} = 0.161$ mm and $D_{90} = 0.653$ mm are quantiles of the cumulative curve of the mean grain size.

For a RUSLE-based erosion model, modified sand (sand without very fine sand) and modified silt (silt and very fine sand) are the relevant grain size separates, which are used to calculate the erodibility factor K. Modified sand is the most dominant separate, with a mean proportion of 60%. Most of the samples contain between 50 and 60% or 60–70% modified sand (41% or 28% of the samples). The mean content of modified silt is around 29%; 50% of the samples contain 20–30% modified silt, 35% contain 30–40%.

79% of the soils under investigation are classified as sandy loams, 13% as loamy sands, 7% as loam and 5% as silt loam according to the USDA classification system.

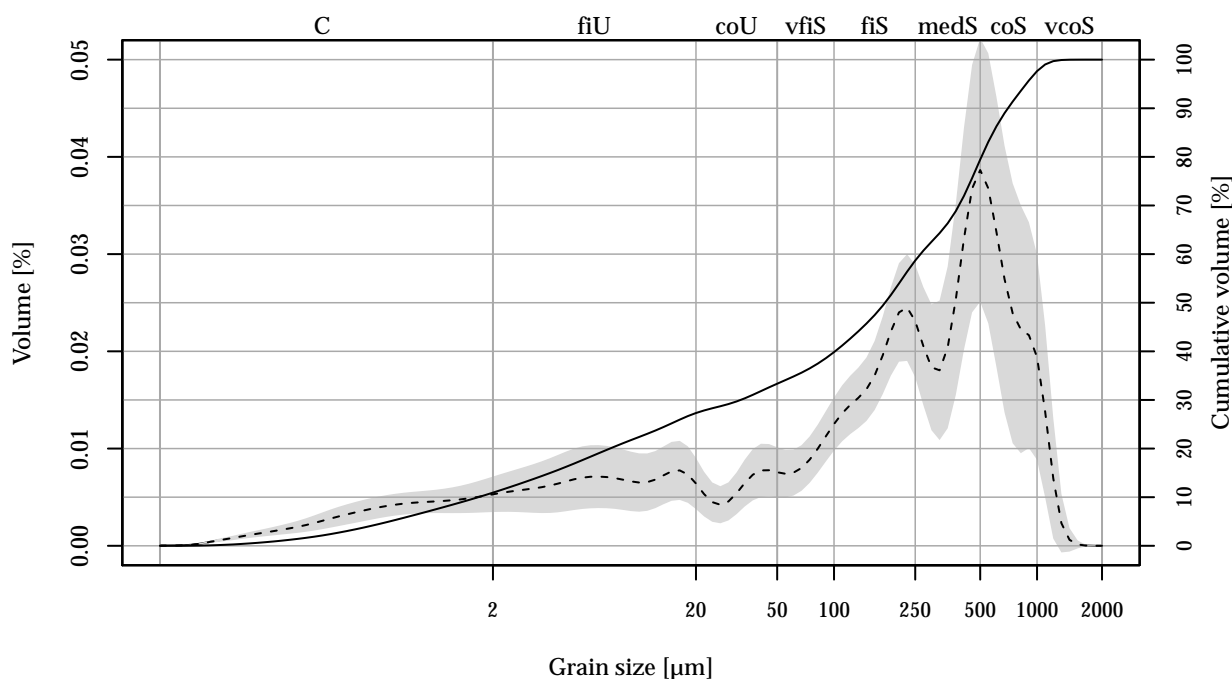


Figure 5.3: Averaged grain size distribution of all samples analysed. The grey shadow marks the standard deviation of the mean. The USDA grain size separates are used for classification (second x-axis, SOIL SURVEY DIVISION STAFF 1993): C is clay, fiU is fine silt, coU is coarse silt, vfiS is very fine sand, fiS is fine sand, medS is medium sand, coS is coarse sand and vcoS is very coarse sand.

Structure

The structure of the coarse soil aggregates was taken down during field work. According to the USDA classification system used for the RULSE's K-factor approximation (USDA 1951), all samples are classified as soil structure class 3 (medium structure). The block-like aggregates of the soil samples are described as medium subangular blocky (10–20 mm). The more spheroidic aggregates are as well classified as of a medium soil structure, due to a medium granular or crumb structure (2–5 mm).

Erodibility

Erodibility factor values are calculated for 36 samples from 33 sites, where all necessary parameters are available for calculation. The results of all samples are shown in Table 5.3; in Figure 5.4 the results are plotted in relation to the input parameters. The most frequent K-values groups are 0.015–0.020 and 0.025–0.030 $\text{ton acre h } 100^{-1} \text{ acre}^{-1} \text{ ft}^{-1} \text{ tonf}^{-1} \text{ in}^{-1}$ (9 and 12 samples in each of the groups). For one site, a K-value lower 0.010 is estimated, whereas three samples have an approximated K-value greater than 0.035; one of these has values greater than 0.040. The mean K value is 0.023 ± 0.007 ; the values range from 0.009

Table 5.3: K-values and input parameter for all samples. Soil structure class s is not printed because it is constant ($s=3$). OM is organic matter, Ks is hydraulic conductivity, p is the permeability class, modS is modified sand (250–2000 μm), modU is modified silt (2–250 μm), U is silt (2–100 mm), AGG is the fraction of aggregates 200–630 mm, and K_{trop} is the tropical K-value according to NILL (1993).

ID	OM [%]	Ks [in hr^{-1}]	p	modS [%]	modU [%]	U [%]	AGG [%]	K [SI]	K [US]	K_{trop} [US]	K_{trop} [SI]
Nk1	7.7	1.567	2	57	32	26	24	0.011	0.09	0.09	0.012
Nk10F	3.5	0.652	3	40	49	43	62	0.038	0.29	0.31	0.041
Nk10N	5.7	1.522	2	55	32	24	27	0.016	0.12	0.13	0.017
Nk11	2.2	0.233	3	58	29	22	56	0.025	0.19	0.21	0.028
Nk13	7.3	0.035	6	51	33	25	72	0.025	0.19	0.21	0.027
Nk14	2.8	0.158	4	63	26	18	67	0.025	0.19	0.21	0.028
Nk15	4.3	0.179	4	56	30	23	41	0.024	0.18	0.20	0.026
Nk16	5.6	0.305	3	48	37	29	78	0.021	0.16	0.18	0.023
Nk17	3.8	0.583	3	56	32	26	74	0.024	0.18	0.20	0.026
Nk18	6.6	0.091	4	22	66	58	84	0.036	0.28	0.30	0.040
Nk19	3.4	0.569	3	54	31	24	78	0.023	0.18	0.20	0.026
Nk2	2.6	2.686	1	56	30	23	–	0.018	0.14	0.15	0.020
Nk20F	5.0	0.469	3	61	27	20	66	0.018	0.14	0.15	0.020
Nk20N	5.5	0.236	3	61	27	20	65	0.017	0.13	0.14	0.019
Nk22	9.4	0.004	6	68	26	18	34	0.019	0.15	0.16	0.021
Nk23	5.8	0.337	3	67	22	18	56	0.014	0.11	0.12	0.016
Nk24	3.6	1.840	2	61	29	22	44	0.020	0.15	0.17	0.022
Nk26	8.6	0.044	5	73	21	15	74	0.016	0.12	0.13	0.018
Nk27	6.4	0.490	3	71	21	15	57	0.013	0.10	0.11	0.014
Nk28	5.9	0.278	3	77	16	12	62	0.011	0.09	0.09	0.012
Nk3	4.5	4.663	1	61	28	22	44	0.013	0.10	0.11	0.014
Nk30	5.6	0.023	6	69	23	16	65	0.025	0.19	0.21	0.027
Nk31	4.5	0.226	3	72	20	14	53	0.015	0.11	0.13	0.017
Nk33	4.1	0.429	3	69	21	17	–	0.016	0.12	0.14	0.018
Nk35	1.6	0.331	3	45	33	29	49	0.026	0.20	0.22	0.029
Nk36	2.2	0.225	3	61	26	21	66	0.023	0.17	0.19	0.025
Nk37	5.6	0.002	6	72	20	15	53	0.023	0.18	0.20	0.026
Nk38	5.0	0.022	6	65	25	20	61	0.027	0.21	0.23	0.030
Nk39	5.6	0.083	4	67	24	19	28	0.019	0.15	0.16	0.021
Nk4	5.1	1.504	2	56	31	23	50	0.017	0.13	0.14	0.018
Nk42	6.3	0.425	3	57	28	21	58	0.015	0.12	0.13	0.017
Nk6	6.0	0.725	3	52	39	28	60	0.023	0.17	0.19	0.025
Nk7	8.9	1.125	2	57	31	24	32	0.008	0.06	0.07	0.009
Nk8	5.3	0.210	3	36	54	47	77	0.034	0.26	0.29	0.038
Nk9F	4.3	0.159	4	53	33	26	47	0.026	0.20	0.22	0.029
Nk9N	4.4	1.807	2	55	32	25	47	0.019	0.14	0.16	0.021

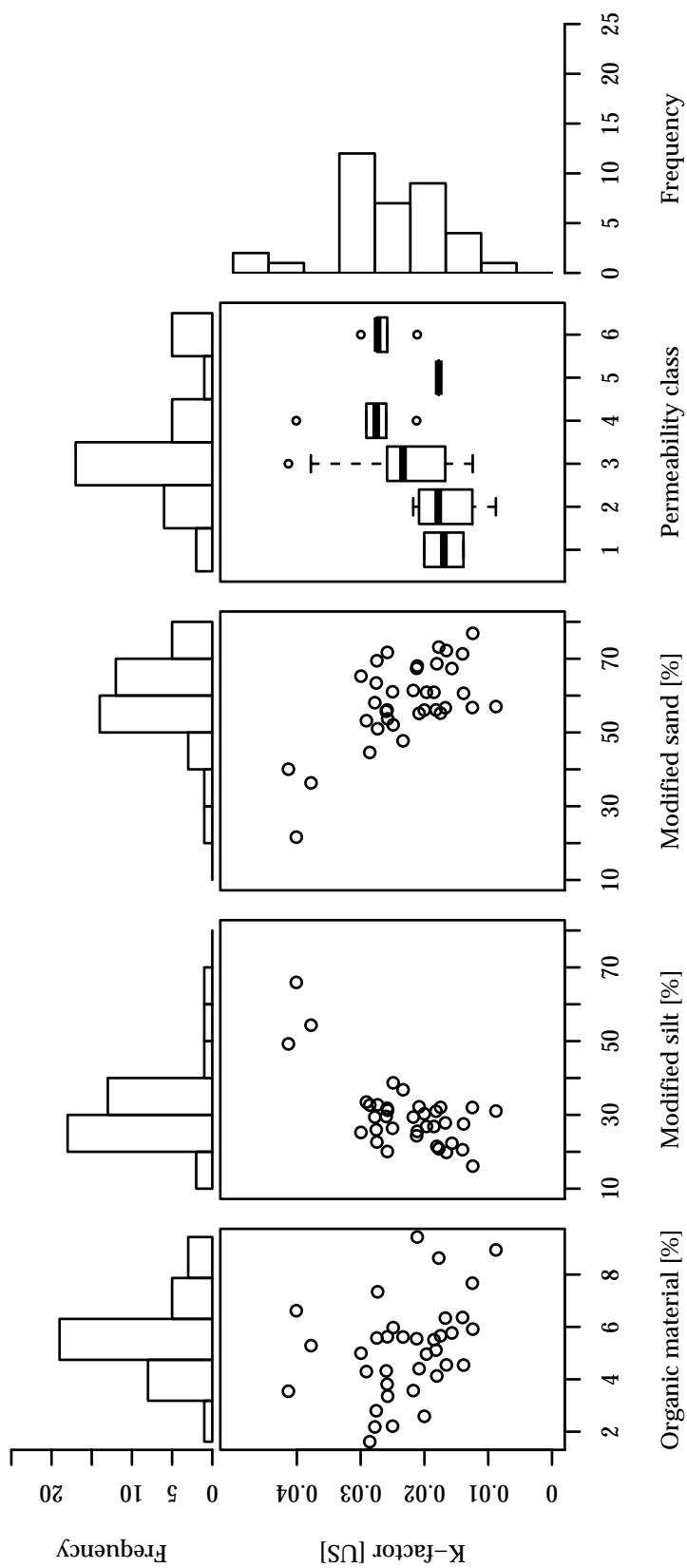


Figure 5.4: Overview on the results of the parameters determining the K-factor in relation to the K-values.

to a maximum of 0.041. Samples with a high content of the modified silt separate and accordingly a low content of modified sand have the highest K-values (Figure 5.4). Those samples with more than 40% modified silt have K-values between 0.033 and 0.040. Sites with a relatively low K-value are characterized by the lowest permeability class 1 and more or less high organic material contents. The samples containing 7% or more percent organic material have K-values less than 0.020. Low-K samples do not show a remarkable tendency to a higher modified sand content (Figure 5.4). Sites with high K-values have more than 50% modified silt—what is remarkably high. But in contrast to the low K samples, these sites are only classified in medium permeability classes (3–4) and have a mean organic matter content (Figure 5.4).

Using the approach of NILL 1993, modified K-values (K_{trop}) are calculated, which are better adapted to tropical conditions. The approach is based on the classification on the soil samples in one of three groups. All samples in the study on hand are classified in group 2 (see Equation 4.15) based on pH, bulk density, %silt and the relative content of 200–630 mm dry-sieved aggregates. As pH values and bulk density in 5–10 cm depth were not measured during field work or in the laboratory, mean values are taken from NILL's study. The proportion of the silt fraction is used as shown in Table 5.3, where also the portions of dry sieved aggregates are given. The portion of the silt fraction ranges from 24% to 84% of air dried sample weights; the mean proportion of the 200–630 mm-aggregates is $56 \pm 23\%$. The high variability in the dry-sieved aggregate content can not be explained by organic matter content, mean grain size or land use and land cover.

Based on the measured values of the soil samples from the Upper Mefou subcatchment and the relations calculated by NILL, the tropical K-value of the present soil samples is linear to the Wischmeier and Smith's erodibility factor with a conversion factor of 1.1 (group 2 of NILL's classification). The values of K_{trop} are listed in Table 5.3.

Interpolated K-values

Although organic matter content and hydraulic conductivity partly show a significant difference between the mean values of four land use types, there is no significant difference between the K-values of the land use types (Wilcoxon rank-sum test); the mean values of the modified silt or modified sand content did not differ significantly. Due to that fact, it is deemed justifiable to use an interpolation method that is not driven by an external drift such as land use.

The K_{trop} -values are interpolated using a Multilevel B-Spline Approximation (MBA) with 4 iterations (i). The number of iterations is tested in loop with 1–8 iterations. Using $i = 4$

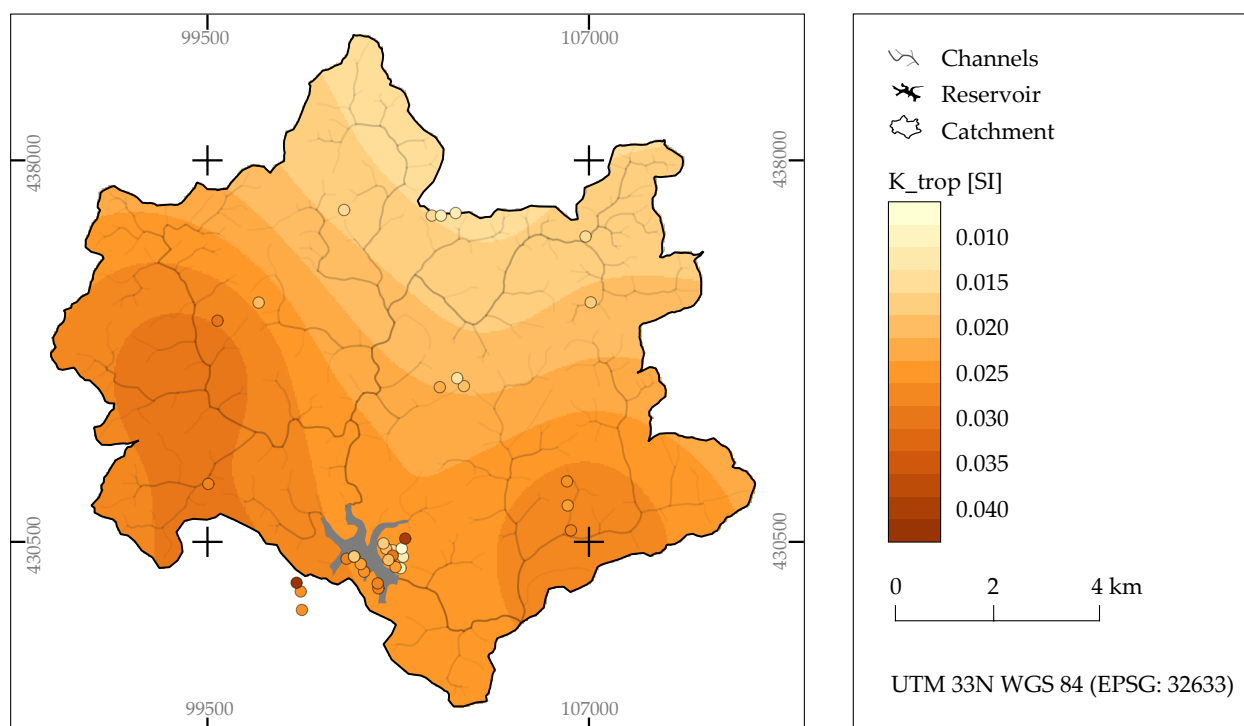


Figure 5.5: Interpolated K_{trop} [t ha h ha⁻¹ MJ⁻¹ mm⁻¹] values using a Multilevel B-Spline Approximation. Coloured bullets (●) mark the location of the soil samples and their K-values.

has the advantage that the whole catchment does not have the same values—what is more or less the case if $i < 4$. Then, also the dispersion of values is much lower than the actual dispersion of the samples. Using more iterations than 4 results in a great heterogeneity in areas with a high density of samples and the interpolation does not give a mean value for that areas.

The western inselbergs of the Upper Mefou subcatchment have the highest interpolated K-values (0.030–0.0325, Figure 5.5). In the southeastern—more or less periurban—areas, the values are as well relatively high. The lowest values are interpolated for the northern areas of the catchment (0.0150–0.0175); there is a general tendency of lower values in the north and higher values in the south. Around the Mefou Reservoir, K-values are on a medium level. In this area, the density of point samples is the highest, with approximated K-values less than 0.010 and more than 0.040.

5.3 Topographic potential

Two derivatives of a Digital Elevation Model (DEM) are used to model the topographic potential of soil loss, the RUSLE3D's LS factor. Catchment area per unit contour width

(contributing area) is shown in Figure 5.6b (slope map: Appendix, p. vi); the multiple flow direction algorithm (MFD) and the deterministic infinity algorithm (D_∞) are used to calculate contributing area for both an ASTER and a SRTM DEM.

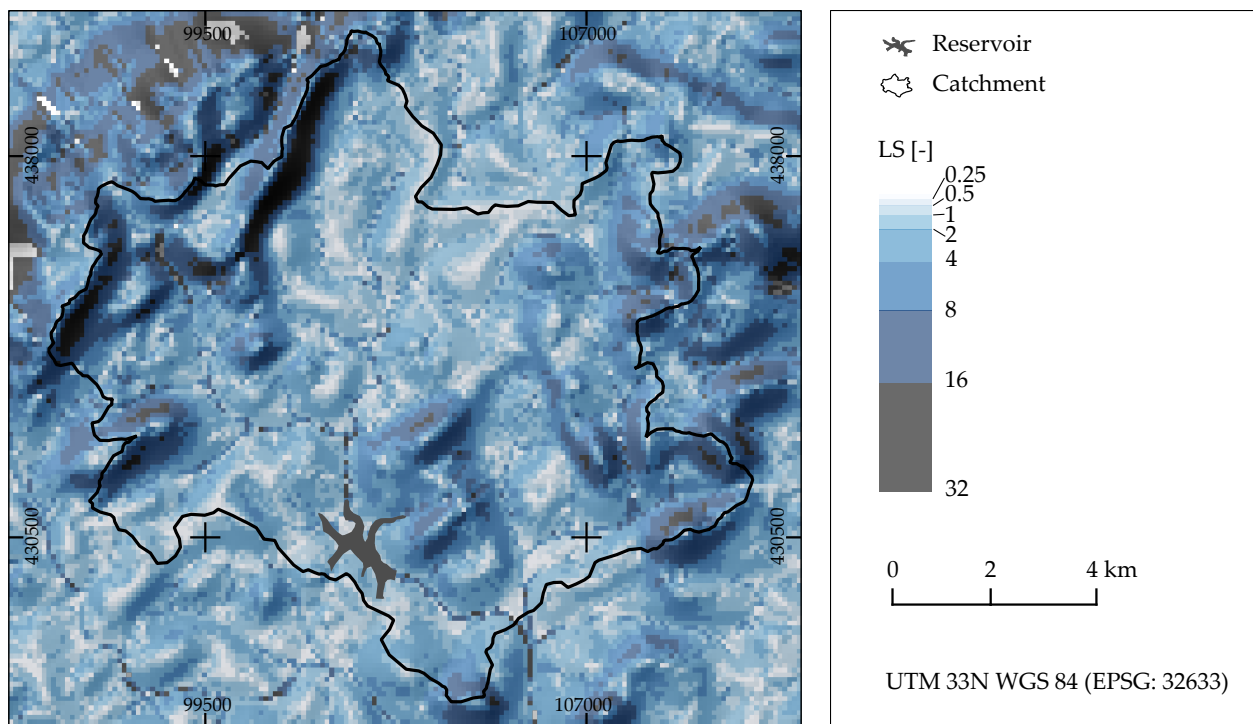
Both algorithms to calculate catchment area show a similar pattern. According to the lower resolution of the SRTM DEM, the flow pattern is coarser than the ASTER DEM; less flow lines are visible. Lines of concentrated flow using the ASTER DEM are more straight than the SRTM flow lines. In comparison to D_∞ , MFD shows extended areas with high flow around concentrated flow lines (both DEMs). In Table 5.4 mean values of slope and catchment area per unit contour width are shown. The values of the different DEMs differ significantly (notches of a boxplot); mean flow accumulation per unit contour width is—regardless to the algorithm used—higher when calculated on the basis of an ASTER DEM. In contrast, mean slope is higher when calculated for the SRTM DEM. The mean slope of both DEMs differs also significantly (notches of a boxplot): the slope of the SRTM DEM is slightly higher.

Due to the more realistic non-linear pattern of concentrated flow, ASTER-based LS-factors are used to model soil loss in a further step. The D_∞ flow algorithm is applied to calculate the final LS-factor map, because high areas of concentrated flow around flow lines seem to be unrealistic and do not match to what has been observed in the catchment during field work.

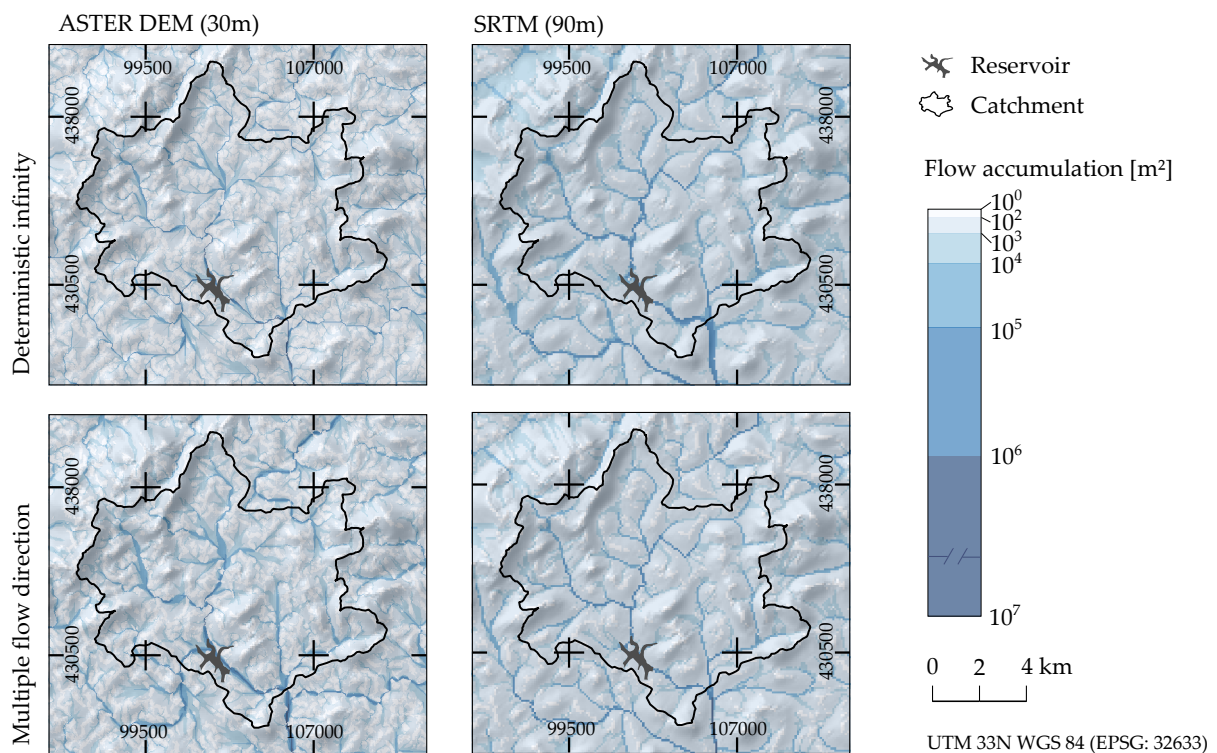
The LS-factor is mapped in Figure 5.6a. Most parts of the catchment, especially in the central north, northwest of the Mefou Reservoir and in the valley between the central and eastern inselbergs are characterized by a pattern of low LS-factors. The summits of the rolling hills are characterized by very low values, whereas the slopes of the river valleys are characterized by slightly higher LS-factors. Due to concentrated flow, LS-values are very high in streams. On the central hills, the hill in the western part of the catchment as well as in the mountains in the northwest and in the east, the LS-factor values are the highest.

Table 5.4: Mean values of DEM derivatives using different algorithms and DEMs. Medians of all values are significantly different (notches of a boxplot: MCGILL et al. 1978).

<i>Derivat</i> , algorithm	ASTER DEM (30 m)	SRTM DEM (90 m)
<i>Catchment area (per unit contour width)</i>		
Deterministic Infinity	6715 m	6066 m
Multiple Flow Direction	7431 m	6235 m
<i>Slope</i>		
Fit 2. Degree Polynom	14.6°	15.3°



(a) Map of the LS factor ($m=0.1$) calculated on the basis of an ASTER DEM and the D_∞ flow routing algorithm.



(b) Map of flow accumulation calculated on the basis of an ASTER DEM and a SRTM DEM applying the flow routing algorithms D_∞ and MFD.

Figure 5.6: Map of the LS factor used to calculate soil loss and different approaches to calculate flow accumulation (Database: NASA AND JAPAN ASTER PROGRAM 2011; UNITED STATES GEOLOGICAL SURVEY (USGS) 2012).

5.4 Cover and crop management factor

Estimation

The cover and crop management factor C is estimated using a linear model of the reflectance of a Landsat 8 scene and the C -factor values of bare ground and dense forest pixels as seen on Google Earth. Three different indices are used to appropriately represent reflectance of different land use and land cover types: A forest disturbance index (DI), the Normalized Difference Vegetation Index (NDVI) and a band ratio. To select the most suitable band ratio, correlation coefficient of all possible band ratios and ground truth data is calculated, whereas the ratio of band 5 (near infra-red;) to band 7 (short wavelength infrared) gave the best results ($\tau = -0.71$) and is accordingly used for further calculations.

NDVI values are high for dense forest and low for bare ground. As shown in Figure 5.7a (boxes) the mean NDVI of forest pixels is 0.79 ± 0.02 ; the mean NDVI of bare ground pixels is 0.22 ± 0.08 . There are no outlying values (Figure 5.7a). The NDVI of bare soils have a relatively wide range (between 0.06 and 0.42), while the NDVI of forest cover ranges between 0.73 and 0.82.

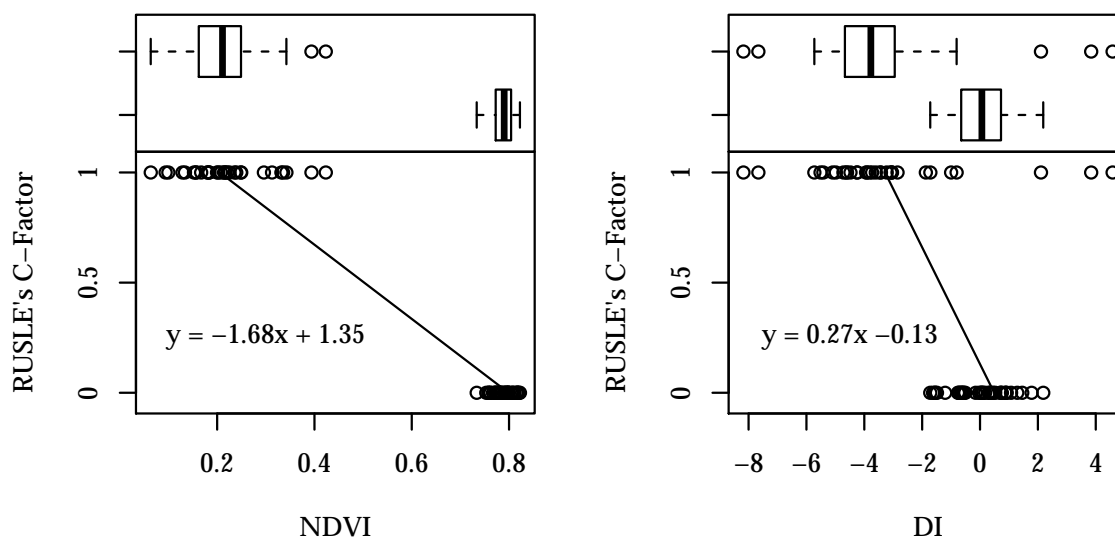
The values of the disturbance index in comparison show a vague image (Figure 5.7b). The mean DI of forest pixels is 0.0 ± 1.0 ; the mean DI of bare ground pixels is -3.3 ± 2.7 . As it is indicated by the high deviation of the mean, the ranges of the two land cover types are overlapping: While the values for bare ground range from -8.2 to 4.6 , the values for forest cover range from -1.7 to 2.2 . The linear model plotted in Figure 5.7b shows that modeled bare ground and forest cover values will not differ significantly.

The mean band ratio (5:7) for bare ground or forest is 1.4 ± 0.40 or 6.7 ± 0.49 (not shown).

C-factor validation and model selection

To select an appropriate model for a catchment wide C -factor, a validation data set of ground truth data (Google Earth) of dense forest cover and bare ground pixels is used to test the models of the indices/ratios. As it is shown in Figure 5.9 all indices/ratios gave good results for bare ground; the mean difference between modelled and ground truth C -factor values is -0.07 using the Disturbance Index, 0.03 using the NDVI and 0.00 using the band ratio. Only the DI-based values have some outliers. DI is not considered to be valid, because modelled value for forest cover differ clearly from ground truth values (mean-deviance 0.2). The deviances of NDVI and the band ratio are both much smaller (Figure 5.8).

A second validation is based on land use and land cover mapped during field work (Nov/Dec 2012). For all mapped land use and land cover types, mean, maximum and minimal published



(a) Normalized Difference Vegetation Index (b) Disturbance Index

Figure 5.7: Linear models and measured values for ground truth points with known C-Factor for bare ground ($C=1$) and dense forest ($C=0.002$) as seen on a Google Earth image

C-factor values are taken from literature (ROOSE 1977; NILL et al. 1996) as shown in Table 5.6. Only 59% percent of the DI-modelled C-factor values fit to the range of literature C-values. Both NDVI or the band ratio-based values fit to the range much better (70% or 66%). The mean deviation of the modelled values from the mean literature values is the lowest for NDVI, while again the DI-based values are worse. The deviation of the NDVI-C-factor is always smaller than 0.5 and in 41% of the samples smaller than 0.1. While the DI tends to overestimate C-factor values, both NDVI and brand ratio underestimate C-Factor values. In 39% of the point samples, the NDVI modelled the most accurate values; the band ratio estimated best values in 29% and the DI in 32% of the cases.

For further calculations, NDVI-derived C-factor values are used, because the index is the best estimator for C-factor values, either using bare-forest samples or C-factors of mapped land use and land cover (literature values) for validation, the NDVI-based C-values give most accurate results (overall accuracy is 70%).

C-factor distribution in the Upper Mefou subcatchment

A map to the modelled C-factors is shown in Figure 5.9. The relatively flat areas in the north, the hills and mountains in the western part of the Mefou catchment as well as the hill in the east—in the catchment of the Afeumev river—and the central hills are the areas with

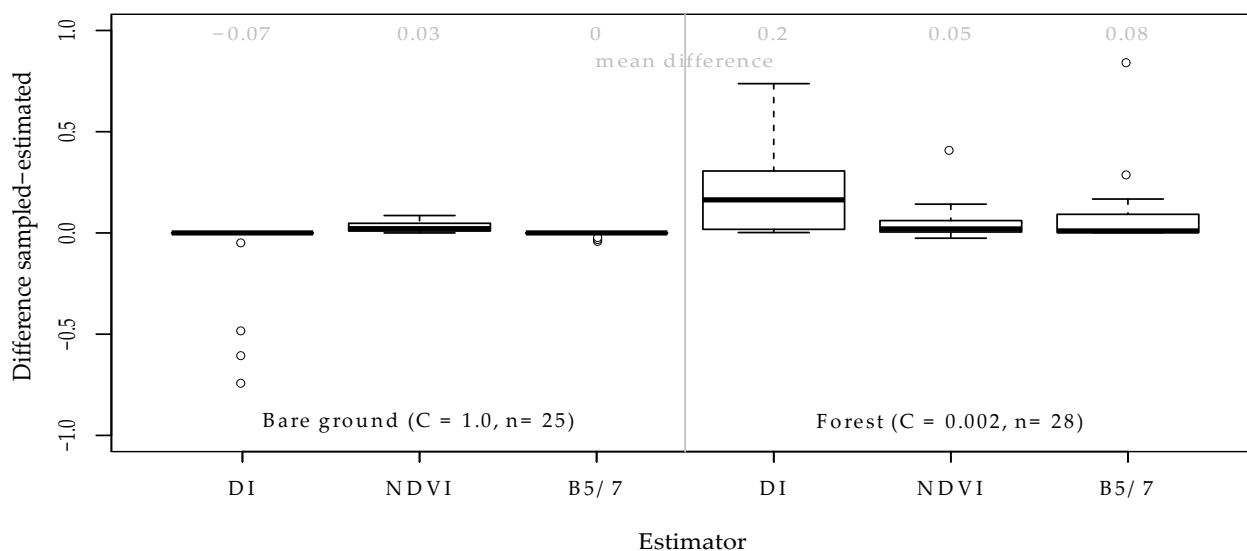


Figure 5.8: Box plots of difference between modelled C-factor and a validation set of ground truth information for bare ground and dense forest as seen on a Google Earth image.

the highest density of low C-factors (<0.15). These values are typical values for dense forest or secondary forest and bushes. (Also plantations with low tree spacing have low C-factors.) C-factors between 0.15 and 0.3 are typical for mixed-cropping systems, sometimes with intergrowing trees. The areas with the highest density of such factors are the flat areas north of the Mefou Reservoir and some relatively steep slopes in the upstream areas of the Mefou river. C-factors typical for mono-cropping systems range from 0.3 to 0.6; these values have been modelled for areas around the villages north of the reservoir and—more frequent—for areas around the densely settled parts of periurban Yaoundé and especially for areas in direct vicinity of the Mefou Reservoir. Extremely high C-factors (>0.6) are modeled mainly for sparsely vegetated areas with rocky outcrops, such as the the slopes of the inselbergs close to the reservoir and Yaoundé.

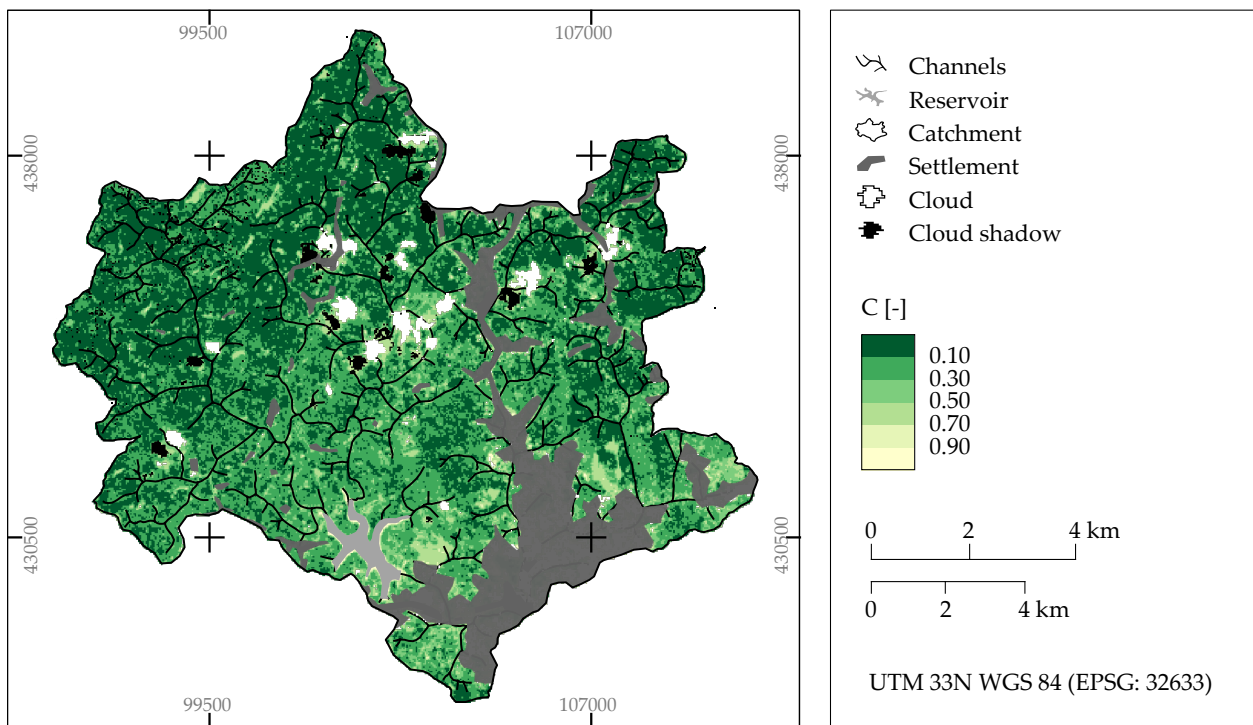
Table 5.5: Validation of C-factor estimation using field sampling of land use ($n = 34$).

Parameter	DI	NDVI	Band ratio 5:7
Fits Range	59%	70%	66%
Best Estimator	32%	39%	29%
Mean deviation	0.36	0.22	0.27
Deviation <0.5	78%	100%	94%
Deviation <0.1	28%	41%	34%
Deviation <0.01	9%	13%	3%
Overestimation	80%	37%	69%
Underestimation	20%	63%	31%

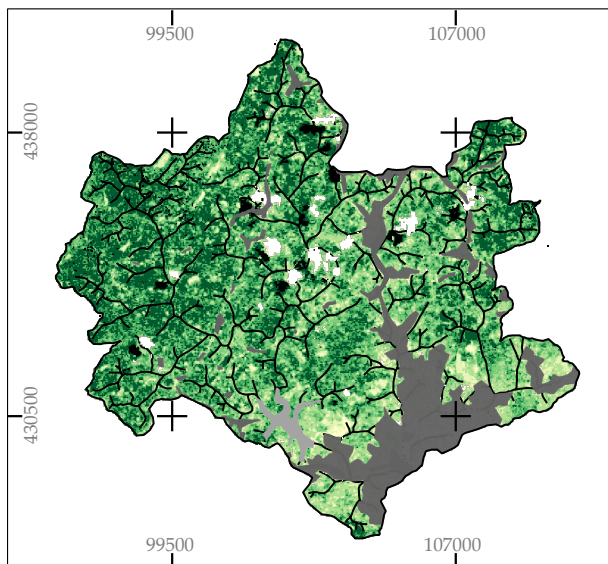
Table 5.6: Validation of C-factor estimation using field sampling of land use and C-values from literature.

ID	Estimator			Mean	Literature values		Source
	DI	NDVI	B5/7		Min	Max	
1	0.64	0.16	0.49	0.27	0.16	0.47	†
2	0.76	0.07	0.29	0.34	0.21	0.8	†
4	0.61	0.09	0.29	0.39	0.16	0.82	†
6	0.56	0.18	0.47	0.001	0.001	0.1	‡
7	0.62	0.14	0.45	0.42	0.1	0.83	†
8	0.03	0.11	0.15	0.02	0.00007	0.3	† ‡
9	0.41	0.17	0.37	0.39	0.16	0.82	†
10	0.41	0.22	0.53	0.18	0.02	0.59	†
11	0.25	0.2	0.35	0.18	0.02	0.59	†
12	0.4	0.18	0.32	0.39	0.16	0.82	†
13	0	0.39	0.33	0.001	0.001	0.1	‡
14	0.82	0.14	0.39	0.18	0.02	0.59	†
15	0.82	0.17	0.47	0.18	0.02	0.59	†
16	0.6	0.06	0.13	0.1	NA	NA	‡
17	0.44	0.29	0.59	0.39	0.16	0.82	†
18	0.11	0.33	0.68	0.1	NA	NA	‡
19	1	0.19	0.59	0.39	0.16	0.82	†
20	0.7	0.13	0.36	0.39	0.16	0.82	†
21	0.69	0.07	0.16	0.18	0.02	0.59	†
22	0.07	0.1	0.16	0.1	NA	NA	‡
23	0.9	0.09	0.5	0.001	0.001	0.1	‡
24	0.52	0.21	0.54	0.39	0.16	0.82	†
25	0.8	0.4	0.72	0.39	0.16	0.82	†
29	0.16	0.1	0.25	0.42	0.1	0.83	†
31	0.84	0.19	0.55	0.2	0.1	0.3	‡
33	0.06	0.67	0.82	0.36	0.12	0.56	†
34	0.53	0.07	0.19	1	NA	NA	
35	0.73	0.19	0.44	0.39	0.16	0.82	†
36	0.91	0.45	0.77	0.18	0.02	0.59	†
37	0.31	0.05	0.14	0.001	0.001	0.1	‡
38	0.01	0.16	0.38	0.02	0.00007	0.3	† ‡
39	0.4	0.01	0.01	0.001	0.001	0.1	‡
40	0.19	0.12	0.36	1	NA	NA	
42	0.51	0.03	0.1	0.39	0.16	0.82	†

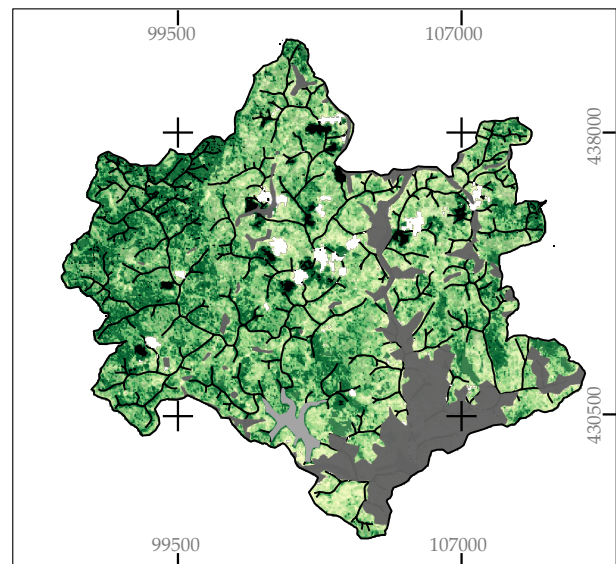
† NILL et al. (1996); ‡ ROOSE (1977)



Normalized Difference Vegetation Index



Ratio band5:band7



Disturbance Index

Figure 5.9: Cover and crop management factor based on three different linear models. The C-factor based on the Normalized Difference Vegetation Index is used for the calculation of soil loss (Database: NASA AND JAPAN ASTER PROGRAM 2011).

5.5 Erosion

5.5.1 Soil loss

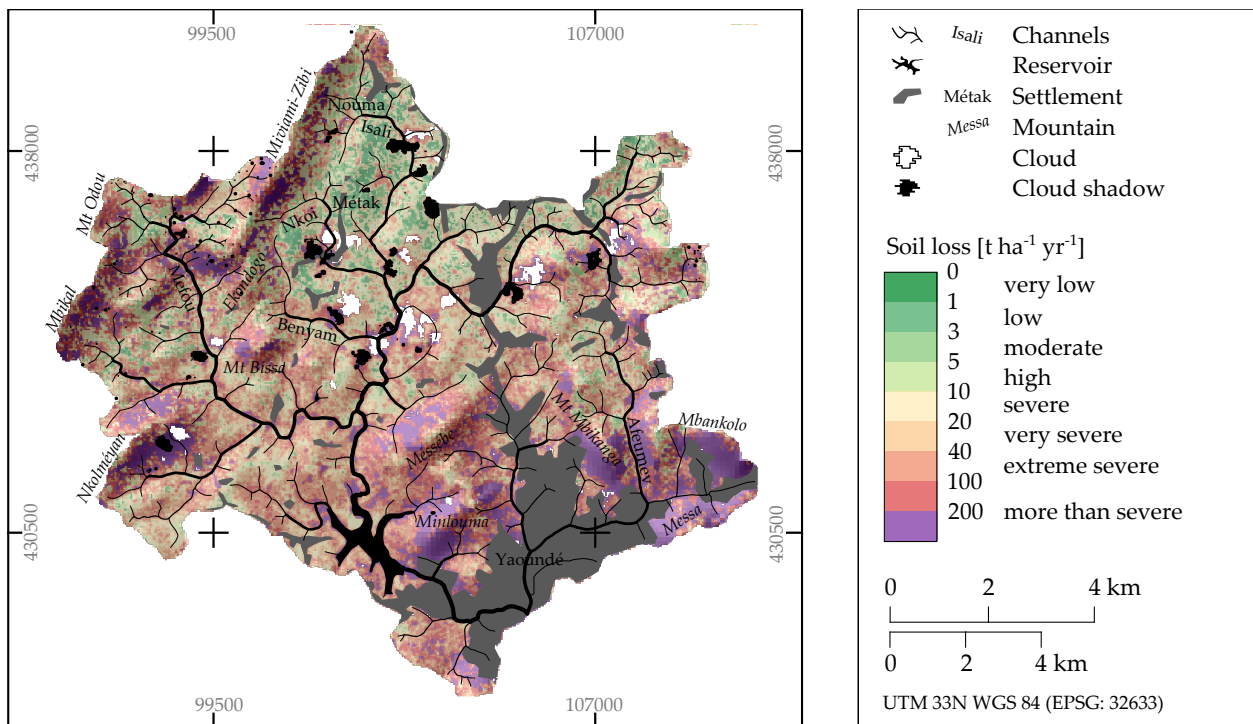
Modelled soil loss of the Upper Mefou catchment ranges from very low to more than severe; the maximum area specific soil loss is $1878 \text{ t ha}^{-1} \text{ yr}^{-1}$, the mean soil loss is $20 \text{ t ha}^{-1} \text{ yr}^{-1}$; the total amount of soil loss is $119\,328 \text{ t yr}^{-1}$. Based on the system of VAN DER KNIJFF *et al.* (2000), soil erosion in the Upper Mefou subcatchment is classified into nine soil loss classes, which range from very low ($0\text{--}1 \text{ t ha}^{-1} \text{ yr}^{-1}$) up to more than extremely severe ($> 200 \text{ t ha}^{-1} \text{ yr}^{-1}$). Very low and low erosion (classes 1 and 2) is modeled for 13.8% of the catchment area, moderate erosion for 6.9% of the catchment and high to severe erosion for 30.1% of the catchment. 49.2% of the area are subject of very or extreme severe erosion (classes 6 and 7), whereas erosion exceeds $100 \text{ t ha}^{-1} \text{ yr}^{-1}$ in 10.4% of the catchment.

As erosion has always to be seen in relation to soil loss tolerance, it is important to know the percentage of area exceeding the acceptable threshold. A general value for the maximal tolerable soil loss is $12.5 \text{ t ha}^{-1} \text{ yr}^{-1}$ (USDA 1983), whereas for the tropics a value of $2 \text{ t ha}^{-1} \text{ yr}^{-1}$ is often used (*cf.* EL-SWAIFY *et al.* 1982). In 63.1% of the Upper Mefou subcatchment, soil loss is higher than the global maximum value, and in 90.5% of the area higher than the tropical value.

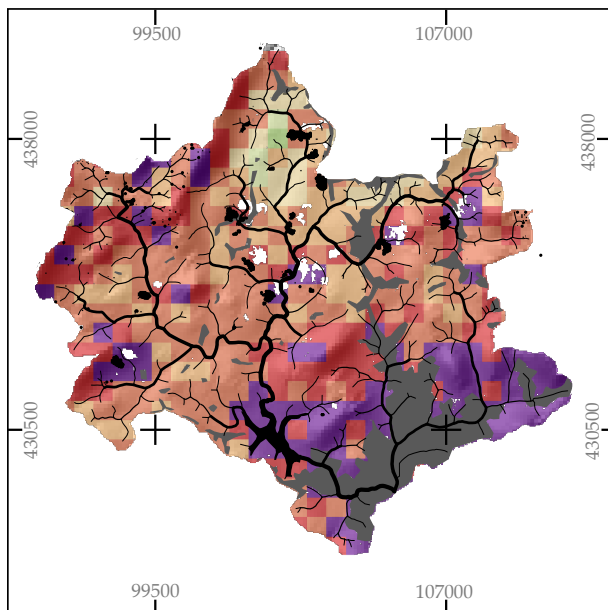
Mean annual modeled soil loss is the highest for areas with C-factors typical for all types of agricultural land ($123.8 \text{ t ha}^{-1} \text{ yr}^{-1}$; C-factor 0.18–0.41). Soil loss of mono-cropping areas (C-factor 0.18–0.28) is also extremely severe ($111.67 \text{ t ha}^{-1} \text{ yr}^{-1}$). The soil loss of areas with C-factors higher than agricultural land (>0.41) are in contrast clearly less $90.0 \text{ t ha}^{-1} \text{ yr}^{-1}$. On areas covered with sparse bush, fallows or plantations, soil loss is clearly less, averaging $31.2 \text{ t ha}^{-1} \text{ yr}^{-1}$; on forests, soil loss is even less ($2.6 \text{ t ha}^{-1} \text{ yr}^{-1}$).

Soil loss is higher on the steep slopes of the hills than on the flat areas of the catchment. Modeled erosion in nearly level and gently undulating areas (slope gradient classes 1 and 2; WISCHMEIER & SMITH 1978) averages less than $0.9 \text{ t ha}^{-1} \text{ yr}^{-1}$, whereas erosion in class 3—strongly undulating areas—is $4.8 \text{ t ha}^{-1} \text{ yr}^{-1}$. Erosion on strongly rolling slopes (class 5) is $15.8 \text{ t ha}^{-1} \text{ yr}^{-1}$ and 50.0 on steep slopes (class 7) and reaches $112.0 \text{ t ha}^{-1} \text{ yr}^{-1}$ on very steep slopes and $105.7 \text{ t ha}^{-1} \text{ yr}^{-1}$ on very extremely steep slopes (Table 5.7).

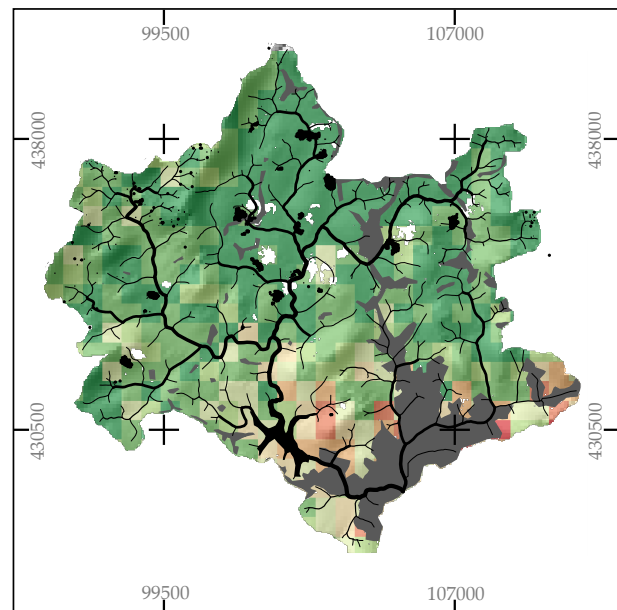
A map of soil losses is shown in Figure 5.10. In the northern part of the catchment—in the watersheds of the Isali, Nkoli and Benyam rivers south of the village of Nouma and around Métak—soil loss is low. Also in the flat valleys of the headwaters, soil erosion is relatively low: This is true for the Mefou River in the northwest as well as the river in the northeast and the Afeumev River in the east. Areas with moderate soil loss values are located all over



30 m resolution



Mean resampled (500 m)



Min resampled (500 m)

Figure 5.10: Map of modeled actual soil loss: The upper image shows soil loss in a 30 m resolution, the lower left shows soil loss resampled to a 500 m grid (*mean* of the 30 m grid cells) and the lower right image shows soil loss resampled to a 500 m grid (*minimal value* of the 30 m grid cells).

Table 5.7: Classified soil loss values and mean values of the USLE input K, C and LS without and with deposition areas

	Erosion class (soil loss [$\text{t ha}^{-1} \text{yr}^{-1}$])								
	(1)	(2)	(3)	(4)	(5)	(6)	(7)	(8)	(9)
	< 1	1–3	3–5	5–10	10–20	20–40	40–100	100–200	> 200
<i>Erosion</i>									
Area [ha]	410	582	493	904	1258	1416	1381	498	247
Area [%]	5.7	8.1	6.9	12.6	17.5	19.7	19.2	6.9	3.4
Mean K [SI]	0.019	0.020	0.020	0.021	0.023	0.023	0.023	0.023	0.024
Mean C [-]	0.00	0.02	0.03	0.05	0.07	0.08	0.11	0.14	0.23
Mean LS [-]	0.8	1.6	2.0	1.3	1.4	2.0	3.2	4.9	6.2
<i>Erosion/Deposition</i>									
Area [ha]	207	289	252	455	647	729	748	292	157
Area [%]	2.9	4.0	3.5	6.3	9.0	10.1	10.4	4.1	2.2
Mean K [SI]	0.018	0.020	0.021	0.021	0.023	0.023	0.023	0.023	0.024
Mean C [-]	0.00	0.02	0.03	0.05	0.06	0.08	0.10	0.13	0.22
Mean LS [-]	0.8	1.6	1.9	1.4	1.4	2.1	3.5	5.2	6.4

the catchment, but tend to be more frequent in the north than in the south (around the periurban parts of Yaoundé and the Mefou Reservoir) of the catchment. High soil loss values show a similar distribution pattern: low in the north and high in the periurban south and southwest. Areas experiencing severe and very severe erosion are located mainly in the south and the west of the catchment: in the periurban areas as well as on the steep inselbergs.

Extremely severe soil loss is abundant around the Mefou Reservoir and on the slopes of the central inselbergs (Méssébe and Minlouma), the western inselbergs (Nkolméyan and Mt Bissa), the inselbergs in the east (Mt Mbikanga, Messa and Mbankolo) and the inselbergs in the northwest (Mbikal, Mt Odou, Ekondogo and Miviami-Zibi). In the northwest, the valley of the Mefou is excluded from extreme severe erosion, as it is the valley of the Afeumev river in the east. The areas in close proximity to periurban Yaoundé are also subject of extreme severe erosion. Around the rural settlements, erosion is not higher, apart from the villages in the northeast of the catchment. As it is shown in the coarse, resampled soil loss map (Figure 5.10), the main area of the highest loss values is around periurban Yaoundé and the Mefou Reservoir, especially on steeper slopes.

In Figure 5.11 the potential erosion risk is shown. In comparison to the actual erosion risk (Figures 5.10 and 5.13, Table 5.7), the potential erosion risk takes erodibility, erosivity and topographic potential into account as well, but not the present vegetation cover. Therefore, the potential soil erosion risk of different types of land cover and land use is highlighted. (Land

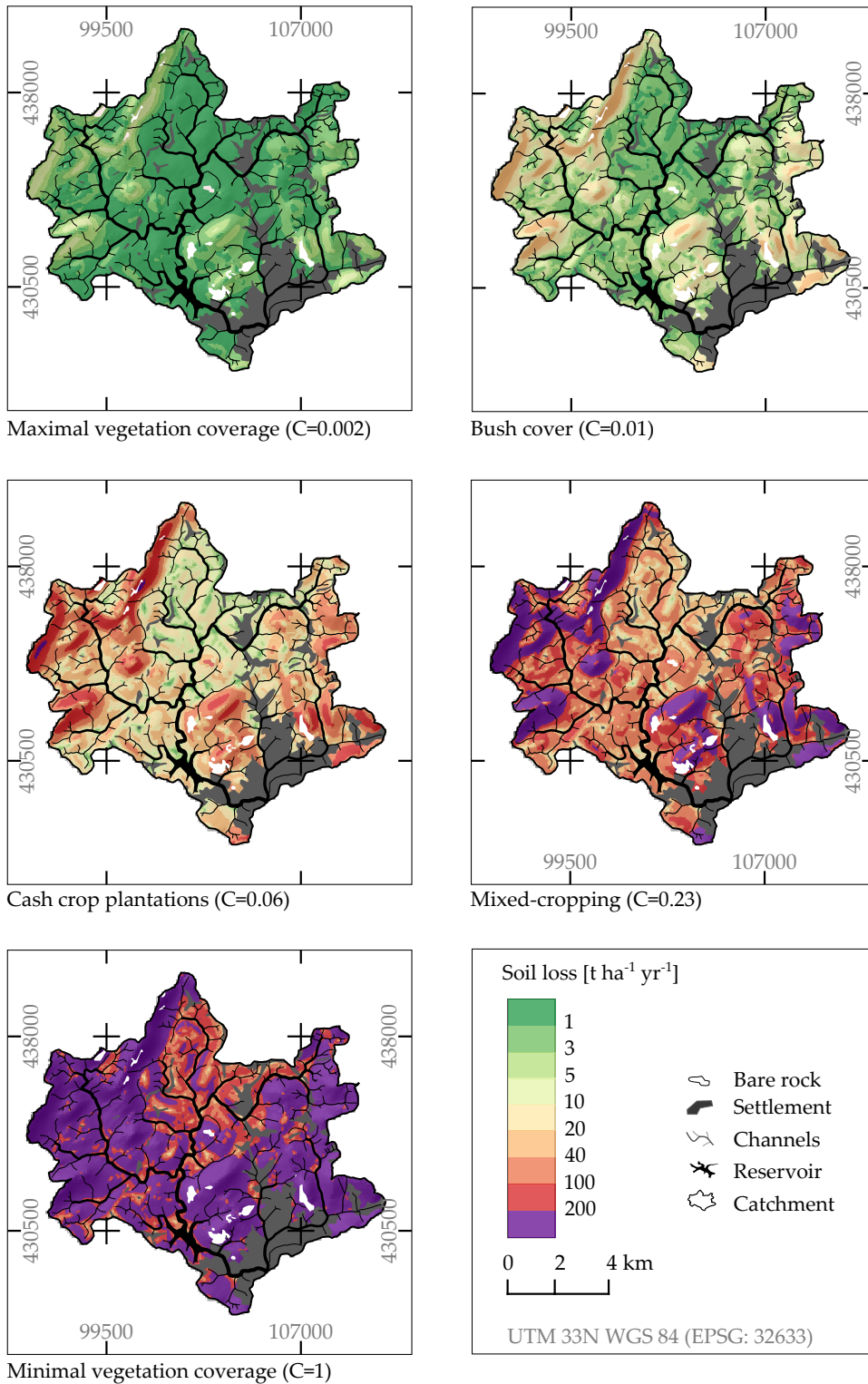


Figure 5.11: Potential soil loss of five different land use and land cover assumptions (dense natural vegetation cover to a worst case: bare ground (Database: INSTITUE GÉOGRAPHIQUE NATIONAL 1956; EL-SWAIFY et al. 1982; NILL et al. 1996; JARVIS et al. 2008; NASA AND JAPAN ASTER PROGRAM 2011)).

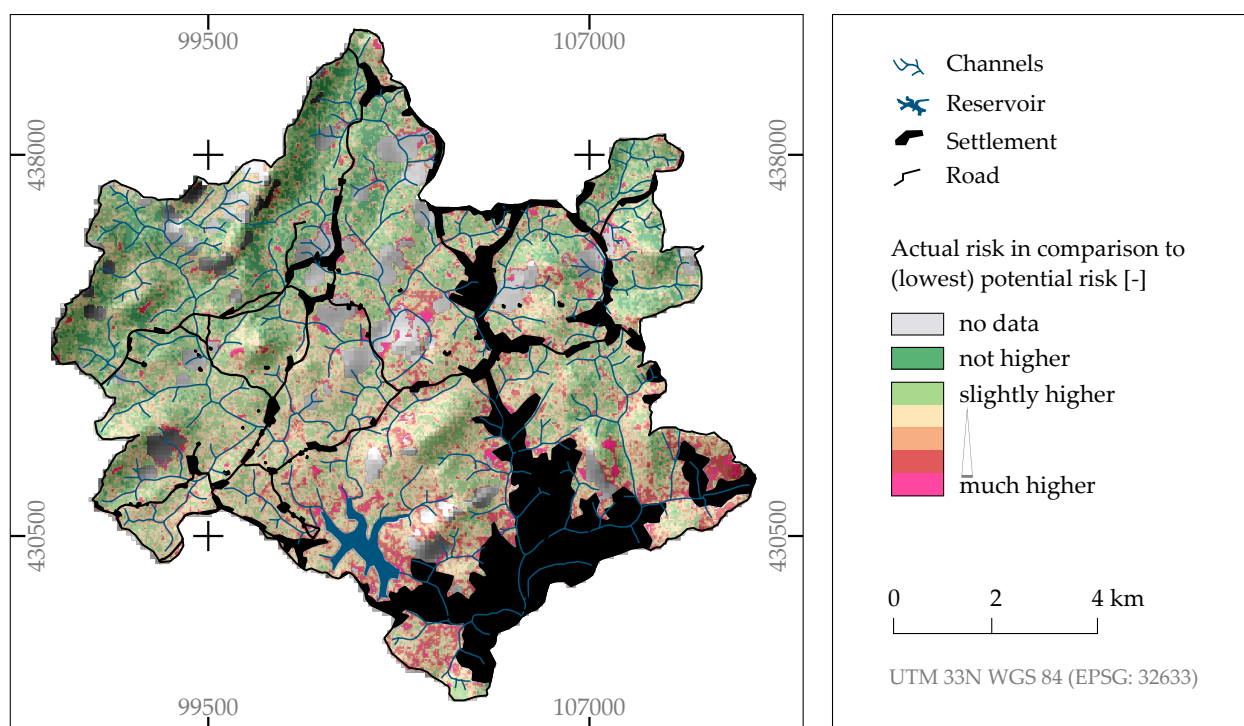


Figure 5.12: Comparison of actual and potential soil loss: Actual soil loss divided by the potential soil loss of an Upper Mefou catchment completely covered with dense forest ($C=0.002$). Classes according to the third quartile and the 90%, 95% and 99% percentiles (Database: JARVIS et al. 2008; NASA AND JAPAN ASTER PROGRAM 2011).

use and land cover change scenarios are shown and described in Section 5.6). The potential risk is the highest on the inselbergs in the northwest, the central part of the catchment and in the east. The northern undulating hills have a smaller potential risk than the southern part. Assuming a dense natural vegetation cover (humid forest), the soil erosion risk in the Upper Mefou subcatchment is relatively low ($< 1 \text{ t ha}^{-1} \text{ yr}^{-1}$)—also on the steep inselbergs, where the potential soil erosion does not exceed $10 \text{ t ha}^{-1} \text{ yr}^{-1}$). Also in the case of a bush coverage in the entire catchment, the erosion risk is relatively low ($< 3 \text{ t ha}^{-1} \text{ yr}^{-1}$), but the steepest parts of the inselbergs experience a higher risk ($> 40 \text{ t ha}^{-1} \text{ yr}^{-1}$). Assuming cash crop production or even food crop production in the catchment, the potential erosion risk is high. The potential soil loss of the zero-coverage case is severe; only in the flattest parts in the lowlands—especially in the north—the potential soil erosion risk is relatively low.

5.5.2 Deposition

As the RUSLE3D models erosion in the entire catchment, deposition areas are excluded from soil loss with a topographic erosion/deposition index. Excluding net deposition areas from

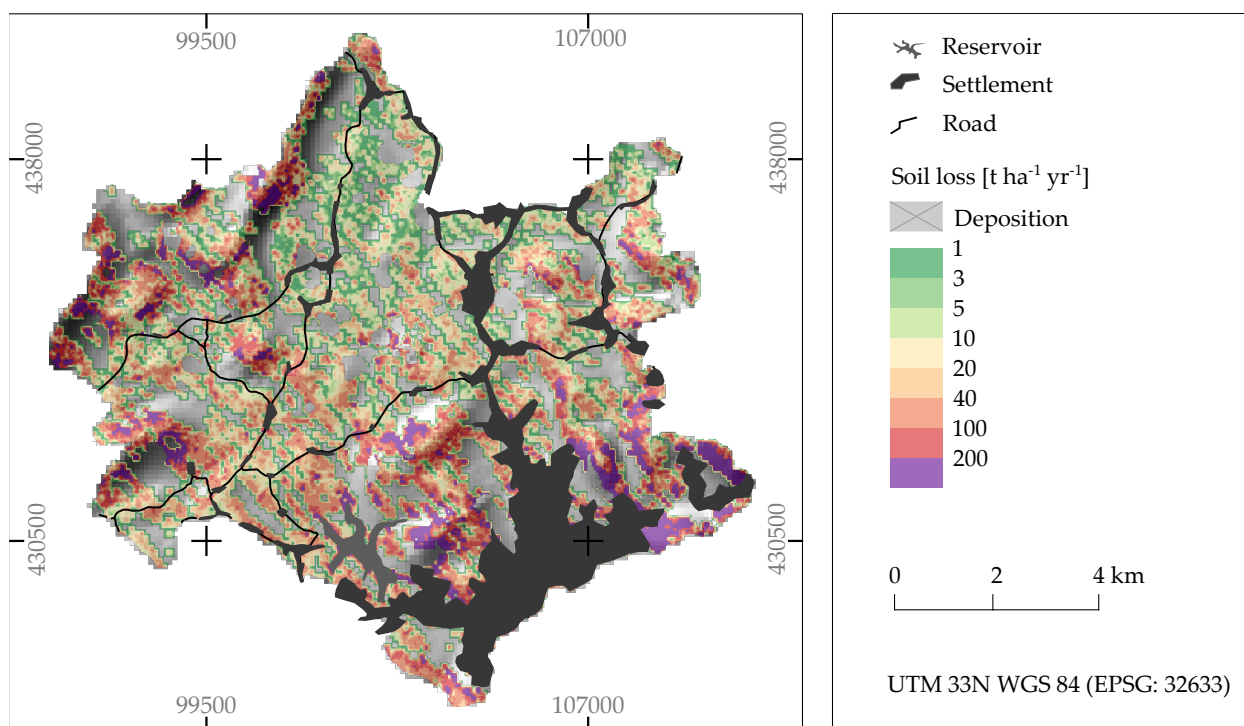


Figure 5.13: Erosion/deposition: Actual soil loss excluding all topographical depositional areas (Database: NASA AND JAPAN ASTER PROGRAM 2011).

soil loss, the mean annual soil loss is $9.5 \text{ t ha}^{-1} \text{ yr}^{-1}$, total annual soil loss in the Upper Mefou subcatchment is 92 537 t. 23% of the area are subject of very low or low erosion, *only* 1925 ha are subject of very severe or extremely severe erosion compared to 2331 ha when assuming erosion on topographically deposition areas (Table 5.7, Figure 5.13).

5.5.3 Validation: Reservoir sediment survey

A reservoir sediment survey is conducted to validate the results of RUSLE3D and the topographic erosion/deposition index. Due to the fact that the Mefou Reservoir is under rehabilitation during field work in November/December 2012, it was easily possible to measure the thickness of the sediment layer ($n = 6$).

Thickness ranges from 3 to 7 cm; mean thickness is used to approximate the sediment volume of the entire reservoir surface (105 ha) and sediment weight calculated based on a dry sediment bulk density of 1 g cm^{-3} . The Mefou Reservoir (*aka* Mopfou Reservoir) was constructed in 1969, abandoned 1976–2005 and again in operation from 2005 until 2011 (cf. BECKER et al. 2013). From 2012 to 2014, the dam was under construction. Thus, it is assumed that the duration of sediment deposition was ca. 6 years (2005–2011); the building contractor (*FAYAT S.A.: Razel-Bec S.A.S., Orsay, France*) did not reworked the sediments before

Table 5.8: Input parameters and calculated values of the Mefou Reservoir sediment survey: Validation of the modeled soil loss values.

Parameter	Value	Source
<i>Mefou Reservoir</i>		
Reservoir catchment	ca. 70,9 km ²	<i>own calculation</i>
Storage capacity (before 2014)	ca. 5 Mio. m ³	FAO-AQUASTAT (2013)
Trap efficiency	90%	catchment–capacity ratio (cf. BROWN 1943; VERSTRAETEN & POESEN 2000)
Surface area of the reservoir	105 ha	BECKER et al. (2013)
Years of operation	2005–2011 (6 yrs)	BECKER et al. (2013)
<i>Sediment yield</i>		
Thickness of the sediment layer	4.85 ± 1.7 cm	field survey (n=6)
Sediment bulk density	1.00 g cm ⁻³	<i>own approximation</i>
Sediment yield (SY)	8486 ± 2928 t yr ⁻¹	
Area specific sediment yield (SSY)	1.20 ± 0.41 t ha⁻¹ yr⁻¹	
<i>Sediment delivery</i>		
Gross erosion – deposition (Upper Mefou catchment, 97.9 km ²)	92537 t yr ⁻¹	(see pp. 68)
Erosion in the reservoir catchment	ca. 9.5 t yr ⁻¹ yr ⁻¹	
Sediment delivery ratio (SDR)	0.105 ± 0.077	EL-SWAIFY et al. (1982) and EBISEMIJU (1990)
Proportion of soil loss from settlements, roads and trails	42% ± 14.8 pp	DOUGLAS (2003), RIJSDIJK (2005), and DE MEYER et al. (2011a)
Area specific sediment delivery	1.62 ± 1.04 t ha⁻¹ yr⁻¹	

the recommissioning of the dam 2013 (pers. comm., a construction worker, Nov. 2012, cf. OTT 2014). The trap efficiency (90%) is taken from the lower envelope of the Brown curve (BROWN 1943; cf. VERSTRAETEN & POESEN 2000) for a capacity–catchment ratio of 5 000 000 m³ : 70.9 km²; the lower envelope is suitable for fine sediments. Sediment delivery of the catchment is estimated taking into account that modeled soil loss only includes soil loss from non-linear land use and land cover and only partly from settlements; an average ratio of soil loss from unconsolidated roads, trails and landing sites is taken from literature (42% ± 14.8 pp); the sediment delivery of the reservoir catchment is increased proportionately (the contribution of roads and trails is discussed in detail in Section 6.2). Sediment delivery ratio (SDR) is taken from literature: As values for the humid tropics are rare, it is referred to

two values only; SDR=0.05 (EL-SWAIFY et al. 1982) and SDR=0.16 (EBISEMIJU 1990). The mean of these values (SDR=0.105) and its standard deviation are used for calculation. The area specific sediment delivery (SSD) is $1.62 \pm 1.04 \text{ t ha}^{-1} \text{ yr}^{-1}$, whereas the area specific sediment yield (SSY) is $1.20 \pm 0.41 \text{ t ha}^{-1} \text{ yr}^{-1}$. Thus, SSD and SSY differ, but are not importantly different.

5.6 Land use change scenarios

The change in annual soil loss of five land use change scenarios is calculated for the Upper Mefou subcatchment. Scenario 1b is based on the transformation of forest to mixed-cropping. Total soil loss in this scenario increases from $20.0 \text{ t ha}^{-1} \text{ yr}^{-1}$ to $64 \text{ t ha}^{-1} \text{ yr}^{-1}$ (values excluding deposition areas are given in Table 5.9).

Table 5.9: Modeled soil loss of five land use scenarios

	Soil loss [$\text{t ha}^{-1} \text{ yr}^{-1}$]		Area affected
	Erosion	Erosion/Deposition	
<i>Actual situation</i>	20.1	9.5	100%
<i>Scenario 1a:</i> Transformation of forest to mixed-cropping	64.1	17.1	10%
<i>Scenario 1b:</i> Transformation of bush, plantations and fallows to mixed-cropping / shorter fallow period	67.9	18.8	52%
<i>Scenario 2:</i> Land use intensification: Change from mixed-cropping to mono-crop cultivation	45.5	12.6	7%
<i>Scenario 3:</i> Forest clearing and new plantations	47.5	13.0	10%
<i>Scenario 4:</i> Forest regrowth – abandonment of agricultural land	19.5	9.2	12%

Areas with an extreme increase of soil loss are mainly located on the slopes of the northwestern inselbergs and—to a clearly less extent—on the slopes of the eastern inselbergs and the western inselbergs.

In the vicinity of Nouma in the central north of the catchment, soil loss would slightly increase. In the case of a change from fallows, bush or plantations to mixed-cropping, the mean annual soil loss would increase to $47.5 \text{ t ha}^{-1} \text{ yr}^{-1}$; 52% of the catchments surface would be affected, where again on the northwestern inselbergs soil loss would increase, but the western as well as the central hills and the hills in the east would be more clearly affected. Around periburan Yaoundé and in the areas north of the Mefou Reservoir, soil loss would increase

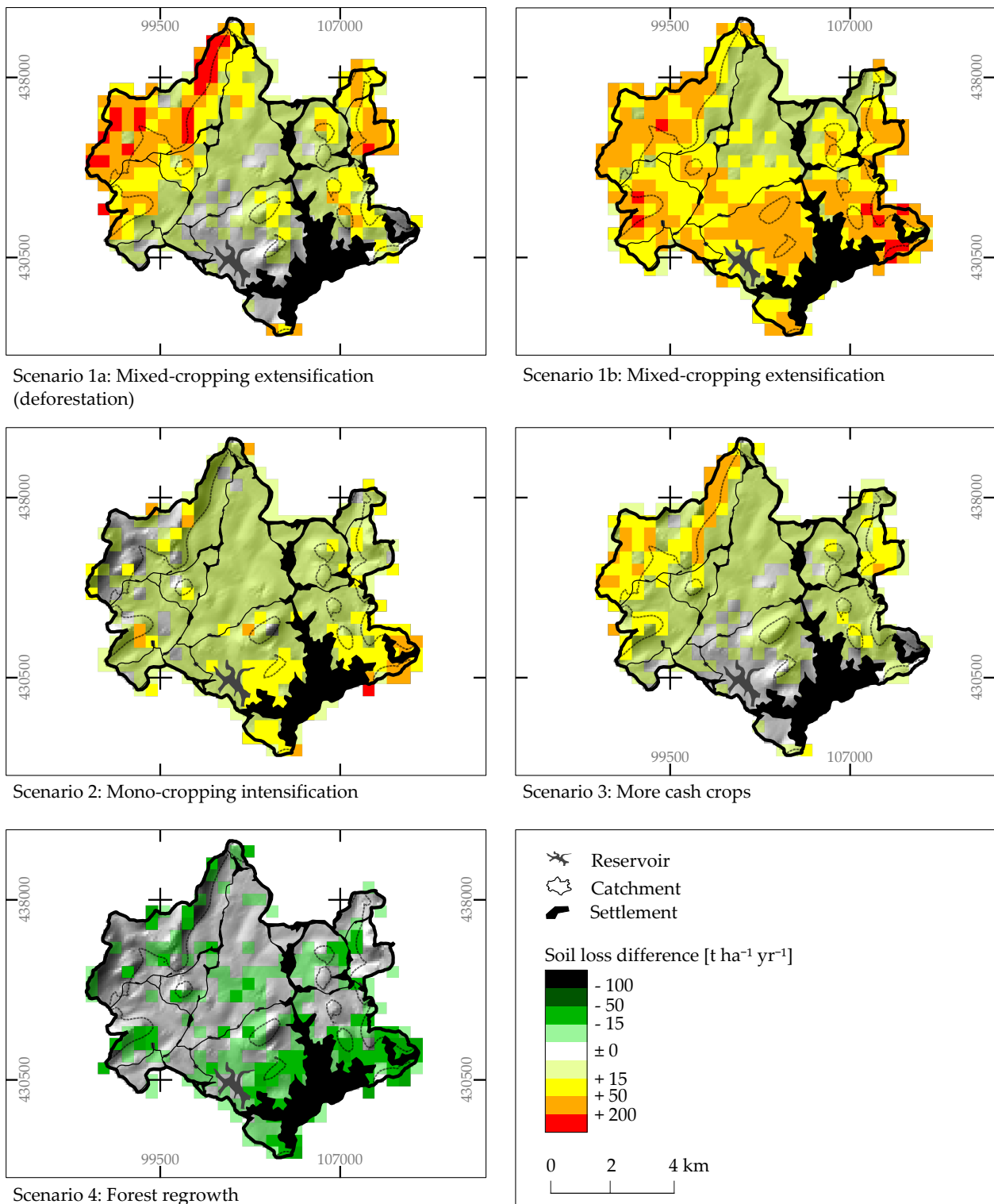


Figure 5.14: Modeled change of soil loss for five land use/cover scenarios. Medium resolution (30 m) information can be found on the digital appendix (Database: JARVIS et al. 2008; NASA AND JAPAN ASTER PROGRAM 2011).

slightly. An intensification of land use—the use of mixed-cropping field for mono-cropping (Scenario 2)—would result in an increase of erosion to $26.5 \text{ t ha}^{-1} \text{ yr}^{-1}$. 7% of the area would be subject of the change, which is mainly located around the Mefou Reservoir as well as in the southeastern periurban areas. Nevertheless, the entire catchment would be affect, excluding the inselbergs in the northwest. Scenario 3—the use of forest areas for plantations—also affects huge parts of the Upper Mefou subcatchment, but slightly more pronounced the inselbergs in the northwest. Areas around Yaoundé and the Mefou Reservoir are not subject of change in that scenario. The overall soil loss would raise to $47.5 \text{ t ha}^{-1} \text{ yr}^{-1}$. The regrowth of forest in cultivated areas would result in a decreased soil loss (Table 5.9), especially some slopes of the western hill, areas around periurban Yaoundé and the Mefou Reservoir.

6 Discussion

6.1 Soil loss

The validation of the soil loss results shows that the modelled sediment delivery of the catchment is similar to the sediment yield obtained by a reservoir sediment survey. Thus, the modelled results seem to be not far away from reality and at least in the order of magnitude of the sediment yield.

Excluding deposition areas, modelled actual soil loss in the Upper Mefou catchment averages $9.5 \text{ t ha}^{-1} \text{ yr}^{-1}$; values for the lumped-erosion case of the RUSLE3D seem to be fairly to high. The potential soil loss under natural conditions is much lower (dense forest: $0.7 \text{ t ha}^{-1} \text{ yr}^{-1}$; bush: $3.4 \text{ t ha}^{-1} \text{ yr}^{-1}$).

The value of $9.5 \text{ t ha}^{-1} \text{ yr}^{-1}$ fits in the overall range of values published for tropical regions world wide and also in the range of values for West and Central Africa (EL-SWAIFY et al. 1982). The general erosion hazard risk map of Fournier (as shown in EL-SWAIFY et al. 1982) shows soil loss values for the Southern Cameroon Plateau between 10 and $20 \text{ t ha}^{-1} \text{ yr}^{-1}$. This is quite somewhat higher than the present values. However, WALLING (1984) notes that the general view of Fournier is substandard and maps soil losses between 1 and $10 \text{ t ha}^{-1} \text{ yr}^{-1}$ for the Southern Cameroon Plateau. WALLING & WEBB (1996) mapped also values within that range (Table 6.1), which are all in accordance with the modelled values. General values for Africa (STOCKING 1984) are far below the present values, but also extrapolated over a huge area including soil loss of e. g. deserts.

In general, the intercomparability of different erosion studies is complex, due to varying methodology, topography, land use and land cover and soils. Most of the soil loss values published for the wider study area are from plot experiments, where slope and vegetation cover are constant and slope length is short. Thus, the values in Table 6.1 give only an overview of some typical values for different land uses.

The published soil loss values of natural vegetation and bush fallows are low: all values summarized by EL-SWAIFY et al. (1982) do not exceed $0.1 \text{ t ha}^{-1} \text{ yr}^{-1}$; EHUI et al. (1990) measured $0.42 \text{ t ha}^{-1} \text{ yr}^{-1}$ on a bush fallow in southwest Nigeria and BARTHES et al. (2000) reports a loss of $0.8 \text{ t ha}^{-1} \text{ yr}^{-1}$ on a savanna plot in northern Cameroon. Erosion is up to two orders of magnitude higher on bare plots. 33.8 , 102 or $307.5 \text{ t ha}^{-1} \text{ yr}^{-1}$ soil loss were measured on 4%, 7% or 20% sloping plots near Abijan, Ivory Coast (cf. ROOSE & SARRAILH 1989). ROOSE (1977) published even higher values up to $570 \text{ t ha}^{-1} \text{ yr}^{-1}$.

Table 6.1: Soil loss [$\text{t ha}^{-1} \text{yr}^{-1}$] in different study areas in the (humid) tropics of western Africa in relation to slope angle and land use/cover. Values for different types of cropping or slope length are averaged. Catchment based values are calculated from sediment yield maps with sediment delivery ratios (0.05; 0.16), so that ranges are reported. Values marked with an asterisk (*) are from continental erosion hazard risk maps or sediment yield maps.

Soil loss	Context	Slope	LULC	Reference
<i>Experimental plots</i>				
2.9	Cameroon and Nigeria, tropical soils		cultivated areas	NILL (1993)
1.53	SW Nigeria, sandy oxic soil, 1100-1500 mm	7%	bush fallow	EHUI et al. (1990)
13.5	Benin, 1000–1600 mm, sandy clay loam	<5%	intercropping	BARTHES et al. (2000)
0.8	Cameroon, 1000-1600 mm, loamy sand	<5%	savanna	BARTHES et al. (2000)
17.5	Cameroon, 1000-1600 mm, loamy sand	<5%	cropped	BARTHES et al. (2000)
0.42	SW Nigeria, sandy oxic soil, 1100-1500 mm	7%	bush fallow	EHUI et al. (1990)
0.89	SW Nigeria, sandy oxic soil, 1100-1500 mm	7%	shifting cultivation	EHUI et al. (1990)
0.5	Abijan, Ivory Coast, 2500 mm	4%	pine apple	ROOSE & SARRAILH (1989)
1.2	Abijan, Ivory Coast, 2500 mm	7%	pine apple	ROOSE & SARRAILH (1989)
25.7	Abijan, Ivory Coast, 2500 mm	20%	pine apple	ROOSE & SARRAILH (1989)
33.8	Abijan, Ivory Coast, 2500 mm	4%	bare soil	ROOSE & SARRAILH (1989)
102.0	Abijan, Ivory Coast, 2500 mm	7%	bare soil	ROOSE & SARRAILH (1989)
307.5	Abijan, Ivory Coast, 2500 mm	20%	bare soil	ROOSE & SARRAILH (1989)
15	Yaoundé area, Cameroon	24%	disk-harrow ploughing	AMBASSA-KIKI & NILL (1999)
14	Yaoundé area, Cameroon	24%	no tillage	AMBASSA-KIKI & NILL (1999)
1	Yaoundé area, Cameroon	24%	intercropping	AMBASSA-KIKI & NILL (1999)
9	Yaoundé area, Cameroon	24%	bare fallow	AMBASSA-KIKI & NILL (1999)
<i>Continental scale / global values</i>				
0.47	<i>Africa</i>		variable	STOCKING (1984)
0.8–555	Tropical regions worldwide		variable	EL-SWAIFY et al. (1982)
0.1–1.3	Central Cameroon*		variable	WALLING & WEBB (1996)
5.0–6.3	Central Cameroon*		variable	WALLING & WEBB (1996)
10–20	Central Cameroon*		variable	EL-SWAIFY et al. (1982)

continued ...

... continued

Soil loss	Context	Slope	LULC	Reference
1–10	Central Cameroon*		variable	WALLING (1984)
0.01–0.07	West Africa		natural vegetation	ROOSE (1977)
0.1–90	West Africa		cropland	ROOSE (1977)
3–570	West Africa		bare fallow	ROOSE (1977)
<i>Area specific sediment yields</i>				
3.1	Ibadan, Nigeria		cultivated	LAL (1996)
3–9.6	Congo basin		variable	EL-SWAIFY et al. (1982)
1.19–3.8	Niger basin		variable	BALEK (2011)
4.8–15.4	Benue basin		variable	BALEK (2011)
2.3–7.4	Niger-Benue basin and Congo basin		variable	BALEK (2011)
0.35–1.12	Songkwé catchment (2.7 km ²), southern Cameroon	>25%	variable	WATERLOO et al. (2000)
0.2	Songkwé catchment (2.7 km ²), southern Cameroon	>25%	variable	NTONGA et al. (2002)
1.1–3.4	Nyangong catchment (6.8 km ²), southern Cameroon	>15%	variable	WATERLOO et al. (2000)
1.0–12.9	Nyangong catchment (6.8 km ²), southern Cameroon	>15%	variable	NTONGA et al. (2002)
2.1–6.8	Biboo-Minwo catchment (7.7 km ²), southern Cameroon	>25%	variable	WATERLOO et al. (2000)
0.3–12.7	Biboo-Minwo catchment (7.7 km ²), southern Cameroon	>25%	variable	NTONGA et al. (2002)

Both, published values for bare ground and natural vegetation fit to the modelled *potential* soil loss in the Upper Mefou subcatchment: Maximal values in the catchment are as high, especially on even steeper slopes, where the potential soil erosion risk is more than severe ($> 200 \text{ t ha}^{-1} \text{ yr}^{-1}$). Nevertheless, pure bare soil is, except sports fields, not modelled in the study at hand, due to the fact that the coarse resolution of the erosion model ($30 \times 30 \text{ m}$) results in mixed pixels (see Section 6.3.2). Assuming that the Upper Mefou subcatchment would only be covered with dense natural vegetation, soil loss would be below $1 \text{ t ha}^{-1} \text{ yr}^{-1}$ (see Section 5.5.1).

The values measured on cultivated plots in Central/West Africa have a wide range ($0.89\text{--}29.6 \text{ t ha}^{-1} \text{ yr}^{-1}$, Table 6.1). Under similar conditions, soil loss is clearly higher on steeper slopes (ROOSE & SARRAILH 1989): On a pineapple plot, average soil loss is 0.5, 1.2 or $25.7 \text{ t ha}^{-1} \text{ yr}^{-1}$ at 4%, 7% or 20% slope. The mean catchment slope of the Upper Mefou subcatchment is 5.8%—however, the Bornhard type inselbergs are very steep. The results of AMBASSA-KIKI & NILL (1999) show that also the type of ploughing is a determining factor of soil erosion. In the study at hand, this could not be taken into account, what limits the meaning of the presented values to a broader scale.

Catchment sediment yield and erosion

In general, it is problematic to extrapolate plot values to catchments (i. a. BOARDMAN 1998). Value comparison with those from catchment experiments might help to avoid that problem. In comparison to the amount of plot studies, these types of studies are seldom in West/Central Africa. In a catchment experiment in Ibadan, Nigeria, LAL (1996) applied different methods of clearing and tillage: he measured a mean soil loss value of $3.1 \text{ t ha}^{-1} \text{ yr}^{-1}$. Values from other catchment experiments or suspended load studies are also difficult to compare with that of the study on hand, since they suffer from the sediment delivery problem. Sediment yields have to be *converted* to erosion, what is done here by applying a factor of 0.05 and 0.16. Only ranges of values are given for catchment surveys (Table 6.1). On a broad scale, the basin erosion of the major rivers in western Africa can be consulted, although sediment delivery depends on catchment size (WALLING 1983). Soil erosion in the Congo basin is reported to be $3.0\text{--}9.6$ or $2.3\text{--}7.4 \text{ t ha}^{-1} \text{ yr}^{-1}$ (EL-SWAIFY et al. 1982; BALEK 2011). The erosion values of the study at hand are in the upper 10% of the first range and exceed the second range. They are also higher than the values of the Niger basin and the Niger–Benué basin (Table 6.1), where the basin characteristics are completely different. Values are in the range of that from the Benué basin (Table 6.1), where land cover is partly similar to the Southern Cameroon Plateau. Sediment yield was measured in three small catchments ($2.7\text{--}7.7 \text{ km}^2$) in southern

Cameroon, where land use is similar to that of the Upper Mefou catchment: Up to one third are agricultural areas (WATERLOO et al. 2000; NTONGA et al. 2002). In the first investigation period (WATERLOO et al. 2000) soil loss was 0.35–1.12 t ha⁻¹ yr⁻¹ in the Songkwé catchment, 1.07–3.4 in the Nyangong catchment and 2.1–6.8 in the Biboo-Minwo catchment. Modelled soil loss in the study at hand exceeds these values. Nevertheless, in the second investigation period in the same catchments, soil loss was partly higher due to clearing and logging. The values fit to the range of the long-term Mefou-values. Soil loss in the second period was 0.2–0.6 t ha⁻¹ yr⁻¹, 4.6–14.6 and 2.7–8.6 t ha⁻¹ yr⁻¹, respectively (NTONGA et al. 2002). Two third of the values are again exceeded by the present soil loss, but the values of the Upper Mefou catchments are in accordance with the values of the Nyangong catchment.

Conservative ratios are used to convert sediment yields from the catchments in Southern Cameroon. If one would rely on catchment size for calculating the SDR, they would be higher (Roehl 1962, cited in WALLING 1983). Thus it can be presumed that the soil loss rates of the present study exceed published values and are high, but they are in same order of magnitude.

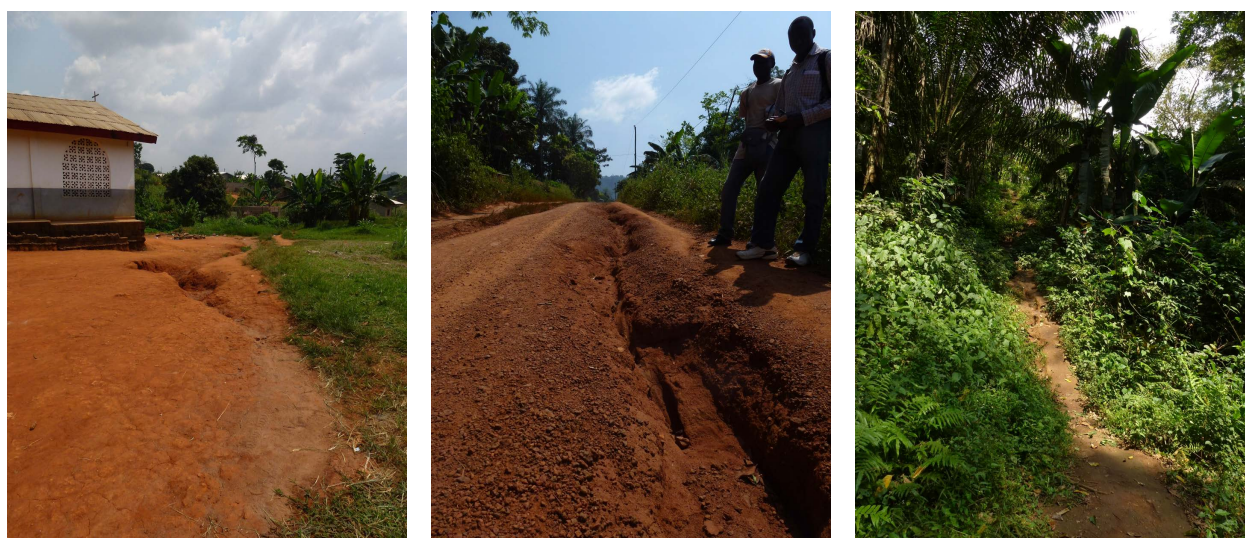
Values vs risk

The values of modelled potential as well as actual soil erosion are on the same level as published values. The mean soil loss of the catchment is nevertheless higher than the mean soil loss of other catchments in Cameroon as obtained by the analysis of sediment yields; the validation has shown that the modelled erosion is slightly overestimated. In addition, the high values of some areas in the study at hand ($> 200 \text{ t ha}^{-1} \text{ yr}^{-1}$) are far from reality.

As it is described in detail in Section 2.3, not the quantitative results of erosion modelling are important for soil erosion risk assessment, but only the relative values, which indicate areas of high risk. This is done in the study at hand. The map of the actual erosion risk shows where erosion is relatively high, the comparison of actual and potential erosion risk highlights that erosion is extraordinary high around the reservoir and the periurban area and the simulation of the future erosion risk shows where a land use and land cover change would have the most severe impacts.

6.2 Soil erosion from roads and trails

As the discussed soil erosion risk does not take erosion from roads or tracks into account, it might even be higher at some places.



(a) Rill erosion on a yard adjacent to a church in a periurban settlement (Nkolbisson).

(b) Rill erosion and loss of fine material on an unpaved road in the rural lowlands of the catchment.

(c) Small erosion feature on a trail used for the transport of water from a source in the headwaters.

Figure 6.1: Erosion features on roads, trails and settlement areas (Photos: F. Becker, December 2012)

Soil erosion from unconsolidated roads, paths and trails is a topic in the literature in various contexts (FORMAN & ALEXANDER 1998), either in urban areas (VOGLER & BUTLER 1996), hicking areas (BRATTON et al. 1979) or even in an agricultural setting, where small trails are used by farmers to reach their fields. The erosion impact of unconsolidated roads and trails is determined by direct erosion on the surface or by landslides and gullies triggered by road construction (FORMAN & ALEXANDER 1998). Roads might also be a sediment trap or reduce runoff (FORMAN & ALEXANDER 1998). While the latter effect will not be discussed here, soil loss on unconsolidated roads and trails is important to be mentioned: The amount of soil eroded from roads is huge—and not considered in the RUSLE3D.

In a two years study on St. Croix, Virgin Islands, RAMOS-SCHARRÓN et al. (2014) got soil loss values which were one to three orders of magnitude higher on unconsolidated roads than on hillslopes. DOUGLAS (2003) conducted a short term experiment on forest roads after logging on Malaysian Borneo. He measured a soil loss of 0.53 t ha^{-1} on a one-year-abandoned skid trail, while the soil loss was only 0.38 t ha^{-1} in a primary forest. Also in tropical southeast Asia (Java), the contribution of non-vegetated surfaces to the total sediment yield was 38.8%, where the amount of soil eroded from trails (24.5%) was higher than from roads (4.3%) or settlement (10.0%) (RIJSDIJK 2005). DE MEYER et al. (2011b) estimated soil loss rates in the Lake Victoria Basin in Uganda and found out that erosion from roads and trails considerably amounts to total erosion; while 7.5% of the sediment yield are from “landing

sites”, 2.2% originate from footpaths and 19.5% from unpaved roads. In addition, they found out that on older roads, erosion was less due to progressive compaction of the soil layer and a consequently reduced erodibility.

Soil loss from roads, trails or settlement areas—which comes to 29%–58% in the mentioned studies in the humid tropics—is not covered by the RUSLE3D. Thus, it can be assumed that total soil loss is higher in the Upper Mefou subcatchment than the modelled amount of 9 t yr^{-1} . Small trails are common in the catchment. Especially around the Mefou Reservoir, where land use is more extensive and intensive than in other parts of the catchment (see Section 3.4), these paths are frequent. Rill erosion on roads and settlement areas is frequent in the catchment (Figure 6.1).

6.3 Erosion determining factors

As the application of USLE-family models in a context other than the original study areas is complicated, an application is only useful if all factors of the models are reasonably adapted to the actual study area. Therefore it is imperative to discuss the results of the single factors.

6.3.1 Soil erodibility

The mean approximated K-values of the Upper Mefou subcatchment is 0.023 ± 0.007 [SI]. Only 3 of 36 values exceed 0.03, only 1 is below 0.1. These values fit very well in the range of values presented for tropical soils on a global or African scale (Table 6.2: items 1–7). They are also in accordance with the values quoted by ROOSE (1977), who tested the application of the USLE in West Africa and deemed the use of the erodibility nomograph acceptable for West African ferralitic soils. Studies with a regional focus on humid Nigeria draw a more ambivalent image. While the values approximated by OLORUNLANA (2013) and VANELSLANDE et al. (1984) on clayed eutric Nitisols are far below the values of the present study (maximum: 0.011, Table 6.2: 9–10), other studies found much higher values on Nitisols and Acrisols (Table 6.2: 11).

This aspect emphasizes that not only the value range of tropical (West) African erodibilities is very high, also the variability on similar soil types might be enormous, what stresses the need to have a more specific view on sandy loams and Ferralsols (Oxisols), which is the major texture or soil type in the Upper Mefou subcatchment. The mean approximated erodibility value of Nigerian sandy loams (n=14) given by VANELSLANDE et al. (1987) is similar to the erodibility approximated for the Mefou catchment. The values for southern Nigerian Ferralsols are in generally higher than the values in the present hand (Table 6.2: 9–17, 12–14).

Table 6.2: Erodibility of African and tropical soils: ‡ estimated value (nomograph, approximation); † measured values. An astrisk (*) marks review papers.

	Location	Soil	K-value [SI]	Reference
1	Global	tropical soils	0.008–0.063	EL-SWAIFY et al. 1982
2		tropical ferruginous soils	0.026–0.040	ROOSE 1996*
3	Tropical Africa	ferralitic soils on granite	0.016	ROOSE 1996*
4		ferralitic soils on schist	0.026	
5		ferralitic soils on volcanic deposits	0.053	
6	Humid Africa	ferralitic soils	0.001–0.05†	ROOSE & SARRAILH 1989*
7	Mountainous Africa	ferralitic soils	0.004–0.0358†	ROOSE & SARRAILH 1989*
8	West Africa	Tropical ferruginous and ferralitic soils	0.001–0.042	ROOSE 1977*
9	South-west Nigeria	–	0.007–0.011‡	OLORUNLANA 2013
10	Southern and central Nigeria	clayed eutric Nitosol	0.01‡	VANELSLANDE et al. 1984
11	Southern Nigeria	Nitrosols and Acrisols	0.03–0.06‡	IGWE 2003
12	Nigeria	sandy loams	$\bar{x}=0.024\pm 0.013^\dagger$	VANELSLANDE et al. 1987
13			$\bar{x}=0.013\pm 0.013^\dagger$	
14	Southern and central Nigeria	sandy ferric Acrisol and xanthic Ferralsol	0.03 and 0.06‡	VANELSLANDE et al. 1984
15	South-east Nigeria	Ferralitic soils	0.004–0.053‡	IDAH et al. 2008
16	Southern Nigeria	Ferralsol	0.05‡	IGWE 2003
17	Humid Nigeria	Oxisols	0.005–0.063	LAL 1985*
18	Central Cameroon	Oxisols	0.001–0.037 †	NILL 1993
19	Upper Mefou subcatchment	Oxisols	0.023±0.007‡	<i>study at hand</i>

Also on Ferralsols, NILL (1993) measured values from 0.001 to 0.037—fostering the above mentioned problem of high variability within similar soil types. For example VANELSLANDE et al. (1984) tested ferralsols, but organic matter content was considerably less and the percentage of the clay fraction considerably greater. A comparison of values is furthermore hampered due to the application of different methods to calculate the K-factor. Nevertheless, the K-values for the Mefou catchment do not seem to be out of range. In comparison to the other studies, the values are on a medium level.

Organic matter

Triple determination of the total inorganic carbon content of three samples shows that most of the variation is less than 0.1 pp with a maximum variation of 0.25 pp. TIC values measured for CaCO_3 (12% TIC) range from 11.2% to 14.0%; the mean deviation from the expectation is ca. 1 pp (8.6%). Although this error seems to be high, it might be acceptable due to the relatively low overall TIC values ($0.3\% \pm 0.2$ pp); the uncertainties will not result in importantly wrong organic matter (OM) contents. Double determination of TC values revealed that the error is less than 5%. When comparing the measured OM-values with published values from other sites with similar conditions, it is important to consider that there is no standard procedure to test for organic carbon; most studies used the Walkley–Black method, others dry combustion. The results of both methods have a high correlation coefficient, but absolute values might differ due to differences in parameters (cf. SOON & ABBOUD 1991; SLEUTEL et al. 2007; SATO et al. 2014). What is also relevant is that the conversion factor to calculate OM from TOC differs between studies or is not reported. Thus, published values are given here, the values from publications only giving OC-values were converted with a factor 2 (PRIBYL 2010). The difference between the traditional factor 1.724 and 2 might also be relevant for total K-values or consequently soil loss values. High OM-values of the study on hand might partly be explained by a high conversion factor.

AMBASSA-KIKI & NILL (1999) analysed organic carbon content (OC) of soils in the vicinity of Yaoundé, ranging from 1.1% at a bare-fallow to 3.2% in a secondary forest. The mean value of the OC-contents in the Upper Mefou catchment fits with this range ($2.6\% \pm 0.9$ pp), but is relatively high. Also NOUNAMO (2001) reported slightly lower OC-values for the humid tropics of southern Cameroon (1.8–2.6% in sandy soils), whereas in a sandy loam in southern Nigeria, OM-values were clearly lower (OBI & NNABUDE 1988). The OC-values of YEMEFACK (2005) from Ferralsols in southern Cameroon’s forests—averaging $3.17\% \pm 0.18$ pp—are in contrast higher than the values in the present study. In all the studies, OC/OM-contents strongly depend upon land use type or intensity (YEMEFACK 2005). Forest soils have the highest values, whereas cultivated soils have medium values and bare-fallows the lowest values (OBI & NNABUDE 1988; AMBASSA-KIKI & NILL 1999; NOUNAMO 2001); in the Upper Mefou catchment, forests and plantations have a significantly higher OM-content than fields, whereas the difference between fallows and other land uses is not significantly different. Altogether, the values presented here fit to published values, but some are relatively high.

A critical question concerning organic matter content is whether the applied formula to calculate K-values is suitable for high OM-values. The erodibility nomograph (WISCHMEIER et al. 1971) is only valid for $\text{OM} < 4\%$. For the algebraic approximation, no maximum OM-

content is mentioned in the RUSLE manual (RÖMKENS et al. 1997). Still, EL-SWAIFY et al. (1982) notes that the nomograph—including the approximation—was developed from a limited database; the maximum OM-value of this database is 5.5%. Around half of the present samples exceed this value. As a definite conclusion on the suitability of the nomograph for high OM soils can not be drawn here, this point has at least to be considered when discussing K-values.

Permeability

The results of the infiltration testing demonstrate the parameter's variability; the mean conductivity is $0.5 \pm 0.6 \cdot 10^{-3} \text{ cm s}^{-1}$, but values range from 0.016 to $3.290 \cdot 10^{-3} \text{ cm s}^{-1}$. Conductivities measured by WATERLOO et al. (2000) and NTONGA et al. (2002) tend to be much higher. They range from 0.9 to $9.7 \cdot 10^{-3} \text{ cm s}^{-1}$ on forest soils in southern Cameroon. OBI & NNABUDE (1988) observed higher values as well, with a minimum of $2.5 \cdot 10^{-3} \text{ cm s}^{-1}$ and a maximum of $2.4 \cdot 10^{-2} \text{ cm s}^{-1}$. These differences do not necessarily point out that the values are incorrect. They rather show that infiltration and conductivity values cover a wide range of values. The high values of OBI & NNABUDE can be explained by a very high proportion in the sand fraction up to 90%. The values measured in the Mefou catchment may not be similar to other values from the ferralitic soil of the humid tropics, but fit to a generalized table of conductivity and texture, as it is presented by BEAR (1988).

Measured infiltration in southern Nigeria is ordered from high to low rates as follows (OBI & NNABUDE 1988): butterfly pea > Panicum > tilled cocoyam > non-tilled cocoyam > tilled groundnut > non-tilled groundnut > bare fallow. This is quite different to the values at hand, where the values follow the order field > (bush) fallow > plantation > forest/bush. Only the means of fields and forests and fields and plantations differ significantly. The order seems to be the other way round: fields have greater values than fallow; natural vegetation has the lowest infiltration rate, not the highest. At least the high values of fields in the Mefou catchments seems to be reasonable because of seed-bed preparation with hoes after clearance. The high influence of tillage is illustrated by higher infiltration values on ridges than between ridges.

Grain size

The influence of grain size on approximated K-values is relatively high; firstly, two of five parameters of the nomograph—modified silt and modified sand—are grain size variables; secondly, the samples with high K-values have an *outlying* proportion of the silt separate, but only average values in the other parameters (Figure 5.4). The sensitivity analysis of

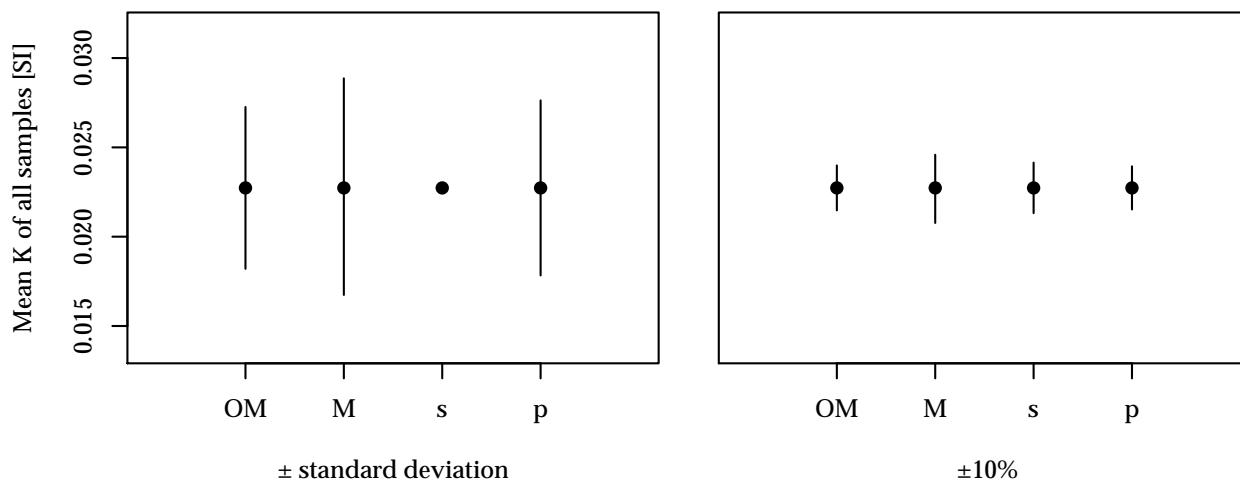


Figure 6.2: Sensitivity analysis (one-factor-at-a-time) of the erodibility factor K : The mean K -value of all samples is marked with a bullet (\bullet), the lines ($|$) show the change of the mean K -value when one of the input parameters of the K -approximation is changed by either its standard deviation (left plot) or by 10% (right plot); OM = organic matter, M = function of modified silt and modified sand, s = structure class, p = permeability class. Note that s is constant for all samples and that a change of the non-metric classified parameters (s, p) by their standard deviations or 10% is somewhat incorrect, but done for comparative reasons. K is given in SI-units ($\text{t ha h ha}^{-1} \text{MJ}^{-1} \text{mm}^{-1}$).

the K -factor (one-factor-at-a-time) shows that the grain size parameter M (a function of modified silt and modified sand) is the most sensitive (Figure 6.2).

In comparison with other studies on soil erodibility, the silt content is slightly higher in the Upper Mefou subcatchment. The sand content is higher and the clay content is clearly lower. AMBASSA-KIKI & NILL (1999) reported clay contents of 13%, 20% and 30% for three samples from the vicinity of Yaoundé; NILL (1993) reported even higher values averaging 40% clay ($n=13$); IGWE (2003) reported a mean clay content of 16%. The samples from the Upper Mefou subcatchment have a mean clay content of $11\% \pm 3 \text{ pp}$. As clay is a factor reducing soil erodibility due to its ability to bind particles, the low clay contents measured here are of great importance. Three reasons may be given to explain a possible underestimation:

(1) The development of the K -estimation is based on the “standard” procedure to measure grain size (pipette method). Also most studies on erodibility use this method. Laser diffraction—the method applied here—delivers results which are different from that obtained by sieving and the pipette-method. Most studies agree that the percentage clay is *underestimated* by laser diffraction (KONERT & VANDENBERGHE 1997; MUGGLER et al. 1997; BEUSELINCK et al. 1998; BUURMAN et al. 2001). In addition KONERT & VANDENBERGHE (1997) found out that grain sizes $> 2 \mu\text{m}$ are positively biased towards more coarse fractions. Also the determination of the aggregate size distribution is biased towards coarser fractions when

using laser diffraction instead of dry or wet sieving (BEUSELINCK et al. 1999). BUURMAN et al. (2001) demonstrated that factors of 0.42, 0.62 or 0.62 have to be used to get pipette-clay from laser-clay for fluvial, marine or loess deposits. BEUSELINCK et al. (1999) however notes that there is no unique conversion factor for different soil types. The *underestimation* of the clay fraction might be explained by the platy, non-spheric shape of clay particles what does not meet the assumption of particle sphericity; laser diffraction is based on that assumption. Thus, non-spheric particles will have a greater volume. In addition, gas bubbles might cause an overestimation of coarse fractions (LOIZEAU et al. 1994). The *underestimation* of the clay fraction is relevant for erodibility estimation; all samples in the study on hand will have too high K-values if the clay fraction is negatively biased—erodibility is overestimated.

Nevertheless, the effect can be put in relative perspective; the *underestimation* of the laser method is relative to the overestimation of the pipette method, which is biased towards smaller particle sizes (BUURMAN et al. 2001).

Organic rich samples show a problematic weight–volume relationship if organic material is not fully dissolved. Values delivered by laser diffraction are in percentage volume, while the classical pipette values are in percent weight. Organic material has a lower density than mineral components of soil.

(2) Sample preparation for grain size determination included the treatment with hydrogen peroxide to dissolve organic matter. Due to a high content of organic matter, treatment was complicated and a lot of repetitions were necessary in the study at hand. For some samples it might be true that not all organic material is dissolved completely. As it is shown in Figure 6.3, treated and non-treated samples have different grain size distributions. The non-treated samples have a higher proportion of particles in the fine silt separate. The samples Nk18, Nk8 and Nk10F for example show a high proportion in this separate, which is higher than the fourfold standard deviation of the mean grain size of all samples. Especially the percentages of the silt fraction of these samples are probably overestimated, which will result in a high K-value. This is true for the samples mentioned. A study comparing different protocols of hydrogen peroxid treatment and non-treatment got—in contrast—no dramatic differences in grain sizes in sediments, except for marshland samples (GRAY et al. 2010).

The samples from the Upper Mefou subcatchment were not treated with sodium dithionite-citrate-bicarbonate to dissolve sesquioxides. This might lead to an underestimation of the clay fraction: It is often supposed that sesquioxides are an important binding agent of aggregates in ferralitic soils (EMBRECHTS & SYS 1988; BRYAN 2000). Macroaggregates ($> 250 \mu\text{m}$) are more likely dissolved when treated with hydrogen peroxide or even by sonification, because organic components such as plant or root debris are the more important binding agents of

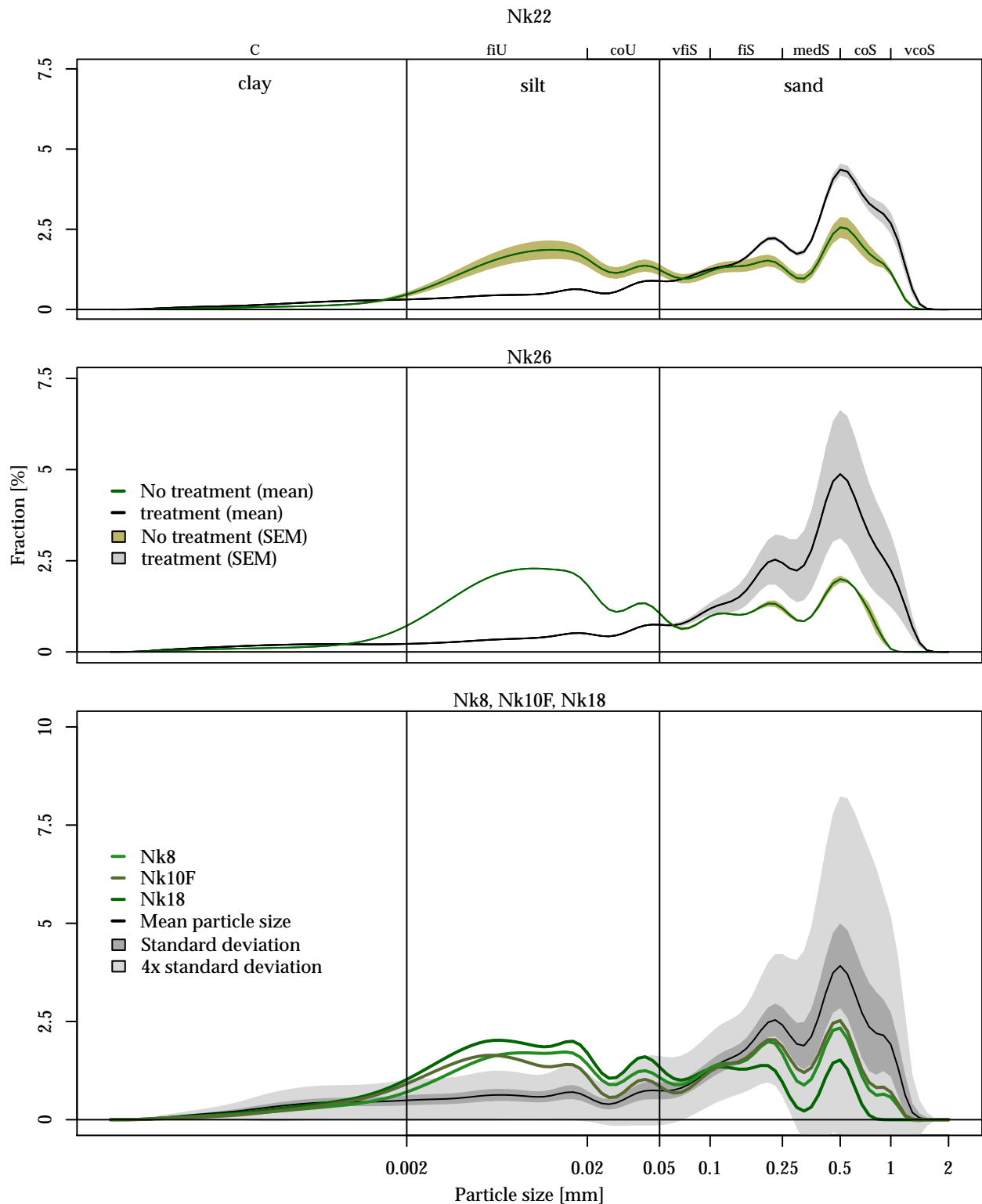


Figure 6.3: Comparison of samples treated with hydrogen peroxide and not chemically treated samples. The content of silt, modified silt and modified sand as well as erodibility values are given in Table 5.3.

macroaggregates (BRYAN 2000). EMBRECHTS & SYS (1988) report a defragmentation of the aggregates in the upper horizon of soils on steep slopes, where the easily dispersable clay (EDC) is laterally transported. In the horizon with less EDC, aggregation is less due to a lower portion of binding agents. Nevertheless, EMBRECHTS & SYS (1988) highlight the role of zoogenic aggregates in the near-surface horizons. These aggregates are dissolved with the preparation procedure applied in the study at hand.

Due to the role of less erodible aggregates, it is often assumed that treatment of samples increases the calculated erodibility. In the study at hand, the opposite is true: The samples of only wetted and sonificated samples have a higher erodibility than pretreated samples. Large macroaggregates might be destroyed during the transport of samples from the study area in Cameroon to the laboratory at Freie Universität Berlin, but are nevertheless taken into account in the structure-subfactor of the erodibility equation (see 4.1.2).

EL-SWAIFY et al. (1982) comment that testing of soil properties for the USLE is method sensitive, especially grain size analysis. 10 Hawaiian soils showed—in comparison with apparent texture—a slightly higher K-value when treated only with water and a clearly lower K-value when treated with sodium hydroxide ($0.018 \pm 0.007 < 0.018 \pm 0.009 > 0.012 \pm 0.008$; EL-SWAIFY et al. 1982). No standard procedure to determine the values of modified silt and modified sand exists for the calculation of RUSLE's K; neither for treatment nor for the method to measure grain size.

Methodological limitations

The use of Wischmeier and Smith's nomograph or its algebraic approximation for estimating soil erodibility is criticized by various others (EL-SWAIFY et al. 1982; VANESLANDE et al. 1984; VANESLANDE et al. 1987). In Table 6.2: 12–13 measured and approximated mean values are given for sandy loams in Nigeria. The measured values are approximately twice higher than the approximated values, which leads the authors to the conclusion that “Values of K estimated using the nomogram . . . do not give a satisfactory measure of erodibility for some soils of the tropics” (VANESLANDE et al. 1984). They propose to take reduction of infiltration rates due to surface sealing during rainfall events into account as well as iron oxides as binding agents. This aspect is taken up by ROTH et al. (1974), who developed a nomograph based on sesquioxides content. Because the role of bounding agents and aggregate stability and size distribution on erodibility is discussed in Section 2.1.2, only a few remarks will be given here. On one hand, the soils of the Mefou catchment were not tested for aggregate stability or mineral composition directly. But on the other hand, at least the percentage of aggregates 0.2–0.63 μm is used to calculate tropical K-values (NIL 1993). Due

to the fact that the clay content is relatively low in the tested soils and the samples were not treated with sodium dithionite-citrate-bicarbonate, aggregates are not completely dissolved and considered in the calculation of soil erodibility as “pseudo-silt” or “pseudo-sand”. As the models and relations of NILL (1993) are based on measured values, it seems to be reasonable to use the tropical K-value, although neither aggregate stability nor sesquioxides were tested. Some authors (ROOSE 1977) consider even estimations based on the Wischmeier–Smith nomograph for correct.

6.3.2 Cover and crop management factor

The Normalized Difference Vegetation Index (NDVI), and even the reflectance of Landsat TM band 5 and 7, are used to classify tropical land use and land cover in shifting cultivation systems. The most relevant problem in doing so is the relation of field or patch sizes and satellite resolution. As some of the patches in the study have only an area of 0.2 ha or even less, a grid cell area of 0.09 ha (30×30 m) seems to result in a high number of mixed pixels. In addition—as noted by YEMEFACK (2005)—most of the patches are covered with vegetation, whether cultivated areas or forests. Only roads or settled areas are without vegetation. Otherwise, LUCAS et al. (2000) used low resolution images to discriminate various regeneration states of tropical humid forests. Regarding the separability of different land use classes, the number of explicit classes seems to be important when using Landsat-images. Often it is possible to discriminate between bare soil and forest with very high accuracy (HARTTER et al. 2008). In a humid forest in southern Cameroon, the NDVI is a sufficient index to separate bare ground from forest or cultivated areas (YEMEFACK et al. 2006).

The NDVI of bare ground and dense forest as seen on a GoogleEarth-image was used to calculate a linear model of the NDVI and RUSLE’s C-factor; C-factors of bare ground and dense forest are well known and are the maximal and minimal possible C-factor values. Using NDVI to model the C-factor is a well known approach which is applied in different environments. In Taiwan, LIN et al. (2002) compared a NDVI-derived C-factor map with a map based on classified land use maps and obtained similar results. GARATUZA-PAYÁN et al. (2005) were able to explain 98% of the temporal variability of erosion with the variation of NDVI values. Also CHILAR (1987) successfully used spectral reflectance to model soil erosion. In contrast, DE JONG (1994) found a low correlation between NDVI and C-factor ($r = -0.67$). They explained the low accuracy of NDVI predicted C-factors with different methodological assumptions. The NDVI—and remotely sensed reflectance values in general—are highly sensitive to plant physiological structure and pigments, whereas the C-factor is an indicator for vegetation cover (DE JONG 1994). Analysis of measured erosion and NDVI-modelled

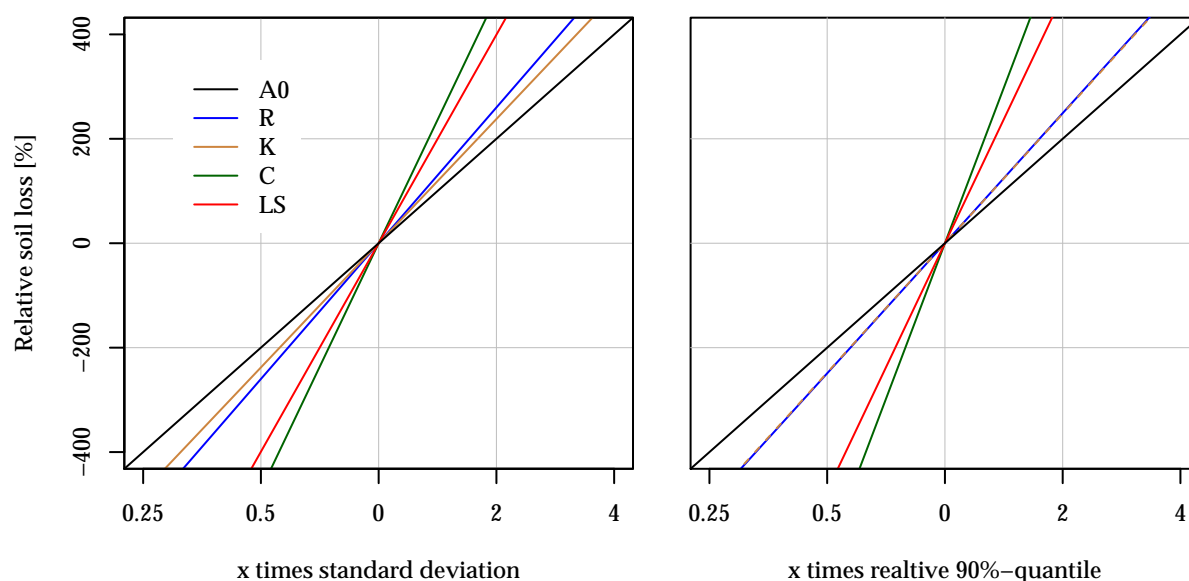


Figure 6.4: Sensitivity analysis (OFAT method) of RUSLE's input values and factors. The soil conservation factor P is constant for the entire catchment and was therefore not tested. The left plot shows the response of soil loss (A) to the change of one input factor by its standard deviation, the second a change of one input factor to its 90%-quantile.

C-factors show that high erosion was incorrectly classified as severe and slight erosion was classified as nil (ASIS & OMASA 2007). In this study, only a small number of C-factor pixels were classified in the group 0–0.1. However, KNIJFF et al. (2002) found out that the predictability of C differs between pixels with small and pixels with great NDVI-values due to the effect of mulch cover. Mulch is important for protection against raindrop impact and normally included in the calculation of the C-factor, but not very well estimated by NDVI due to the higher sensitivity to vitality than cover. NAGLER et al. (2000) in contrast states that the NDVI relevant bands are indeed able to detect litter. Similar results are reported by BIARD & BARET (1997). In addition to KNIJFF et al. (2002), MEUSBURGER et al. (2010) got good results for soils with a ground cover >50%; in their opinion, the albedo effect of soils is important only in that case. Taking into account that the ground cover in the Mefou catchment is often greater than 50% and the fact that some authors successfully used the NDVI to model RUSLE's C, the NDVI is used in the study at hand. Nevertheless, it has to be taken in mind that erosion might tend to extreme low or extreme high values when using NDVI to estimate C.

NILL (1997) mentioned the high variability of the C-factor in the humid tropics, which is far higher than the variability of the other factors. Also in the case of the modelled C-values for the Upper Mefou subcatchment, the variability of the C-factors has the greatest

impact on soil loss values (Figure 6.4). Thus, in some parts of the catchment, the C-factor is low (i. e., dense forest or bush) and high in other parts of the catchment (cultivated or deforested areas). This is shown by comparing the actual soil loss and the potential soil loss in the catchment: Soil loss is much higher where the natural vegetation cover is disturbed. In the Upper Mefou subcatchment, this disturbance is related to settlements, especially the periurban areas of Yaoundé. The consequences of deforestation and urban growth are also shown by other authors for the Southern Cameroon Plateau (VAN SOEST 1998; MERTENS & LAMBIN 2000; SUNDERLIN et al. 2000).

The values of the modelled C-factor are typical for the humid tropics of West/Central Africa (ROOSE 1977; EL-SWAIFY et al. 1982; NILL 1993; NILL et al. 1996; NILL 1997), as large areas are covered with dense forest or are used for intercropping. The distribution of C-values—higher values in the periurban areas and lower values in the rural areas—fit to the general description of land use and land cover in the catchment (Section 3.4).

6.3.3 Rainfall

Eight models were applied to calculate the erosivity factor R of the RUSLE3D. This application of different approaches aims at testing the influence on model selection on the resulting R-value and thereby the uncertainty coming along with the selection of a specific model. Modelled R-values for the Nkolbisson station range from 10 015 to 15 658 MJ mm ha⁻¹ h⁻¹ yr⁻¹, depending on the approach. Values for Yaoundé are quite similar to those of Nkolbisson; the difference is within the margins of the standard error of the mean. Thus, the considerably different length of the observation periods does not effect the results. Nevertheless, it is important to note that precipitation totals changed during the record period of both stations, Yaoundé and Nkolbisson. NICHOLSON et al. (2012b) and NICHOLSON et al. (2012a) used semi-quantitative precipitation data (1801–1900) and rain gauge data (1901–1998) to compile a rainfall data set for Africa. During the recording period of the Nkolbisson station (1956–1980), rainfall changed from precipitation totals higher than the mean to totals below the long term mean. From the mid 1970s until 1998, precipitation is far lower than from 1940 to the mid 1970s and lower than the long-term average (NICHOLSON et al. 2012b). Also LE BARBÉ et al. (2002) show that precipitation in the two decades from 1950 to 1969 was higher than the standard deviation of the long-term precipitation and lower than 1970–1997. A decrease of the precipitation up to 2010 is also reported (MCSWEENEY et al. 2010a; MCSWEENEY et al. 2010b) The approximation in the study on hand based on the period 1956–1980 therefore seems to overestimate present R-values. However, the long-term mean R-values from Yaoundé

(1889–1996)—covering wet and dry periods—are not importantly different and it is therefore appreciated that the R-values used are more or less acceptable.

Moreover, the calculated R-values—irrespective of the applied model—fit to the range of values published. VRIELING et al. (2010) and VRIELING et al. (2014) mapped satellite-based R-values for all of Africa, where the values for the Southern Cameroon Plateau range from 10 000 to 15 000. Also an isoerodent map of West Africa (ROOSE 1977) shows values in the same order of magnitude (12 000–15 000); The values of ARNOLDUS (1980) are slightly higher. FOURNIER (1993) however notes that values in at least the grasslands of western Cameroon are slightly lower than the values for entire West Africa (ROOSE 1977), especially in mountainous regions. The seasonal variability and the higher standard deviation in months with higher erosivity are in accordance with other studies (VRIELING et al. 2014).

In general, the regressions used to model R-values of the Upper Mefou subcatchment are not site-specific. The databases used to get the regressions might include stations with more or less rainfall totals, with different intensities or a different rainfall regime. The only approach taking spatial variability into account is the ARESED model (DIODATO et al. 2013). In the study at hand, the results of this approach seem to be problematic due to a great difference between the results of Yaoundé and Nkolbisson.

The data sets of the regressions and the present study are not identical, what might also effect the accuracy of the modelled results (VRIELING et al. 2014).

Spatial variability of rainfall in the Upper Mefou subcatchment was not taken into account in the present study. According to KIET (1972), annual rainfall totals in Yaoundé depend on altitude and varied between 1579 and 1940 mm in 1970–1971 for an altitude range of approximately 400 m. Unfortunately, KIET does not give any regression equations or sufficient maps to develop a reliable altitude–rainfall relationship.

Lastly, it should be noted that all erosivity models used here are based on either R-value as calculated in the USLE or it's revisited version. It is under discussion if the energy and intensity relationships of both equations are reliable (VAN DIJK et al. 2002); short duration intensities might be underestimated (VRIELING et al. 2014). Other indices of tropical rainfall were developed (see Section 2.1.1, LAL 1976; OBI & NGWU 1988), but no regression for a limited database exists. An lower erosivity when applying RUSLE-based estimations than USLE-based estimations (YU 1998) is not true for the study at hand (Table 5.1).

6.3.4 Topographic factor

The topographic factor of the USLE and its revisions is—especially in the last two decades—the most widely discussed input factor. In contrast to the other factors of the USLE, which

can relatively easily be implemented in Geographical Information Systems (GIS), the original LS-factor (WISCHMEIER & SMITH 1978) is difficult to implement. In the study on hand, the modification of MITASOVA et al. (1996) was therefore used to model the topographic potential of erosion, which is based on catchment area. Various other studies use the approach in the RULSE3D or the USPED model and deem the results to be plausible (WARREN et al. 2005; KUMAR & KUSHWAHA 2013; STANCHI et al. 2013; ZHANG et al. 2013). Some problems of the application of the concept in the present study nevertheless have to be discussed.

The DEM used to calculate slope angle and catchment area is an SRTM DEM with a horizontal resolution of 90 m. In comparison to other studies, this is a very coarse resolution (i. a. MITASOVA et al. 1996: 30 m, KUMAR & KUSHWAHA 2013: 20 m, and GARCIA RODRIGUEZ & GIMENEZ SUAREZ 2012: 10 m). ZHANG et al. (2008) work out that a 30 m SRTM DEM is not suitable for erosion prediction with the WEPP model; they achieved better results with a 10 m DEM. More quantitative, KIENZLE (2004) cites values from KwaZulu-Natal in South Africa where mean soil loss calculated with a 100 m DEM was not clearly different from a 50 m-DEM soil-loss (31.3 and 35.4 t ha⁻¹ yr⁻¹ respectively); however, maximum values of the finer DEM were twice higher. WU et al. (2005) applied a modified USLE and got a third higher soil loss when using a 10 m DEM instead of a 100 m DEM. MUTUA et al. (2006) obtained satisfactory validated soil loss values from a 90 m DEM in Kenya. Slope values calculated on aggregated DEMs from point data of a catchment in the Salzgitter Mountains, Weser Upland, Germany, were lower for coarse DEMs (e. g. 7.05% vs. 5.45% when comparing slope angles derived from a 25 m DEM and a 100 m DEM respectively; KIENZLE 2004). Similar results were obtained for mean slope and for maximum slope (THIEKEN et al. 1999). In the study at hand, slope derived from a 90 m DEM was slightly higher than the slope derived from the 30 m ASTER DEM. Comparing a 30 m DEM with a high resolution DEM, EASTER et al. (2000) note that DEM derivative based on a high number of grid cells— what applies for slope and especially for catchment area—are erroneous even if the DEM is not, what might be explained by the fault propagation. In a comparative study in a “gently rolling landscape” in northern Germany, the catchment-area-based mean slope-length-factor (L) was slightly more than two times higher when using a 90 m DEM in comparison to a 1 m reference DEM; also dispersion was higher (LIU et al. 2011). In contrast, in a subcatchment of the Potomac River, Ridge-and-Valley Appalachians, higher LS factors (LS>2.5) were more frequent when using a 10 m DEM instead of DEMs with resolutions 30–250 m (WU et al. 2005). As it is shown in Figure 5.6b and Table 5.4 catchment area (per unit contour width) is lower for the coarse 90 m SRTM DEM than for the 30 m ASTER DEM. In conclusion, the SRTM DEM applied in the study at hand seems—regarding resolution—to underestimate

Table 6.3: Influence of selected LS rill-to-interrill parameter (m) on soil loss. Values are factors of total soil loss in relation to $m = 0.4$, which is the commonly used value (i. a. MITASOVA et al. 1996). A graphical representation of the influence of m on LS/S—the slope length component of the topographic factor—is shown in the the Appendix (p. viii). In the study on hand, $m = 0.1$ is used to calculate RUSLE3D’s topographic factor LS.

	$m = 0.1$	$m = 0.2$	$m = 0.3$	$m = 0.4$	$m = 0.5$	$m = 0.6$
soil loss factor	0.35	0.49	0.70	1.00	1.46	2.17

the S factor and in some cases also L and therefore also soil loss; while some authors deem erosion estimated with a coarse DEM for not reliable, others obtained good results.

The selection of flow routing algorithms also influences the LS factor. The LS-factor calculated on basis of the Multidirectional flow algorithm (FREEMAN 1991; QUINN et al. 1991) got more extended areas with high catchment area in valleys than the two-directional flow algorithm (TARBOTON 1997). Thus, the mean LS-factor of the Upper Mefou subcatchment was higher in the first case. LIU et al. (2011) notes that the selection of one from five algorithms was less important for a low resolution DEM in northern Germany; for a more pronounced relief, it might be more important. The D_{∞} -algorithm applied in the study at hand is recommended—at least for a 10 m DEM—for LS calculation by GARCIA RODRIGUEZ & GIMENEZ SUAREZ (2012), who tested nine algorithms in the Arroyo del Lugar basin, Central Spain. Also HOFFMANN et al. (2013) suggest to use the D_{∞} -algorithm to compute LS.

Besides catchment area and slope angle, two parameters are used to calculate MITASOVA et al. (1996)’s LS. The slope parameter n will not be discussed here, due to the fact that $n = 1.3$, as proposed by MITASOVA et al., is widely used and accepted. For the water/flow parameter m different values were used, which are also different from the originally proposed values ($m = 0.4$ or $m = 0.6$). WISCHMEIER & SMITH (1978) calculated m as a function of slope angle; in the RUSLE (RENARD et al. 1997) m is defined as the rill-interrill ratio, which is also a function of slope. MITASOVA et al. (1996) describes m as an exponent reflecting the interaction of different types of flow and soil detachment and transport. For a combination of sheet flow and turbulent flow, m is 0.4, whereas for prevailing rill and gully erosion and highly turbulent flow, m is 0.6. The underlying assumption is that flow on steeper slopes is more turbulent (HOFFMANN et al. 2013). The hydrological effect of vegetation cover might also be incorporated in the parameter. MITASOVA et al. (1996) propose $m = 0.6$ for disturbed vegetation, $m = 0.5$ for sparse grassland, $m = 0.4$ for grassland and $m = 0.2$ for forests, HOFFMANN et al. (2013) propose to use $m = 0.4$ for catchments with alternating land use and $m = 0.1$ for a dense plant cover. Other authors used $m = 0.6$ or $m = 0.4$ for *forests* (SIMMS et al. 2003; FERREIRA et al. 2008), however, without elaborating on the

reasons to choose these values. In the study at hand, $m = 0.1$ is selected. On the one hand because of an absence of pronounced rills in the catchment after rainfall, on the other hand due to a relatively dense vegetation cover. However, it should be noted that based on slope angle, m should be higher. Soil loss values would be much higher in the Upper Mefou catchment if $m > 0.1$ (Table 6.3), what emphasizes the influence of the LS-factor and the parameter selection on total soil loss values in the catchment. Nevertheless, the often reported overestimation of soil loss by the USLE is i. a. attributed to slope length: DIKAU (1986) showed that the ratio of modelled to measured value is a function of slope length, with higher ratios on longer slopes. So, a low m -value seems to be appropriate here.

To close with the comments on the topographic potential of erosion in the catchment, the general usability of MITASOVA et al.'s approach should be discussed. Several authors brought out that manual methods to calculate LS underestimate the topographic potential (HOFFMANN et al. 2013). Thus, in comparison to other studies, the soil loss values in the study at hand might be relatively high. For the methodological discussion if MITASOVA et al.'s method is theoretically a sufficient replacement of the original LS-factor see the comments of DESMET & GOVERS (1997) and the reply of MITASOVA et al. (1997).

The problem of cut-off of flow paths is also relevant for the study at hand, where small tracks and roads are relevant for runoff and erosion (see Section 6.2, cf. LIU et al. 2011). Deposition areas are excluded in the study at hand using the unit stream power based *topographic erosion/deposition potential index*, which is elaborated in HOFIERKA et al. (2009) (cf. MITASOVA et al. 1996; MITAS & MITASOVA 1998; MITASOVA & MITAS 2001).

6.4 Validation

The validation applied in the study at hand is only a *very rough* approximation. Sediment layer thickness in the reservoir was only measured at a few sites, where dispersion of the thickness is wide; thickness divers within the bathmetry of the lake and the position in relation to outflow and inflow.

The dry bulk density of the sediments in the Mefou Reservoir was only approximated and is assumed to be constant over the entire reservoir. This is fairly difficult. In their study on retention ponds in Central Belgium, VERSTRAETEN & POESEN (2001: p. 375) conclude that “frequent and dense sampling of sediments is necessary to calculate a representative value of the dry sediment bulk density”. They found a dry sediment bulk density (dBD) of 1.02–1.66 g cm⁻³ in the Hammeveld pond, where dBD is not only a function of texture, but also of distance from inlet and water depth. The overall coefficient of variation of their pond

dBDs ranged from 7 to 80%; the error of using prediction equations ranged from -72 to $+16\%$. A comparably low dBD in the study at hand prevents from overestimation of the sediment yield. The value of 1.00 g cm^{-3} used here fits very well to a value presented for a lake in the vicinity of the Mefou Reservoir ($\bar{x}=1.06 \text{ g cm}^{-3}$, Lac Municipale de Yaoundé, NAAH 2013).

Also the calculation of trap efficiency—based on catchment area and reservoir capacity—is problematic, as it might also be a function of timing and amount of inflow. The reservoirs used to develop the Brown curve are not automatically suitable for other climates than the climate of the original area (BRUNE 1953). Also the velocity of the water in a reservoir is a factor influencing trap efficiency, as it is implemented in the Churchhill curve and its revisited versions (cf. BUBE & TRIMBLE 1986). Nevertheless, the Brown curve is still a method accepted for reservoirs (VERSTRAETEN & POESEN 2000). The application of a more appropriate curve is limited by data availability and still, the curves are not adapted to the climate of the present study area.

Excluding the operation period 1969–1976 from the sedimentation duration seems acceptable, as sediments might be naturally removed after 1976; they were intentionally removed in 2005. It is until now not known that there has been some removal of sediments on a large scale after the beginning of the rehabilitation of the dam in 2011. Only some very small businesses use lake sediments to sell it as construction material, what might not have affected the locations of sediment sampling.

The most critical point of the reservoir sediment survey is the sediment delivery ratio (SDR; WALLING 1983). In the study at hand, an average value from literature is used. Only two values were found, which are more or less suitable for the humid tropics. SDRs are normally calculated as a function of catchment size. It is assumed that most sediments are delivered from steeper slopes, which have a higher percentage in small catchments. In addition, possibilities of sediment storage are larger in huge catchments (FERRO & MINACAPILLI 1995). Other equations calculate SDR as a function of length of the major stream and altitude difference between outlet and the watershed divides of its headwaters areas (ROEHL 1962). Some of these equations would result in a clearly higher SDR of the Mefou Reservoir catchment. Their application is nevertheless problematic as they are strongly influenced by local parameters (FERRO & MINACAPILLI 1995; DE VENTE et al. 2007) and are not suitable for land use and land cover or flow and soil characteristics in the humid tropics; sediment connectivity might also be different (cf. WALLING 1983; BRACKEN & CROKE 2007; FRYIRS 2013). The lack of studies coping with SDRs in the humid tropics is brought in by LAL (1985) and later repeated by the same author (LAL 2005).

The contribution of unconsolidated roads, trails and landing sites to soil loss, which is an important factor of the validation, is discussed in Section 6.2.

7 Conclusions

Soil erosion risk and conservation

Soil erosion in the Upper Mefou catchment is relatively high compared to other regions with similar climate or soils in West and Central Africa; in some regions in the humid tropics soil loss is, however, far lower or even higher. Besides uncertainties in modeling—there are some factors of soil erosion which cause high soil loss in the catchment. In a huge proportion of the watershed, soil loss exceeds the tolerable soil loss for tropical soils. However, the potential erosion risk in the catchment is low.

- (I) Annual **rainfall erosivity** in the catchment is very high—the intra-annual variability of erosivity is distinct: Rainfall erosivity is the highest in April, September and October. “Erosive” rainfall has a short recurrence interval and a lot of wet days in the rainy seasons are erosive. In April and September, planting of maize, sweet potato, groundnut, beans, etc. is still ongoing. In October, planting of cassava is ongoing. Harvest, clearing and felling/burning takes place during dry season, where erosive days are seldom and erosivity is low.

It is fairly difficult to change rainfall erosivity. That’s why recommended measures to reduce the impact of rainfall is to adapt the planting of cassava to seasonal rainfall erosivity—i. e., avoiding to seed cassava beyond mid September.

- (II) The soils in the study area are quite resistant against soil erosion. Compared to other studies on tropical (ferralitic) soils in West and Central Africa, **soil erodibility** is on a medium level. Soils are fairly more erodible than the most resistant soils in other studies in the region, but also fairly less erodible than the most erodible soils in the humid tropics. Organic matter content of the soils is high, but low in some soils with maize or cassava monocropping. This is especially true for soils around the Mefou Reservoir and the periurban parts of the catchment, where the fallow duration is much shorter. Permeability is high on cultivated soils, but there are also some less draining soils. Most of the soils tested are sandy; only a few samples have a relatively high silt content. Erodibility is relatively high in the western part of the catchment and in the periurban areas or around the Mefou Reservoir. As present land use has no significant effect on soil erodibility, the length of the fallow period might explain the variation of erodibility.

Table 7.1: Tabular summary of the soil erosion risk assessment (Objective 1 and 2) and proposed soil conservation measures. The first two columns and rows are faithful to the principles of erosion depicted in Figure 2.1; the conservation measures are roughly ranked by their suspected feasibility and straightforwardness of implementation: + *easily practicable*; ° *practicable*; - *hardly practicable*.

Risk assessment		Conservation
Forces/difficulties	Resistance and protection	
<i>Natural sphere</i>		
<ul style="list-style-type: none"> • high rainfall erosivity • steep inselbergs (high topographic erosion potential) • location in the transition zone between dense equatorial forest, semi-deciduous forest and savanna • low tolerable soil loss 	<ul style="list-style-type: none"> • very low potential soil erosion risk • dense natural vegetation • low soil erodibility • low to nil erosivity in December and January • relatively gentle lowlands 	<ul style="list-style-type: none"> • avoidance of deforestation/cultivation of steep inselbergs + • reduction of cultivation in the periurban areas - • protection zone around the reservoir ° • potential of relatively low erosion risk cultivation in the northern lowlands + • contour parallel ridge tillage + • upkeep of tillage system which reduces the permeability of soils + • avoidance of structure-destabilizing tillage methods + • adaption of cropping calendar to rainfall erosivity ° • manuring: control of organic carbon + • avoidance of bare areas in villages ° • buffer strips around fields in areas with extensive cultivation + • reduction of erosion on roads and paths: water diversion °, stabilization with vegetation -; avoidance of the construction of new roads (highest soil loss on new roads) ° • reduction of rainfall erosivity -
<i>Human sphere</i>		
<ul style="list-style-type: none"> • intensive farming in periurban areas • short fallowing in periurban areas • bare roads and paths (high sediment delivery) • relatively high erodibility in periurban areas • seeding of cassava during the wet/erosive season • no contour-parallel ridge tillage 	<ul style="list-style-type: none"> • intercropping of different crops • intercropping of plantain/palms and food crops • low erosion risk in long time fallow (succession) • contour parallel ridge tillage • tillage reduces low permeability compared to bush/forest • manuring practiced (reduced erodibility) 	

Conservation strategies to reduce soil erodibility in the catchment might include a longer fallow period and a shorter duration of cultivation as organic carbon is higher under bush/fallow; erodibility is lower in areas with longer fallow duration and a shorter cultivation period. As the permeability of tilled soils is much higher, ridge tillage is a possibility to reduce soil erodibility.

- (III) The **topographic potential** of erosion is very high on the inselbergs, especially those in the northwest of the catchment. Using parameters proposed for the setting of the catchment to calculate LS, the topographic potential is mainly dominated by slope steepness. There are areas on the foot slopes of the inselbergs and in the lowlands where deposition exceeds erosion. These areas are less prone to erosion.

The change of the impact of topography on soil erosion is generally reduced by mechanical measures, such as terraces. In the Upper Mefou subcatchment, it does not seem to be necessary to implement such techniques. There is a large portion of flat and gentle land, where the erosion risk is relatively low, even if intercropping is practised. Thus, it is recommended to exclude the slopes of the inselbergs from cultivation and also construction.

- (IV) As a system of mosaic shifting-cultivation is practised in the catchment, land use is fragmented and distribution of the **protective cover** is divers. Nevertheless, there is a tendency of a less protective cover around the Mefou Reservoir and periurban areas, whereas there is a higher protective cover around the villages and a quite higher protective cover on the inselbergs in the northwest of the catchment . Ridge tillage might reduce the erosion risk—however, ridges are not always contour-parallel. A short fallow period—especially in the periurban areas—results in a long-term reduced mean vegetation cover and therefore increases the risk of soil erosion. Mono-cropping is also not seldom in the catchment, what in addition accelerates the risk of soil erosion, as maize or cassava do not have a high ground cover. Due to the system of splash-and-burn farming, litter cover is reduced. Land use and land cover are of special importance for soil loss in the Mefou catchment, as other factors—soil organic matter and infiltration capacity—are controlled by land use significantly.

A long fallow period is important—also for a protective vegetation cover. Intercropping should always be preferred instead of monocropping. Especially intercropping of cassava and sweet potato or beans protects the soil from erosion and is better recommended than other intercroppings as two different stories are covered by the different crops. Again, the area around the reservoir and the periurban part of the catchment should be focused on firstly, as monocropping, especially of maize, is more frequent here. The

actual tillage practices in the catchment help to increase permeability and therefore to reduce erodibility; ridge tillage helps to protection against soil erosion. Nevertheless, is is recommended to implement only contour-parallel ridges. Otherwise, erosion is accelerated. Ridges might be favored over mounds, as they are a more effective conservation measure: Mounds might even accelerate the risk of soil erosion as the microtopography of mouds foster soil erosion (cf. NILL 1997).

Changing land use – changing erosion risk

The soil erosion risk in the catchment is strongly influenced by land use: The potential risk is very low, the actual risk is relatively high, but the “worst case” potential risk (a bare catchment) is severe.

According to the five scenarios, land use and land cover change (LULCC) scenarios have effects on different areas of the catchment. Intensification or extensification of food crop production has the most severe effects around the Mefou Reservoir and in the periurban areas, deforestation has the most severe effects on the inselbergs; deforestation for cash crop production has a slightly smaller impact than land use intensification. A more severe impact is modelled for the transformation of forest or bush/fallow to cultivated land. As land use change is mainly driven by a macroeconomic situation, the reasons and extent of LULCC might be complicated to change within the framework of IWM. Nevertheless, the main aim should be to protect areas where LULCC might have the most severe consequences— in periurban Yaoundé and on the slopes of the inselbergs.

Methodological implications

As erosion modelling using USLE-family models has it’s limitations—especially in the humid tropics—, some concluding remarks should be given concerning the methodology of the study (Table 7.2):

- The selection of a suitable slope length parameter for the calculation of the topographic factor in RUSLE3D remains difficult as it is not well documented which value should be used for humid tropical conditions.
- Pretreatment of grain size samples effects both, sand content and silt content; non-treated samples have a higher silt/pseudo-silt content and a higher erodibility; although pretreatment with hydrogen peroxide destroys macroaggregates (and therefore pseudo-sand), relative sand content is higher in pretreated samples—and erodibility therefore lower.

Table 7.2: Methodological view on the factors of RUSLE3D as applied in the Upper Mefou subcatchment. The colours highlight the difficulty of the factor: not problematic , slightly problematic , problematic , very problematic .

Factor	Values	Sensitivity	Model selection	Methodical problems
R	high, fit to values for Central/West Africa	medium	high variability between models (factor: 1.55) and daily and annual data sets (c. 1.3); models are not specific for the study region	no pluviograph data available, daily/annual data do not cover the last decades
K	some values extraordinary high, but in general low erodibility (typical for tropical soils)	low	higher erodibility (factor: 1.1) applying a tropical approximation (developed in the study region)	treatment with hydrogen peroxid reduces approximated erodibility; overestimation of erodible silt fraction using laser diffraction; high variability of permeability
LS	high values on inselbergs; values meaningful	high	significant difference between DEMs and flow algorithms; but different relatively small (factors: 1.05 or 1.002); selection of slope/flow parameter m (factor: 24) is decisive for modeled soil loss, often ambiguous use in literature	DEM resolution problematic
C	high in periurban areas, low on remote inselbergs; values meaningful and fit to published values	very high	different between indices used for linear model, but some models have a very low accuracy	physical basis of indices and C-factor differs; small paths and mixed-cropping difficult to map with Landsat-resolution

- The erodibility-reducing pseudo-sand is not important for the samples at hand, because pseudo-silt dominates non-treated samples.
- It is necessary to test in further studies if the nomograph-approximation is suitable for an organic matter content $>5\%$.
- The procedure to determine OM-content is not determined for the USLE; authors use different approaches and conversion equations. The procedure and the conversion factor applied here result in a higher OM-content and a reduced erodibility.

There are a lot of different procedures to calculate K for the humid tropics—the calculation used here is based on a regression developed on similar soils in the vicinity of Yaoundé—but

there is no standard procedure. Procedures how to determine OM and grain size differ a lot and might result in different erodibility values. Thus, it is recommended to develop such a procedure. At least it should be kept in mind that approximated K-values are always method sensitive and procedures should be compared before comparing values of K or soil loss. The high variability of the erodibility of tropical soils—as reported by EL-SWAIFY et al. (1982) and NILL (1997; 1998)—might not be alone a characteristic of the specific soils, but also a result of methodological sensitivity.

The same is true for rainfall erosivity values: Disregarding the estimation approach, rainfall erosivity in the Upper Mefou subcatchment is always very high; nevertheless, the amplitude of difference is wide—depending on temporal data resolution and the applied regression equation. The topographic factor LS is not sensitive to data input and algorithm selection: The difference between LS based on an ASTER DEM and a SRTM DEM as well as between the flow algorithms MFD and D_{∞} is significant, but not weighty.

Final remarks

The goodness-of-fit of the mean catchment erosion/deposition values and the results of the rough validation show that the application of the RUSLE3D model is—apart from some limitations—possible in the catchment. Nevertheless, the quantitative values have not to be taken at face value; for a semi-quantitative risk assessment, they are good relative values to map areas with high potential, actual and future risk. The identification of areas with a higher risk using the RUSLE3D model is therefore possible and fits to the observations made in the field, gathered by interviews or obtained doing literature reviewing: Urban growth, deforestation and land use intensification and extensification accelerate the naturally low soil erosion, as the erodibility might increase and the protective cover is reduced—also on long term due to a reduced fallow duration. The inselberg-topography of the catchment results in high erosion (risk) in some areas in the catchment, especially of those inselbergs close to the Mefou Reservoir and periurban Yaoundé. Here, future land use changes are followed by an accelerated soil erosion risk.

On the entire Southern Cameroon Plateau, the soil erosion risk might be lower than in the study area: the Yaoundé mountains are one of the prominent mountains on the Plateau; their summit is the highest elevation at least in the Nyong basin. The location of the Upper Mefou subcatchment in the vicinity of Yaoundé is also a unique feature of the catchment and an important cause of a high erosion risk.

Within the framework of the project *Integrated Watershed Management Research and Development Capacity Building* it should be aspired to reduce the soil erosion and to focus on areas

around the Mefou Reservoir and the periurban parts of Yaoundé in a catchment management plan.

References

- ACHARD, F.; EVA, H. D.; STIBIG, H.-J.; MAYAUX, P.; GALLEGU, J.; RICHARDS, T. & MALINGREAU, J.-P. (2002): Determination of Deforestation Rates of the World's Humid Tropical Forests. In: *Science* **297**(5583), 999–1002.
- AHNERT, F. (1982): Untersuchungen über das Morphoklima und die Morphologie des Inselberggebietes von Machakos, Kenia. In: AHNERT, F.; ROHDENBURG, H. & SEMMEL, A. (eds.): Beiträge zur Geomorphologie der Tropen: (Ostafrika, Brasilien, Zentral- u. Westafrika). Catena Supplement 2. Braunschweig, Germany: Catena Verlag, 1–72
- AHNERT, F. (2009): Einführung in die Geomorphologie. 4th ed. Stuttgart, Germany: UTB. 393 pp.
- ALBERT, M.; ANDLER, J.; BAH, T.; BARBRY-BLOT, P.; BARRAUD, J.-F.; BAXTER, B.; BEARD, J.; BINTZ, J.; BIRO, A.; BISHOP, N.; BLOCHER, J.; BÖCK, H.; BOHRE, H.; BOLDEWYN; BORGMANN, D.; BOUCLET, B.; BREUER, H.; BROBERG, G.; BROWN, C.; BRUBAKER, M.; BRUNO, L.; BUCULEI, N.; BYAK, B.; CACLIN, P.; CALDWELL, I.; CARMICHAEL, G.; CATMUR, E.; CELORIO, C.; CEUPPENS, J.; CHYLA, Z.; CLAUSEN, A.; CLIFF, J.; COOK, K.; CROMWELL, B.; CROSBIE, R.; CRUZ, J.; DE-COOMAN, A.; DEREZYNSKI, M.; DÍAZ, D.; DILLY, B.; DOOLITTLE, L.; DWYER, T.; DZIUMANENKO, M. V.; ENGELEN, J.; ERDELYI, M.; ERIKSON, U.; FALZON, N.; FELFE, F.; FITZSIMON, A.; FLICK, E.; FLORYAN, M.; FOWLER, B.; F.; GEMY, C.; GIANNINI, S.; GONDOUN, O.; GOULD, T.; GREEF, T. DE; GROSBERG, M.; HARRINGTON, B.; HARVEY, D.; HECKERT, A. A.; HETHERINGTON, C.; HIRTH, J.; HOCHREINER, H.; HOLDER, T.; HOLDSWORTH, J.; HORKAN, A.; HUFTHAMMER, K. O.; HUGHES, R.; HURST, N.; INDUCTIVELOAD; INGHAM, T.; IRISSON, J.-O.; JAMISON, B.; JESUSDA; KAPLINSKI, L.; KERBY, L.; KIIRALA, N.; KILFIGER, J.; KIVLIGHN, J.; KNOTH, A.; KOSIŃSKI, K.; KOVAR, P.; LAVORATA, B.; LEONE, A.; LERAY, J.; LEVIEN, R.; LIEROP, D. VAN; LINDGREN, N.; LIPATOV, V.; LOUETTE, I.; MARC, P.; MARMION, A.; MARQUARDT, C.; MASTRUKOV, D.; M.; MEEKS, M.; MENA, F.; MENTALGUY; MONNIER, A.; MONTAGNE, V.; MOONEY, T.; MOORE, D.; MOULDER, P.; MÜLLER, J.; NAKAI, Y.; NAVEZ, V.; NEUMAIR, C.; NILSSON, A.; OKA, M.; OWENS, M.; PENNER, A.; PHILLIPS, J.; PODOBNY, Z.; PROKODINE, A.; REINHARD, J.-R.; REMIZOV, A.; RODRIGO, F.; RODRIGUES, H.; RUDSATZ, J.; CONDE RUEDA, X.; SILVA SANCHES, F. CORRÊA DA; SCHALLER, C.; SCHOLTEN, M.; SCHWERDTNER, T. VON; ŠEGAN, D.; SHIVAKEN; SLOAN, M.; SMITH, J.; ŠPETIČ, B.; SPIKE, A.; SRIDHARAN, K.; STEPHAN, R.; STOJEK, D.; SUV; SUCHA, M.; SUWALSKI, P.; TARABEN, A.; TEBBY, H.; TERMEAU, J.; TURNER, D.; TWUPACK, A.; UROŠEVIĆ, A.; VALAVANIS, A.; VIEITES, L.; WYBROW, M.; YACOB, D.; YAMATO, M. & YIP, D. and (2013): *Inkscape*.
- AMBASSA-KIKI, R. & NILL, D. (1999): Effects of different land management techniques on selected topsoil properties of a forest Ferralsol. In: *Soil and Tillage Research* **52**(3), 259–264.
- ANGIMA, S. D.; STOTT, D. E.; O'NEILL, M. K.; ONG, C. K. & WEESIES, G. A. (2003): Soil erosion prediction using RUSLE for central Kenyan highland conditions. In: *Agriculture Ecosystems & Environment* **97**(1), 295–308.

- ANGULO-MARTÍNEZ, M. & BEGUERÍA, S. (2009): Estimating rainfall erosivity from daily precipitation records: A comparison among methods using data from the Ebro Basin (NE Spain). In: *Journal of Hydrology* **379**(1), 111–121.
- ARNOLDUS, H. (1980): An Approximation of the Rainfall Factor in the Universal Soil Loss Equation. In: DE BOODT, M. & GABRIELS, D. (eds.): *Assessment of Erosion*. Chichester, U. K. [u.a.]: John Wiley & Sons
- ASIS, A. M. DE & OMASA, K. (2007): Estimation of vegetation parameter for modeling soil erosion using linear Spectral Mixture Analysis of Landsat ETM data. In: *ISPRS Journal of Photogrammetry and Remote Sensing* **62**(4), 309–324.
- BACHELIER, G. (1959): Etude pédologique des sols de Yaoundé : Contribution à l'étude de la pédogenèse des sols ferrallitiques. In: *Agronomie Tropicale* **14**(3), 279–305.
- BAHRENBERG, G.; GIESE, E. & NIPPER, J. (2010): *Univariate und bivariate Statistik*. 5th ed. Teubner Studienbücher der Geographie. Stuttgart, Germany: Teubner.
- BAIG, M. H. A.; ZHANG, L.; SHUAI, T. & TONG, Q. (2014): Derivation of a tasseled cap transformation based on Landsat 8 at-satellite reflectance. In: *Remote Sensing Letters* **5**(5), 423–431.
- BALEK, J. (2011): *Hydrology and Water Resources in Tropical Africa*. Developments in Water Science. Amsterdam, Netherlands: Elsevier. 212 pp.
- BARTHES, B.; AZONTONDE, A.; BOLI, B. Z.; PRAT, C. & ROOSE, E. (2000): Field-scale run-off and erosion in relation to topsoil aggregate stability in three tropical regions (Benin, Cameroon, Mexico). In: *European Journal of Soil Science* **51**(3), 485–495.
- BARTHÈS, B. G.; KOUAKOUA, E.; LARRÉ-LARROUY, M.-Ch.; RAZAFIMBELO, T. M.; LUCA, E. F. DE; AZONTONDE, A.; NEVES, C. S. V. J.; FREITAS, P. L. DE & FELLER, Ch. L. (2008): Texture and sesquioxide effects on water-stable aggregates and organic matter in some tropical soils. In: *Geoderma* **143**(1), 14–25.
- BEAR, J. (1988): *Dynamics of Fluids in Porous Media*. Mineola, NY, USA: Dover Publications. 396 pp.
- BECK, J.; BUSCH, K.; ECKHART, E.; FRAYER, J.; HAHL, R.; HUNDHAUSEN, C.; REICHE, S.; SCHWERTFECHTER, Ch.; STUMPTNER, A.; ABEBE, T.; AMARE, G.; AYALEW, N.; BANTIE, W.; BERHE, T.; KIROS, N.; LEGESSE, G.; MULUNEH, Z.; SIYNUM, B.; TAFERE, M. & WALELIGN, Z. (2004): Soil Erosion Risk and Water balance of the Gina River Catchment. In: SCHÜTT, B. (ed.): *Watershed Management in the Abaya-Chamo Basin, South Ethiopia*. **20**. Occasional Paper Geographie. Berlin, Germany, 15–73.
- BECKER, F.; DAY, J.; BELLE, J.; NDAM, J. R.; ATIBU, P. K.; FEUMBA, R. F. & THIEMANN, S. (2013): *Integrated Watershed Management for Upper Mefou Sub-catchment Area – An Overview*. Integrated Watershed Management Research and Development Capacity Building. Yaoundé, Cameroon: Freie Universität Berlin, IWM Expert GmbH and Université de Yaoundé I.
- BEUSELINCK, L.; GOVERS, G.; POESEN, J.; DEGRAER, G. & FROYEN, L. (1998): Grain-size analysis by laser diffractometry: comparison with the sieve-pipette method. In: *CATENA* **32**(3), 193–208.
- BEUSELINCK, L.; GOVERS, G. & POESEN, J. (1999): Assessment of micro-aggregation using laser diffractometry. In: *Earth Surface Processes and Landforms* **24**(1), 41–49.

- BÖHNER, J.; McCLOY, K. R. & STROBL, J. (2006): SAGA-analysis and modelling applications. **115**. Göttinger Geographische Abhandlungen. Göttingen, Germany: University of Goettingen. 130 pp.
- BIARD, F. & BARET, F. (1997): Crop residue estimation using multiband reflectance. In: Remote Sensing of Environment **59**(3), 530–536.
- BIVAND, R. & RUNDEL, C. (2013): rgeos: Interface to Geometry Engine - Open Source (GEOS). R package version 0.3-2.
- BIVAND, R.; KEITT, T. & ROWLINGSON, B. (2013a): rgdal: Bindings for the Geospatial Data Abstraction Library. R package version 0.8-14.
- BIVAND, R. S.; PEBESMA, E. & GÓMEZ-RUBIO, V. (2013b): Applied Spatial Data Analysis with R. 2nd ed. Berlin and Heidelberg, Germany: Springer. 405 pp.
- BLUME, H.-P.; BRÜMMER, G. W.; HORN, R.; KANDELER, E.; KÖGEL-KNABNER, I.; KRETZSCHMAR, R.; STAHR, K.; WILKE, B.-M.; WELP, G. & THIELE-BRUHN, S. (2010): Scheffer/Schachtschabel: Lehrbuch der Bodenkunde. 16th ed. Heidelberg and Berlin, Germany: Spektrum Akademischer Verlag. 570 pp.
- BOARDMAN, J. (1998): An average soil erosion rate for Europe: Myth or reality? In: Journal of Soil and Water Conservation **53**(1), 46–50.
- BOELLSTORFF, D. & BENITO, G. (2005): Impacts of set-aside policy on the risk of soil erosion in central Spain. In: Agriculture, Ecosystems & Environment **107**(2), 231–243.
- BORK, H.-R. & SCHRÖDER, A. (1996): Quantifizierung des Bodenabtrags anhand von Modellen. In: BLUME, H. P.; FELIX-HENNINGSSEN, P.; FISCHER, W. R.; FREDE, H.-G.; GUGGENBERGER, G.; HORN, R. & STAHR, K. (eds.): Handbuch der Bodenkunde. Weinheim, Germany: Wiley-VCH, 1–44
- BORRELLI, P. (2011): Risk Assessment of Human-induced Accelerated Soil Erosion Processes in the Intermountain Watersheds of Central Italy. A Case Study of the Upper Turano Watershed (Latium-Abruzzi). Dissertation. Berlin, Germany: Freie Universität Berlin, Department of Earth Sciences. 255 pp.
- BORRELLI, P. & SCHÜTT, B. (2014): Assessment of soil erosion sensitivity and post-timber-harvesting erosion response in a mountain environment of Central Italy. In: Geomorphology **204**, 412–424.
- BORRELLI, P.; MÄRKER, M.; PANAGOS, P. & SCHÜTT, B. (2014): Modeling soil erosion and river sediment yield for an intermountain drainage basin of the Central Apennines, Italy. In: CATENA **114**, 45–58.
- BOU KHEIR, R.; CERDAN, O. & ABDALLAH, Ch. (2006): Regional soil erosion risk mapping in Lebanon. In: Geomorphology **82**(3), 347–359.
- BOX, G. E. P. & COX, D. R. (1964): An analysis of transformations. In: Journal of the Royal Statistical Society, 211–252.
- BRACKEN, L. L. & CROKE, J. (2007): The concept of hydrological connectivity and its contribution to understanding runoff-dominated geomorphic systems. In: Hydrological Processes **21**(13), 1749–1763.
- BRATTON, S. P.; HICKLER, M. G. & GRAVES, J. H. (1979): Trail erosion patterns in Great Smoky Mountains National Park. In: Environmental Management **3**(5), 431–445.
- BRENNING, A. (2008): Statistical geocomputing combining R and SAGA: The example of landslide susceptibility analysis with generalized additive models. In: BÖHNER, J.; BLASCHKE, T. & MONTANARELLA, L.

- (eds.): SAGA – Seconds Out. Hamburger Beiträge zur Physischen Geographie und Landschaftsökologie 19. Hamburg, Germany: Universität Hamburg, 23–32
- BRESCH, J. (1993): Die Erosivität der Niederschläge Kameruns. Unpublished Master's thesis. Munich, Germany: Technische Universität München.
- BRIONES, N. D. (1991): Estimating Erosion Cost: A Philippine Case Study in the Lower Agno River Watershed. In: EASTER, K. W.; DIXON, J. A. & HUFSCHEIDT, M. M. (eds.): Watershed Resources Management – Studies from Asia and the Pacific. ISEAS Environment and Development Series. Honolulu, HI, USA and Singapore: East-West Center and Institute of Southeast Asian Studies, 191–204
- BROWN, C. B. (1943): Discussion of Sedimentation in reservoirs, by J. Witzig. In: Proceedings of the American Society of Civil Engineers **69**, 1493–1500.
- BROWN, D. R. (2004): Beyond Boserup: Cameroonian Agroforestry Systems in Space and Time. SSRN Scholarly Paper ID 601278. Rochester, NY: Social Science Research Network.
- BROWN, L. C. & FOSTER, G. R. (1987): Storm Erosivity Using Idealized Intensity Distributions. In: Transactions of the American Society of Agricultural Engineers **30**(2), 379–386.
- BRUNE, G. M. (1953): Trap efficiency of reservoirs. In: Eos, Transactions American Geophysical Union **34**(3), 407–418.
- BRYAN, R. B. (1968): The development, use and efficiency of indices of soil erodibility. In: Geoderma **2**(1), 5–26.
- BRYAN, R. B. (2000): Soil erodibility and processes of water erosion on hillslope. In: Geomorphology **32**(3), 385–415.
- BRYAN, R. B.; GOVERS, G. & POESEN, J. (1989): The concept of soil erodibility and some problems of assessment and application. In: CATENA. Selected papers of the Fourth Benelux Colloquium on Geomorphological Processes **16**(4), 393–412.
- BUBE, K. P. & TRIMBLE, St. W. (1986): Revision of the Churchill Reservoir Trap Efficiency Curves Using Smoothing Splines. In: JAWRA Journal of the American Water Resources Association **22**(2), 305–305.
- BUURMAN, P.; PAPE, Th.; REIJNEVELD, J. A.; DE JONG, F. & VAN GELDER, E. (2001): Laser-diffraction and pipette-method grain sizing of Dutch sediments: correlations for fine fractions of marine, fluvial, and loess samples. In: Geologie en Mijnbouw **80**(2), 49–58.
- CARSEL, R. F. & PARRISH, R. (1988): Developing joint probability distributions of soil water retention characteristics. In: Water Resources Research **24**(5), 755–769.
- CENTERS FOR DISEASE CONTROL AND PREVENTION, (ed.): (2010): World Country Admin Boundary Shapefile with FIPS Codes. Epi Info data set. <http://geocommons.com/overlays/33578.html> (2014-10-30): GeoCommons.
- CHAMPETIER DE RIBES, G.; CIROTTEAU, A. & LEROY, B. (1956): Carte Géologique du Cameroun. Ed. by GAZEL, J. & GUIRAUDIE, Ch. Red. by SOCIÉTÉ NOUVELLE DE CARTOGRAPHIE & DIRECTION DES MINES ET DE LA GÉOLOGIE DU CAMEROUN. Paris, France.
- CHILAR, J. (1987): A Methodology for Mapping and Monitoring Cropland Soil Erosion. In: Canadian Journal of Soil Science **67**(3), 433–444.

- COMITE INTERAFRICAIN D'ETUDES HYDRAULIQUES & OFFICE DE LA RECHERCHE SCIENTIFIQUE ET TECHNIQUE OUTRE-MER SERVICE HDROLOGIQUE: République du Cameroun. Précipitations Journalières de L'Origine des Stations a 1972. Tome 1. n. p.
- COMITE INTERAFRICAIN D'ETUDES HYDRAULIQUES; AGENE POUR LA SECURITE DE LA NAVIGATION AERIENNE & INSTITUT FRANCAIS DE RECHERCHE SCIENTIFIQUE POUR LA DEVELOPPEMENT EN CO-OPERATION LABORATOIRE D'HYDROLOGIE, (eds.): (1990): Republique du Cameroun. Precipitations Journalieres de 1973 a 1980. Ouagadougou, Burkina Faso [u.a.]
- CONRAD, O. (2006): SAGA — Entwurf, Funktionsumfang und Anwendung eines Systems für Automatisierte Geowissenschaftliche Analysen. Dissertation. Göttingen, Germany: University of Göttingen.
- CORNELL, R. M. & SCHWERTMANN, U. (2006): The Iron Oxides: Structure, Properties, Reactions, Occurrences and Uses. Hoboken, NJ, USA: John Wiley & Sons. 707 pp.
- CORNILLON, P.-A.; GUYADER, A.; HUSSON, F.; JEGOU, N.; JOSSE, J.; KLOAREG, M.; MATZNER-LOBER, E. & ROUVIÈRE, L. (2012): R for Statistics. Boca Ration, FL, USA: CRC Press. 322 pp.
- DAHL, D. B. (2014): xtable: Export tables to LaTeX or HTML. R package version 1.7-3. <http://CRAN.R-project.org/package=xtable>.
- DE JONG, S. M. (1994): Derivation of vegetative variables from a landsat tm image for modelling soil erosion. In: Earth Surface Processes and Landforms **19**(2), 165–178.
- DE MEYER, A.; POESEN, J.; ISABIRYE, M.; DECKERS, J. & RAES, D. (2011a): Soil erosion rates in tropical villages: A case study from Lake Victoria Basin, Uganda. In: CATENA **84**(3), 89–98.
- DE MEYER, A.; POESEN, J.; ISABIRYE, M.; DECKERS, J. & RAES, D. (2011b): Soil erosion rates in tropical villages: A case study from Lake Victoria Basin, Uganda. In: CATENA **84**(3), 89–98.
- DE VENTE, J.; POESEN, J.; ARABKHEDRI, M. & VERSTRAETEN, G. (2007): The sediment delivery problem revisited. In: Progress in Physical Geography **31**(2), 155–178.
- DE VENTE, J.; POESEN, J.; VERSTRAETEN, G.; VAN ROMPAEY, A. & GOVERS, G. (2008): Spatially distributed modelling of soil erosion and sediment yield at regional scales in Spain. In: Global and Planetary Change **60**(3), 393–415.
- DECAGON DEVICES, Inc., (ed.): (2012): Mini Disk Infiltrometer – User's Manual. 10th ed. Pullman, WA, USA.
- DECKERS, J. A.; NACHTERGAELE, F. & SPAARGAREN, O. C. (1998): World Reference Base for Soil Resources: Introduction. Leuven, Belgium: ACCO. 172 pp.
- DEFRIES, R. S.; RUDEL, Th.; URIARTE, M. & HANSEN, M. (2010): Deforestation driven by urban population growth and agricultural trade in the twenty-first century. In: Nature Geoscience **3**(3), 178–181.
- DEKKERS, J. & KOOMEN, E. (2007): Land-Use Simulation For Water Management. In: KOOMEN, E; STILLWELL, J.; BAKEMA, A. & SCHOLTEN, H. J. (eds.): Modelling Land-Use Change. The GeoJournal Library 90. Luxemburg, Berlin: Springer, 355–374
- DESMET, P. J. J. & GOVERS, G. (1997): Comment on 'Modelling topographic potential for erosion and deposition using GIS'. In: International Journal of Geographical Information Science **11**(6), 603–610.

- DIDUK, S. (1992): The Paradoxes of Changing Land Tenure in Kedjom Chiefdoms, Northwest Province, Cameroon. In: *Paideuma* **38**, 195–217.
- DIKAU, R. (1986): Experimentelle Untersuchungen zu Oberflächenabfluß und Bodenabtrag von Meßparzellen und landwirtschaftlichen Nutzflächen. *Heidelberger Geographische Arbeiten* 81. Heidelberg, Germany: also: Dissertation, Heidelberg University. 195 pp.
- DIODATO, N.; KNIGHT, J. & BELLOCCHI, G. (2013): Reduced complexity model for assessing patterns of rainfall erosivity in Africa. In: *Global and Planetary Change* **100**, 183–193.
- DISTRIBUTED ACTIVE DATA CENTER & EARTH RESOURCES OBSERVATION SYSTEMS DATA CENTER (1996): Global 30-Arc-Second Elevation Data Set. Sioux Falls, SD, USA: US Geological Survey.
- DIXON, J. A. & EASTER, K. W. (1991): Integrated Watershed Management: An Approach to Resource Management. In: EASTER, K. W.; DIXON, J. A. & HUFSCHEMIDT, M. M. (eds.): *Watershed Resources Management – Studies from Asia and the Pacific*. ISEAS Environment and Development Series. Honolulu, HI, USA and Singapore: East-West Center and Institute of Southeast Asian Studies, 3–16
- DOUGLAS, I. (2003): Predicting road erosion rates in selectively logged tropical rain forests. In: BOER, D. DE; FROELICH, W.; MIZUYAMA, T. & PIETRONIRO, A. (eds.): *Erosion Prediction in Ungauged Basins: Integrating Methods and Techniques*. 257. Wallingford, U.K.: IAHS Press
- EASTER, K. W. & HUFSCHEMIDT, M. M. (1985): Integrated watershed management research for developing countries. Honolulu: Environment, Policy Institute, East-West Center, Honolulu, Hawaii, the US Agency for International Development, the University of Minnesota, and the University of Arizona, 39.
- EASTER, K. W.; CHADWICK, O. A. & KYRIAKIDIS, P. C. (2000): Error in a USGS 30-meter digital elevation model and its impact on terrain modeling. In: *Journal of Hydrology* **233**(1), 154–173.
- EBISEMIJU, F. S. (1990): Sediment delivery ratio prediction equations for short catchment slopes in a humid tropical environment. In: *Journal of Hydrology* **114**(1), 191–208.
- EDWARDS, A. P. & BREMNER, J. M. (1967): Microaggregates in Soils. In: *Journal of Soil Science* **18**(1), 64–73.
- EHUI, S. K.; KANG, B. T. & SPENCER, D. S. C. (1990): Economic analysis of soil erosion effects in alley cropping, no-till and bush fallow systems in South Western Nigeria. In: *Agricultural Systems* **34**(4), 349–368.
- EISENBERG, J. (2009): Morphogenese der Flusseinzugsgebiete von Nyong und Ntem in Süd-Kamerun unter Berücksichtigung neotektonischer Vorgänge. Dissertation. Frankfurt/Main, Germany: Johann Wolfgang Goethe-University Frankfurt, Department of Geosciences/Geography.
- EL-SWAIFY, S. A.; DANGLER, E. W. & ARMSTRONG, C. L. (1982): *Soil Erosion by Water in the Tropics*. **24**. Research Extension Series. Honolulu.
- EMBRECHTS, J. & DE DAPPER, M. (1990): Morphologie, genèse et sédimentologie des pédiments de versant de la région du Mont-Fébé (Cameroun méridional). In: LANFRANCHI, R. & SCHWARTZ, D. (eds.): *Paysages Quaternaires de l'Afrique Central Atlantique*. Editions de l'ORSTOM, Collection: Didactiques. Paris, France, 138–154

- EMBRECHTS, J. & SYS, C. (1988): Genesis of subsurface horizons of a soil catena in a humid tropical climate (Yaounde, Cameroon). In: *CATENA* **15**(1), 53–63.
- ERENCIN, Z. (2000): C-Factor mapping using Remote Sensing and GIS : a case study of Lom Sak / Lom Kao, Thailand. Research Paper. Gießen, Germany: Justus Liebig University Giessen.
- EVANS, R. & BRAZIER, R. (2005): Evaluation of modelled spatially distributed predictions of soil erosion by water versus field-based assessments. In: *Environmental Science & Policy* **8**(5), 493–501.
- FAIRFIELD, J. & LEYMARIE, P. (1991): Drainage networks from grid digital elevation models. In: *Water Resources Research* **27**(5), 709–717.
- FAO-AQUASTAT (2013): Dams of Cameroon [CMR_dams_eng.xls]. In: The Geo-referenced database on Dams in Africa. 3rd ed. <http://www.fao.org/nr/water/aquastat/dams/index.stm> (2014-10-11): FAO
- FERREIRA, A. G.; GONÇALVES, A. C. & DIAS, S. S. (2008): Avaliação da Sustentabilidade dos Sistemas Florestais em Função da Erosão. In: *Silva Lusitana* **16** (Especial), 55–67.
- FERRO, V. & MINACAPILLI, M. (1995): Sediment delivery processes at basin scale. In: *Hydrological Sciences Journal* **40**(6), 703–717.
- FFOLIOTT, P. F. (2011): Integrated Watershed Management: A Comprehensive Approach to Land Stewardship. In: *Hydrology and Water Resources in Arizona and the Southwest* **41**.
- FOLK, R. L. & WARD, W. C. (1957): Brazos River bar: a study in the significance of grain size parameters. In: *Journal of Sedimentary Research* **27**(1).
- FORMAN, R. T. T. & ALEXANDER, L. E. (1998): Roads and Their Major Ecological Effects. In: *Annual Review of Ecology and Systematics* **29**(1), 207–231.
- FOSTER, G. R.; MCCOOL, D. K.; RENARD, K. G. & MOLDENHAUER, W. C. (1981): Conversion of the universal soil loss equation to SI metric units. In: *Journal of Soil and Water Conservation* **36**(6), 355–359.
- FOSTER, G. R.; YODER, D. C.; MCCOOL, D. K.; WEESIES, G. A.; TOY, T. J. & WAGNER, L. E. (2000): Improvements in science in RUSLE2. In: *Proceedings of the 2000 ASAE Annual International Meeting, Milwaukee, Wisconsin, USA, 9-12 July 2000*. St. Joseph, MI, USA: American Society of Agricultural Engineers, 1–19
- FOURNIER, J. (1960): *Climate et Erosion*. Paris, France: Presses Universitaires de France.
- FOURNIER, J. (1993): Agressivite Climatique et Risques Erosifs dans la Region de Dschang - Ouest Cameroun. Dschang: Departement de Foresterie - Universite de Dschang.
- FRANQUEVILLE, A. (1979): Croissance démographique et immigration à Yaoundé. In: *Les Cahiers d'Outre-Mer* **128**, 321–354.
- FÖRCH, G. & SCHÜTT, B. (2005): Watershed Management – An Introduction. In: *FWU Water Resources Publications* **4**, 119–133.
- FREEMAN, T. G. (1991): Calculating catchment area with divergent flow based on a regular grid. In: *Computers & Geosciences* **17**(3), 413–422.
- FRYIRS, K. (2013): (Dis)Connectivity in catchment sediment cascades: a fresh look at the sediment delivery problem. In: *Earth Surface Processes and Landforms* **38**(1), 30–46.

- GARATUZA-PAYÁN, J.; SÁNCHEZ-ANDRÉS, R.; SÁNCHEZ-CARRILLO, S. & NAVARRO, J. M. (2005): Using remote sensing to investigate erosion rate variability in a semiarid watershed, due to changes in vegetation cover. In: WALLING, D. E. & HOROWITZ, A. J. (eds.): *Sediment Budgets*. Wallingford, U. K.: IAHS Press
- GARCIA RODRIGUEZ, J. L. & GIMENEZ SUAREZ, M. C. (2012): Methodology for estimating the topographic factor LS of RUSLE3D and USPED using GIS. In: *Geomorphology* **175–176**, 98–106.
- GIORDANO, A.: The corine project on soil erosion risk and land quality. In: *Land Use, Land Cover and Soil Sciences*(3), 144–170.
- GOSLEE, S. C. (2011): Analyzing Remote Sensing Data in R: The landsat Package. In: *Journal of Statistical Software* **43**(4), 1–25.
- GOUDIE, A. S. (1996): *Climate: Past and Present*. In: ADAMS, W. M.; GOUDIE, A. S. & ORME, A.R. (eds.): *The physical geography of Africa*. Oxford regional environments. Oxford, U. K. [u.a.]: Oxford Univ. Press
- GRAY, A. B.; PASTERNAK, G. B. & WATSON, E. B. (2010): Hydrogen peroxide treatment effects on the particle size distribution of alluvial and marsh sediments. In: *The Holocene* **20**(2), 293–301.
- GREGERSEN, H. M.; FFOLIOTT, P. F. & BROOKS, K. N. (2007): *Integrated Watershed Management: Connecting People to Their Land and Water*. Wallingford, U.K. and Cambridge, MA, USA: CAB International. 217 pp.
- HAMILTON, L. S. & PEARCE, A. J. (1991): *Biophysical Aspects in Watershed Management*. In: EASTER, K. W.; DIXON, J. A. & HUFSCHMIDT, M. M. (eds.): *Watershed Resources Management – Studies from Asia and the Pacific*. ISEAS Environment and Development Series. Honolulu, HI, USA and Singapore: East-West Center and Institute of Southeast Asian Studies, 33–52
- HANNA, W. J. & HANNA, J. J. (2009): *Urban Dynamics in Black Africa (sic!): An Interdisciplinary Approach*. Piscataway, NJ, USA: Transaction Publishers. 274 pp.
- HARTTER, J.; LUCAS, Ch.; GAUGHAN, A. E. & LIZAMA ARANDA, L. (2008): Detecting tropical dry forest succession in a shifting cultivation mosaic of the Yucatán Peninsula, Mexico. In: *Applied Geography* **28**(2), 134–149.
- HEALEY, S. P.; COHEN, W. B.; ZHIQIANG, Y. & KRANKINA, O. N. (2005): Comparison of Tasseled Cap-based Landsat data structures for use in forest disturbance detection. In: *Remote Sensing of Environment* **97**(3), 301–310.
- HEATHCOTE, I. W. (2009): *Integrated Watershed Management: Principles and Practice*. Hoboken, NJ, USA: John Wiley & Sons. 465 pp.
- HIJMANS, R. J. (2013): raster: raster: Geographic data analysis and modeling. R package version 2.1-66. <http://CRAN.R-project.org/package=raster>.
- HOARE, J. A. (1991): *The Role of Extension: A Northern Thailand Watershed Case Study*. In: EASTER, K. W.; DIXON, J. A. & HUFSCHMIDT, M. M. (eds.): *Watershed Resources Management – Studies from Asia and the Pacific*. ISEAS Environment and Development Series. Honolulu, HI, USA and Singapore: East-West Center and Institute of Southeast Asian Studies, 159–176

- HOFFMANN, A.; NAVES SILVA, M. L.; CURI, N.; KLINKE, G. & FREITAS, D. A. F. DE (2013): Development of Topographic Factor Modeling for Application in Soil Erosion Models. In: HERNANDEZ SORIANO, M. C. (ed.): *Soil Processes and Current Trends in Quality Assessment*. Rijeka, Croatia: InTech
- HOFIERKA, J.; MITÁŠOVÁ, H. & NETELER, M. (2009): Chapter 17 Geomorphometry in GRASS GIS. In: REUTER, H. I. & HENGL, T. (eds.): *Developments in Soil Science*. **33**. Geomorphometry Concepts, Software, Applications. Amsterdam, Netherlands: Elsevier, 387–410
- HOWELER, R. H.; EZUMAH, H. C. & MIDMORE, D. J. (1993): Tillage systems for root and tuber crops in the tropics. In: *Soil and Tillage Research. Soil Tillage for Agricultural Sustainability* **27**(1), 211–240.
- IDAHO P. A. AND MUSTAPHA, H. I.; MUSA, J. J. & DIKE, J. (2008): Determination of Erodibility Indices of Soils in Owerri West Local Government Area of Imo State, Nigeria. In: *Assumption University Journal of Technology* **12**(2), 130–133.
- IGWE, C. A. (2003): Erodibility of soils of the upper rainforest zone, southeastern Nigeria. In: *Land Degradation and Development* **14**(3), 323–334.
- IGWE, C. A.; MBAGWU, J. S. C. & AKAMIGBO, F. O. R. (1995): Physical properties of soils of southeastern Nigeria and the role of some aggregating agents in their stability. In: *Soil science* **160**(6), 431–441.
- IMBERNON, J. & BRANTHOMME, A. (2001): Characterization of landscape patterns of deforestation in tropical rain forests. In: *International Journal of Remote Sensing* **22**(9), 1753–1765.
- INSTITUE GÉOGRAPHIQUE NATIONAL (1956): Carte au 1/50.000 (Type Outre-Mer) Cameroun: Yaoundé 3 d – Nkolbisson (feuille NA-32-XXIV-3d). Ed. by MINISTRE DES TRAVEUX PUBLICS ET DES TRANSPORTS. Paris, France.
- IRONS, J. R.; DWYER, J. L. & BARSİ, J. A. (2012): The next Landsat satellite: The Landsat Data Continuity Mission. In: *Remote Sensing of Environment. Landsat Legacy Special Issue* **122**, 11–21.
- JARVIS, A.; REUTER, H. I.; NELSON, A. & GUEVARA, E. (2008): SRTM 90m Digital Elevation Database v2; SRTM3N03E011V2; acquisition date: 2000-02-11.
- KALBERER, P. & WALKER, M. (2014): QGIS OpenLayers plugin. In collab. with MOTTA, L.; AKAGI, M.; MINPA, L.; DUIVENVOORDE, R.; KELSO, N. V.; LAROSA, S.; FISCHER, J. E.; MOHAMED, F. & MORTEN, A. Zurich, Switzerland.
- KARYDAS, Ch. G.; SEKULOSKA, T. & SILLEOS, G. N (2009): Quantification and site-specification of the support practice factor when mapping soil erosion risk associated with olive plantations in the Mediterranean island of Crete. In: *Environmental monitoring and assessment* **149**(1-4), 19–28.
- KAUTH, R. J. & THOMAS, G. S. (1976): The tasselled cap—a graphic description of the spectral-temporal development of agricultural crops as seen by Landsat. In: *Proceedings of the Symposium on Machine Processing of Remotely Sensed Data*. **159**. West Lafayette, IN, USA: LARS Symposia, 4B–41–4B–51
- KENDALL, M. G. (1938): A New Measure of Rank Correlation. In: *Biometrika* **30**(1), 81–93.
- KIENZLE, St. (2004): The Effect of DEM Raster Resolution on First Order, Second Order and Compound Terrain Derivatives. In: *Transactions in GIS* **8**(1), 83–111.

- KIET, S. (1972): Hydrologie d'un Bassin de Zone Urbaine. Le Bassin Versant de Yaoundé. Yaoundé, Cameroon: Office de la Recherche Scientifique et Technique Outre-mer - Centre O.R.S.T.O.M. de Yaoundé – Section d'Hydrologie.
- KINNELL, P. I. A. & RISSE, L. M. (1998): USLE-M: empirical modeling rainfall erosion through runoff and sediment concentration. In: Soil Science Society of America Journal **62**(6), 1667–1672.
- KÄMPF, N. & SCHWERTMANN, U. (1983): Goethite and hematite in a climosequence in southern Brazil and their application in classification of kaolinitic soils. In: Geoderma **29**(1), 27–39.
- KNIJFF, J. M. VAN DER; JONES, R. J. A. & MONTANARELLA, L. (2002): Soil erosion risk assessment in Italy. In: RUBIO, J. L.; MORGAN, R. P. C.; ASINS, S. & ANDREU, V. (eds.): Man and soil at the Third Millennium. Proceedings International Congress of the European Society for Soil Conservation, Valencia, Spain, 28 March-1 April, 2000. Volume 2. Logroño, Spain: GEOFORMA Edicions S.L., 1903–1917
- KONERT, M. & VANDENBERGHE, J. (1997): Comparison of laser grain size analysis with pipette and sieve analysis: a solution for the underestimation of the clay fraction. In: Sedimentology **44**(3), 523–535.
- KOTTEK, M.; GRIESER, J.; BECK, Ch.; RUDOLF, B. & RUBEL, F. (2006): World Map of the Köppen-Geiger climate classification updated. In: Meteorologische Zeitschrift **15**(3), 259–263.
- KOTTO-SAME, J.; WOOMER, P. L.; APPOLINAIRE, M. & LOUIS, Z. (1997): Carbon dynamics in slash-and-burn agriculture and land use alternatives of the humid forest zone in Cameroon. In: Agriculture, Ecosystems & Environment **65**(3), 245–256.
- KUMAR, S. & KUSHWAHA, S. P. S. (2013): Modelling soil erosion risk based on RUSLE-3D using GIS in a Shivalik sub-watershed. In: Journal of Earth System Science **122**(2), 389–398.
- LAL, R. (1976): Soil erosion on Alfisols in Western Nigeria: II. Effects of mulch rates. In: Geoderma **16**(5), 377–387.
- LAL, R. (1985): Soil erosion and sediment transport research in tropical Africa. In: Hydrological Sciences Journal **30**(2), 239–256.
- LAL, R. (1996): Deforestation and land-use effects on soil degradation and rehabilitation in western Nigeria. III. Runoff, soil erosion and nutrient loss. In: Land Degradation & Development **7**(2), 99–119.
- LAL, R. (2005): Challenges in Agriculture and Forest Hydrology in the Humid Tropics. In: BONELL, M.; HUFSCHEMIDT, M. M. & GLADWELL, J. S. (eds.): Hydrology and Water Management in the Humid Tropics: Hydrological Research Issues and Strategies for Water Management. Cambridge, U.K.: Cambridge University Press, 395–404
- LAMBIN, E. F.; GEIST, H. J. & LEPEERS, E. (2003): Dynamics of Land-Use and Land-Cover Change in Tropical Regions. In: Annual Review of Environment and Resources **28**(1), 205–241.
- LANGBEIN, W. B. & SCHUMM, S. A. (1958): Yield of sediment in relation to mean annual precipitation. In: Transactions, American Geophysical Union **39**(6), 1076.
- LE BARBÉ, L.; LEBEL, T. & TAPSOBA, D. (2002): Rainfall Variability in West Africa during the Years 1950–90. In: Journal of Climate **15**(2), 187–202.
- LE BISSONNAIS, Y.; MONTIER, C.; JAMAGNE, M.; DAROUSSIN, J. & KING, D. (2002): Mapping erosion risk for cultivated soil in France. In: CATENA **46**(2), 207–220.

- LEE, J.-S.; PAPATHANASSIOU, K. P.; AINSWORTH, T. L.; GRUNES, M. R. & REIGBER, A. (1998): A new technique for noise filtering of SAR interferometric phase images. In: *IEEE Transactions on Geoscience and Remote Sensing* **36**(5), 1456–1465.
- LEE, Jong-Sen (1983): Digital image smoothing and the sigma filter. In: *Computer Vision, Graphics, and Image Processing* **24**(2), 255–269.
- LEFÈVRE, R. (1966): *Etude Hydrologique de la Mefou Supérieure*. Yaoundé, Cameroon: Office de la Recherche Scientifique et Technique Outre-Mer – Section d’Hydrologie.
- LEMON, J. (2006): Plotrix: a package in the red light district of R. In: *R News* **6**(4), 8–12.
- LEVENE, Howard (1960): Robust tests for equality of variances1. In: OLKIN, I.; GHURYE, S. G.; HOEFFDING, W.; MADOW, W. G. & MANN, H. B. (eds.): *Contributions to probability and statistics: Essays in honor of Harold Hotelling*. Standford, CA, USA: Stanford University Press, 278–292
- LIN, Ch.-Y.; LIN, W.-T. & CHOU, W.-Ch. (2002): Soil erosion prediction and sediment yield estimation: the Taiwan experience. In: *Soil and Tillage Research* **68**(2), 143–152.
- LIU, H.; KIESEL, J.; HÖRMANN, G. & FOHRER, N. (2011): Effects of DEM horizontal resolution and methods on calculating the slope length factor in gently rolling landscapes. In: *Catena* **87**(3), 368–375.
- LOIZEAU, J.-L.; ARBOUILLE, D.; SANTIAGO, S. & VERNET, J.-P. (1994): Evaluation of a wide range laser diffraction grain size analyser for use with sediments. In: *Sedimentology* **41**(2), 353–361.
- LUCAS, R. M.; HONZAK, M.; CURRAN, P. J.; FOODY, Giles M. & NGUELE, D. T. (2000): Characterizing tropical forest regeneration in Cameroon using NOAA AVHRR data. In: *International Journal of Remote Sensing* **21**(15), 2831–2854.
- MALA, O. (1993): *Différenciations pédologiques dans la région de Yaoundé (Cameroun): Transformation d’un sol ferrallitique rouge en sol à horizon jaune et relation ave l’évolution du modelé*. Dissertation. Paris, France: Pierre and Marie Curie University (Paris 6).
- MANN, H. B. & WHITNEY, D. R. (1947): On a Test of Whether one of Two Random Variables is Stochastically Larger than the Other. In: *The Annals of Mathematical Statistics* **18**(1), 50–60.
- MARTIN, D. (1967): Géomorphologie et sols ferrallitiques dans le Centre Cameroun. In: *Cahiers ORSTOM, Série Pédologie* **5**(2), 189–218.
- MATI, B. M. & VEIHE, A. (2001): Application of the USLE in a Savannah environment: Comparative experiences from East and West Africa. In: *Singapore Journal of Tropical Geography* **22**(2), 138–155.
- MBAGWU, J.S.C. & SCHWERTMANN, U. (2006): Some factors affecting clay dispersion and aggregate stability in selected soils of Nigeria. In: *International Agrophysics* **20**(1), 23–30.
- MCGILL, R.; TUKEY, J. W. & LARSEN, W. A. (1978): Variations of Box Plots. In: *The American Statistician* **32**(1), 12–16.
- MC SWEENEY, C.; LIZCANO, G.; NEW, M. & LU, X. (2010a): The UNDP Climate Change Country Profiles: Improving the Accessibility of Observed and Projected Climate Information for Studies of Climate Change in Developing Countries. In: *Bulletin of the American Meteorological Society* **91**(2), 157–166.
- MC SWEENEY, C.; NEW, M. & LIZCANO, G. (2010b): *UNDP Climate Change Country Profiles - Cameroon*. Oxford.

- MERRITT, W. S.; LETCHER, R. A. & JAKEMAN, A. J. (2003): A review of erosion and sediment transport models. In: *Environmental Modelling & Software* **18**(8), 761–799.
- MERTENS, B. & LAMBIN, E. F. (2000): Land-cover-change trajectories in southern Cameroon. In: *Annals of the association of American Geographers* **90**(3), 467–494.
- MEUSBURGER, K.; BÄNNINGER, D. & ALEWELL, C. (2010): Estimating vegetation parameter for soil erosion assessment in an alpine catchment by means of QuickBird imagery. In: *International Journal of Applied Earth Observation and Geoinformation* **12**(3), 201–207.
- MILLWARD, A. A. & MERSEY, J. E. (1999): Adapting the RUSLE to model soil erosion potential in a mountainous tropical watershed. In: *CATENA* **38**(2), 109–129.
- MITAS, L. & MITASOVA, H. (1998): Distributed soil erosion simulation for effective erosion prevention. In: *Water Resources Research* **34**(3), 505–516.
- MITASOVA, H. & MITAS, L. (1999): Erosion/deposition modeling with USPED using GIS. URL: <http://www4.ncsu.edu/~hmitaso/gmslab/denix/usped.html>.
- MITASOVA, H. & MITAS, L. (2001): Multiscale soil erosion simulations for land use management. In: HARMON, R. S. & DOE III, W. W. (eds.): *Landscape Erosion and Landscape Evolution Modeling*, 321–347
- MITASOVA, H.; HOFIERKA, J.; ZLOCHA, M. & IVERSON, L. R. (1996): Modelling topographic potential for erosion and deposition using GIS. In: *International journal of geographical information systems* **10**(5), 629–641.
- MITASOVA, H.; HOFIERKA, J.; ZLOCHA, M. & IVERSON, J. (1997): Reply to Comment by Desmet and Govers. In: *International Journal of Geographical Information Science* **11**(6), 611–618.
- MOORE, I. D. & BURCH, G. J. (1986a): Physical basis of the length-slope factor in the Universal Soil Loss Equation. In: *Soil Science Society of America Journal* **50**(5), 1294–1298.
- MOORE, I. D. & BURCH, G. J. (1986b): Sediment Transport Capacity of Sheet and Rill Flow: Application of Unit Stream Power Theory. In: *Water Resources Research* **22**(8), 1350–1360.
- MORGAN, R. P. C. (2009): *Soil Erosion and Conservation*. Hoboken, NJ, USA: John Wiley & Sons. 315 pp.
- MORGAN, R. P. C. & NEARING, M. A., (eds.): (2010): *Handbook of Erosion Modelling*. Hoboken, NJ, USA: John Wiley & Sons.
- MORRIS, G. L. (1998): *Reservoir Sedimentation Handbook: Design and Management of Dams, Reservoirs, and Watersheds for Sustainable Use*. New York City, NY, USA: McGraw Hill Professional. 850 pp.
- MUGGLER, C. C.; PAPE, Th. & BUURMAN, P. (1997): Laser grain-size determination in soil genetic studies, 2. Clay content, clay formation, and aggregation in some Brazilian Oxisols. In: *Soil Science* **162**(3), 219–228.
- MUTEKANGA, F. P.; VISSER, S. M. & STROOSNIJDER, L. (2010): A tool for rapid assessment of erosion risk to support decision-making and policy development at the Ngenge watershed in Uganda. In: *Geoderma* **160**(2), 165–174.
- MUTSAERS, H. J. W.; MBOUÉMBOUÉ, P. & BOYOMO, M. (1981): Traditional food crop growing in the Yaoundé area (Cameroon) Part II. Crop associations, yields and fertility aspects. In: *Agro-Ecosystems* **6**(4), 289–303.

- MUTUA, B. M.; KLIK, A. & LOISKANDL, W. (2006): Modelling soil erosion and sediment yield at a catchment scale: The case of Masinga catchment, Kenya. In: *Land Degradation and Development* **17**(5), 557–570.
- NAAH, M. (2013): Impact Temporel du Développement Urbain du Bassin Versant de la Rivière Mingoa sur la Qualite du Lac Municipal de Yaoundé (Cameroun). Dissertation. Marne-la-Vallée, France: Institut des sciences et technologies de Paris (Paris Institute of Technology) – École des Ponts ParisTech.
- NAGLER, P. L.; DAUGHTRY, C. S. T. & GOWARD, S. N. (2000): Plant Litter and Soil Reflectance. In: *Remote Sensing of Environment* **71**(2), 207–215.
- NASA AND JAPAN ASTER PROGRAM (2011): Advanced Spaceborne Thermal Emission and Reflection Radiometer (ASTER) Global Digital Elevation Model (GDEM) Version 002 — scene: ASTGDEM20N03E011, acquisition date: 2011-10-7. Ed. by U.S. NATIONAL AERONAUTICS AND SPACE ADMINISTRATION (NASA) & JAPAN’S MINISTRY OF ECONOMY, TRADE, AND INDUSTRY (METI).
- NASA LANDSAT PROGRAM (1987): LT51850571987287XXX01_B5 (1987-10-14). Landsat Thematic Mapper multi-spectral (L5). Sioux Falls, SD, USA: US Geological Survey.
- NATURAL EARTH DATA, (ed.): (2013): Rivers + lake centerlines. 1:10m Physical Vectors. <http://www.naturalearthdata.com/downloads/10m-physical-vectors/10m-rivers-lake-centerlines> (download: 2014-10-30).
- NATURAL RESOURCES CONSERVATION SERVICE (1998): Vulnerability to Water Erosion Map. Washington, D.C., USA: United States Department of Agriculture.
- NEARING, M. A.; JETTEN, V.; BAFFAUT, C.; CERDAN, O.; COUTURIER, A.; HERNANDEZ, M.; LE BISSONNAIS, Y.; NICHOLS, M. H.; NUNES, J. P.; RENSCHLER, C. S.; SOUCHÈRE, V. & OOST, K. VAN (2005): Modeling response of soil erosion and runoff to changes in precipitation and cover. In: *CATENA. Soil Erosion under Climate Change: Rates, Implications and Feedbacks* **61**(2), 131–154.
- NEKHAY, O.; ARRIAZA, M. & BOERBOOM, L. (2009): Evaluation of soil erosion risk using Analytic Network Process and GIS: A case study from Spanish mountain olive plantations. In: *Journal of Environmental Management* **90**(10), 3091–3104.
- NGNOTUÉ, T.; NZENTI, J. P.; BARBEY, P. & TCHOUA, F. M. (2000): The Ntui-Betamba high-grade gneisses: a northward extension of the Pan-African Yaoundé gneisses in Cameroon. In: *Journal of African Earth Sciences* **31**(2), 369–381.
- NICHOLSON, Sh. E.; DEZFULI, A. K. & KLOTTER, D. (2012a): A Two-Century Precipitation Dataset for the Continent of Africa. In: *Bulletin of the American Meteorological Society* **93**(8), 1219–1231.
- NICHOLSON, Sh. E.; KLOTTER, D. & DEZFULI, A. K. (2012b): Spatial reconstruction of semi-quantitative precipitation fields over Africa during the nineteenth century from documentary evidence and gauge data. In: *Quaternary Research* **78**(1), 13–23.
- NIGEL, Rody & RUGHOOPUTH, Soonil D.D.V. (2010): Soil erosion risk mapping with new datasets: An improved identification and prioritisation of high erosion risk areas. In: *CATENA* **82**(3), 191–205.

- NILL, D. (1993): Soil erosion from natural and simulated rain in forest-, savannah- and highland areas of humid to sub-humid West Africa and influence of management. Dissertation. Munich, Germany: Technische Universität München.
- NILL, D. (1997): Valuation of Erosion-determining-factors and their Quantitative Influence on Soil Loss in Tropical Africa. In: AUERSWALD, K.; STANJEK, H. & BIGHAM, J. M. (eds.): Soils and environment – Soil processes from mineral to landscape scale. *Advances in Geology* 30. Reiskirchen, Germany: Catena Verlag, 55–67
- NILL, D. (1998): Bodenschutzprobleme in Entwicklungsländern: Geoökologische Einflussfaktoren. In: RICHTER, G. (ed.): Bodenerosion: Analyse und Bilanz eines Umweltproblems. Darmstadt, Germany: Wissenschaftliche Buchgesellschaft, 222–230
- NILL, D.; SCHWERTMANN, U.; SABEL-KOSCHELLA, U.; BERNARD, M. & BREUER, J. (1996): Soil Erosion by Water in Africa – Principles, Prediction and Protection. Rossdorf, Germany: TZ Verlagsgesellschaft. 292 pp.
- NOUNAMO, L. (2001): Farming Systems in the Evergreen Forest of Southern Cameroon: Shifting Cultivation and Soil Degradation. Kribi, Cameroon: Tropenbos-Cameroon. 62 pp.
- NOUNAMO, L. & YEMAFACK, M. (2000): Shifting Cultivation in the Evergreen Forest of Southern Cameroon: Farming Systems and Soil Degradation: Final Report. Kribi, Cameroon: The Tropenbos-Cameroon Project. 54 pp.
- NTONGA, J. C.; WATERLOO, M. J. & AYANGMA, A. B. (2002): Hydrology, Erosion and Nutrient Cycling in a Forest Ecosystem in South Cameroon. **10**. Documents. Tropenbos-Cameroon Programme. 61 pp.
- NZENTI, J. P.; BARBEY, P.; MACAUDIERE, J. & SOBA, D. (1988): Origin and evolution of the late precambrian high-grade Yaounde Gneisses (Cameroon). In: *Precambrian Research* **38**(2), 91–109.
- NZENTI, J. P.; ABAGA, B.; SUH, Ch. E. & NZOLANG, Ch. (2010): Petrogenesis of peraluminous magmas from the Akum-Bamenda Massif, Pan-African Fold Belt, Cameroon. In: *International Geology Review* **53**(10), 1121–1149.
- OADES, JM & WATERS, AG (1991): Aggregate hierarchy in soils. In: *Soil Research* **29**(6), 815–828.
- OBI, M. E. & NGWU, O. E. (1988): Characterization of the rainfall regime for the prediction of surface runoff and soil loss in southeastern Nigeria. In: *Beitraege zur tropischen Landwirtschaft und Veterinaermedizin* **26**(1), 39–46.
- OBI, M. E. & NNABUDE, P. C. (1988): The effects of different management practices on the physical properties of a sandy loam soil in southern Nigeria. In: *Soil and Tillage Research* **12**(1), 81–90.
- OBI, M. E. & SALAKO, F. K. (1995): Rainfall parameters influencing erosivity in southeastern Nigeria. In: *CATENA* **24**(4), 275–287.
- O'CALLAGHAN, J. F. & MARK, D. M. (1984): The extraction of drainage networks from digital elevation data. In: *Computer vision, graphics, and image processing* **28**(3), 323–344.
- OLIVRY, J.-C. (1979): Monographie du Nyong et des fleuves cotiers : Tome 1 : Facteurs conditionnels des régimes hydrologiques. Report. Yaoundé, Cameroon, 523 p.
- OLIVRY, J.-C. (1986): Fleuves et Rivières du Cameroun. Report 9. Paris, France. 733 pp.

- OLORUNLANA, F. A. (2013): Evaluation of erodibility indices in Akoko region of Ondo state, Nigeria. In: *Global Journal of Biology, Agriculture & Health Sciences* **2**(2), 86–89.
- OTT, W. (2014): Access to Drinking Water and Stakeholder Action – Drinking Water Governance in Cameroon from a Political–Ecological Perspective. Case Study: Upper Mefou Watershed, Cameroon. Master’s Thesis. Berlin, Germany: Freie Universität Berlin, Department of Earth Sciences. 97 pp.
- PEBESMA, E. & BIVAND, R. S. (2005): Classes and methods for spatial data in R. In: *R News* **5**(2).
- PEEL, M. C.; FINLAYSON, B. L. & MCMAHON, T. A. (2007): Updated world map of the Köppen–Geiger climate classification. In: *Hydrol. Earth Syst. Sci.* **11**(5), 1633–1644.
- PETERSON, Th. C. & VOSE, R. S. (1997): An overview of the Global Historical Climatology Network temperature database. In: *Bulletin of the American Meteorological Society* **78**(12), 2837–2849.
- PRASUHN, V.; LINIGER, H.; GISLER, S.; HERWEG, K.; CANDINAS, A. & CLÉMENT, J.-P. (2013): A high-resolution soil erosion risk map of Switzerland as strategic policy support system. In: *Land Use Policy* **32**, 281–291.
- PRIBYL, D. W. (2010): A critical review of the conventional SOC to SOM conversion factor. In: *Geoderma* **156**(3), 75–83.
- QGIS DEVELOPMENT TEAM (2013): QGIS Geographic Information System. <http://www.qgis.org>.
- QUINN, P.; BEVEN, K.; CHEVALLIER, P. & PLANCHON, O. (1991): The prediction of hillslope flow paths for distributed hydrological modelling using digital terrain models. In: *Hydrological Processes* **5**(1), 59–79.
- R CORE TEAM (2012): *R: A Language and Environment for Statistical Computing*. Vienna, Austria: R Foundation for Statistical Computing.
- R CORE TEAM (2013): *R: A Language and Environment for Statistical Computing*. Vienna, Austria: R Foundation for Statistical Computing.
- RAMOS-SCHARRÓN, C. E.; REALE-MUNROE, K. & ATKINSON, S. C. (2014): Quantification and modeling of foot trail surface erosion in a dry sub-tropical setting. In: *Earth Surface Processes and Landforms* **39**(13), 1764–1777.
- RENARD, K. G. & FREIMUND, J. R. (1994): Using monthly precipitation data to estimate the R-factor in the revised USLE. In: *Journal of Hydrology* **157**(1), 287–306.
- RENARD, K. G.; FOSTER, G. R.; WEESIES, G. A. & PORTER, J. P. (1991): RUSLE: Revised universal soil loss equation. In: *Journal of Soil and Water Conservation* **46**(1), 30–33.
- RENARD, K. G.; FOSTER, G. R.; WEESIES, G. A.; MCCOOL, D. K. & YODER, D. C. (1997): Predicting soil erosion by water: a guide to conservation planning with the Revised Universal Soil Loss Equation (RUSLE). In: *Agriculture Handbook* (703), 384.
- RENSCHLER, C. S.; MANNAERTS, C. & DIEKKRÜGER, B. (1999): Evaluating spatial and temporal variability in soil erosion risk—rainfall erosivity and soil loss ratios in Andalusia, Spain. In: *CATENA* **34**(3), 209–225.
- RENSCHLER, Ch. S. & HARBOR, J. (2002): Soil erosion assessment tools from point to regional scales—the role of geomorphologists in land management research and implementation. In: *Geomorphology in the Public Eye: Political Issues, Education, and the Public* **47**(2), 189–209.

- RIJSDIJK, A. (2005): Evaluating sediment sources and delivery in a tropical volcanic watershed. In: HOROWITZ, A. J. & WALLING, D. E. (eds.): *Sediment Budgets 2*. Wallingford, U.K.: IAHS Press, 16–23
- RÖMKENS, M. J. M.; YOUNG, R. A.; POESEN, J. W. A.; MCCOOL, D. K.; EL-SWAIFY, S. A.; BRADFORD, J. M. & RENARD, K. G. (1997): Chapter 3. Soil Erodibility Factor (K). In: RENARD, K. G.; FOSTER, G. R.; WEESIES, G. A.; MCCOOL, D. K. & YODER, D. C. (eds.): *Predicting Soil Erosion by Water: A Guide to Conservation Planning With the Revised Universal Soil Loss Equation (RUSLE)*. **703**. Agricultural Handbook
- ROEHL, J. W. (1962): Sediment source areas, delivery ratios and influencing morphological factors. In: *International Association of Scientific Hydrology* **59**, 202–213.
- ROOSE, E. (1996): *Land husbandry: components and strategy*. **70**. Rome, Italy: FAO.
- ROOSE, E. J. (1977): Use of the universal soil loss equation to predict erosion in West Africa. In: ANONYMOUS (ed.): *Soil erosion: prediction and control : the proceedings of a National Conference on Soil Erosion, May 24-26, 1976, Purdue University, West Lafayette, Indiana*. Ankeny, IA, USA: Soil Conservation Society of America, 60–74
- ROOSE, Eric & SARRAILH, Jean-Marie (1989): Erodibilité de quelques sols tropicaux. Vingt années de mesure en parcelles d'érosion sous pluies naturelles. In: *Cahiers Orstom Série Pédologie, Bondy* **25**, 7–30.
- ROTH, Ch. B.; NELSON, D. W. & RÖMKENS, M. J. M. (1974): *Prediction of subsoil erodibility using chemical, mineralogical and physical parameters*. Washington, D. C., USA: Office of Research and Development, US Environmental Protection Agency. 132 pp.
- ROY, D. P.; WULDER, M. A.; LOVELAND, T. R.; C.E., Woodcock; ALLEN, R. G.; ANDERSON, M. C.; HELDER, D.; IRONS, J. R.; JOHNSON, D. M.; KENNEDY, R.; SCAMBOS, T. A.; SCHAAF, C. B.; SCHOTT, J. R.; SHENG, Y.; VERMOTE, E. F.; BELWARD, A. S.; BINDSCHADLER, R.; COHEN, W. B.; GAO, F.; HIPPLE, J. D.; HOSTERT, P.; HUNTINGTON, J.; JUSTICE, C. O.; KILIC, A.; KOVALSKYY, V.; LEE, Z. P.; LYMBURNER, L.; MASEK, J. G.; MCCORKEL, J.; SHUAI, Y.; TREZZA, R.; VOGELMANN, J.; WYNNE, R. H. & ZHU, Z. (2014): Landsat-8: Science and product vision for terrestrial global change research. In: *Remote Sensing of Environment* **145**, 154–172.
- RUBEL, F. & KOTTEK, M. (2010): Observed and projected climate shifts 1901–2100 depicted by world maps of the Köppen-Geiger climate classification. In: *Meteorologische Zeitschrift* **19**(2), 135–141.
- RUTHENBERG, H. & MACARTHUR, J. D. (1980): *Farming systems in the tropics*. Oxford, U.K.: Clarendon Press. 476 pp.
- SABBI, A. & SALVATI, L. (2014): Searching for a downward spiral? Soil erosion risk, agro-forest landscape and socioeconomic conditions in Italian local communities. In: *Land Use Policy* **41**, 388–396.
- SALAKO, F. K. (2006): Rainfall temporal variability and erosivity in subhumid and humid zones of southern Nigeria. In: *Land Degradation & Development* **17**(5), 541–555.
- SALAKO, F. K. (2008): Rainfall variability and kinetic energy in Southern Nigeria. In: *Climatic Change* **86**(1), 151–164.
- SALAKO, F. K. (2010): Development of isoerodent maps for Nigeria from daily rainfall amount. In: *Geoderma* **156**(3), 372–378.

- SALAKO, F. K.; OBI, M. E. & LAL, R. (1991): Comparative assessment of several rainfall erosivity indices in Southern Nigeria. In: *Soil Technology* **4**(1), 93–97.
- SALAKO, F. K.; GHUMAN, B. S. & LAL, R. (1995): Rainfall erosivity in south-central Nigeria. In: *Soil Technology* **7**(4), 279–290.
- SANTOIR, C. & VILLIERS, J. F. (1995): *Atlas Régional Sud Cameroun – Végétation*. ORSTOM Éditiones. Toulouse, France.
- SATO, J. H.; FIGUEIREDO, C. C.; MARCHÃO, R. L.; MADARI, B. E.; BENEDITO, L. E. C.; BUSATO, J. G. & SOUZA, D. M. de (2014): Methods of soil organic carbon determination in Brazilian savannah soils. In: *Scientia Agricola* **71**(4), 302–308.
- SAYER, J. A.; ENDAMANA, D.; RUIZ-PEREZ, M.; BOEDHIHARTONO, A. K.; NZOOH, Z.; EYEBE, A.; AWONO, A. & USONGO, L. (2012): Global financial crisis impacts forest conservation in Cameroon. In: *International Forestry Review* **14**(1), 90–98.
- SCHMENGLER, A. C. (2011): Modeling soil erosion and reservoir sedimentation at hillslope and catchment scale in semi-arid Burkina Faso. Dissertation. Bonn, Germany: Rheinischen Friedrich-Wilhelms-Universität zu Bonn – Hohe Landwirtschaftliche Fakultät.
- SCHWERTMANN, U.; VOGL, W. & KAINZ, M. (1990): *Bodenerosion durch Wasser. Vorhersage des Abtrags und Bewertung von Gegenmassnahmen*. 2. Aufl. Ulmer (Eugen). 64 pp.
- SEIBERT, J. & MCGLYNN, B. L. (2007): A new triangular multiple flow direction algorithm for computing upslope areas from gridded digital elevation models. In: *Water Resources Research* **43**(4), W04501.
- SELIGE, Th.; BÖHNER, J. & RINGELER, A. (2006): Processing of SRTM X-SAR Data to correct interferometric elevation models for land surface process applications. In: *Göttinger Geographische Abhandlungen* **115**, 97–104.
- SHAPIRO, S. S. & WILK, M. B. (1965): An analysis of variance test for normality (complete samples). In: *Biometrika* **52**(3), 591–611.
- SIETCHIPING, R. (2003): Évolution de l'espace urbain de Yaoundé, au Cameroun, entre 1973 et 1988 par télédétection. In: *Télédétection* **3**, 229–236.
- SIETCHIPING, R. (2004): *A Geographic Information Systems and Cellular Automata-Based Model of Informal Settlement Growth*. Ph. D. thesis. Melbourne, Australia: The University of Melbourne, School of Anthropology, Geography and Environmental Studies. 233 pp.
- SIMMS, A.; WOODROFFE, C. & JONES, B. (2003): Application of RUSLE for erosion management in a coastal catchment, southern NSW. In: *Proceedings of the MODSIM 2003: International Congress on Modelling and Simulation, volume 2, Integrative Modelling of Biophysical, Social and Economic Systems for Resource Management Solutions (14-17 July 2003)*. Faculty of Science - Papers. Townsville, Australia: University of Wollongong
- SLEUTEL, S.; DE NEVE, S.; SINGIER, B. & HOFMAN, G. (2007): Quantification of organic carbon in soils: A comparison of methodologies and assessment of the carbon content of organic matter. In: *Communications in soil science and plant analysis* **38**(19), 2647–2657.

- SOIL SURVEY DIVISION STAFF (1993): Soil survey manual. **18**. U.S. Department of Agriculture Handbook. Washington, D.C., USA: USDA Soil Conservation Service.
- SOON, Y. K. & ABBOUD, S. (1991): A comparison of some methods for soil organic carbon determination. In: *Communications in Soil Science and Plant Analysis* **22**(9), 943–954.
- STABLER, B. (2013): shapefiles: Read and Write ESRI Shapefiles. R package version 0.7.
- STANCHI, S.; FREPPAZ, M.; GODONE, D. & ZANINI, E. (2013): Assessing the susceptibility of alpine soils to erosion using soil physical and site indicators. In: *Soil Use and Management* **29**(4), 586–596.
- STOCKING, D. E. (1984): Rates of erosion and sediment yield in the African environment. In: WALLING, D. E.; FOSTER, S. S. D. & WURZEL, P. (eds.): *Challenges in African hydrology and water resources. Proceedings of the Harare Symposium, July 1984, convened and organized by the Ministry of Water Resources and Development and the Department of Civil Engineering, University of Zimbabwe, in cooperation with UNEP, UNESCO, WMO, IAH and IAHS*. **144**. IAHS publications. Wallingford, U.K.: IAHS Press, 265–284
- SUNDERLIN, W. D.; NDOYE, O.; BIKIÉ, H.; LAPORTE, N.; MERTENS, B. & POKAM, J. (2000): Economic crisis, small-scale agriculture, and forest cover change in southern Cameroon. In: *Environmental Conservation* **27**(3), 284–290.
- TARBOTON, D. G. (1997): A new method for the determination of flow directions and upslope areas in grid digital elevation models. In: *Water Resources Research* **33**(2), 309–319.
- TARDY, Y. & NAHON, D. (1985): Geochemistry of laterites, stability of Al-goethite, Al-hematite, and Fe³⁺-kaolinite in bauxites and ferricretes: an approach to the mechanism of concretion formation. In: *Am. J. Sci* **285**(10), 865–903.
- TERRANOVA, O.; ANTRONICO, L.; COSCARELLI, R. & IAQUINTA, P. (2009): Soil erosion risk scenarios in the Mediterranean environment using RUSLE and GIS: An application model for Calabria (southern Italy). In: *Geomorphology* **112**(3), 228–245.
- THIEKEN, A. H.; LÜCKE, A.; DIEKKRÜGER, B. & RICHTER, O. (1999): Scaling input data by GIS for hydrological modelling. In: *Hydrological Processes* **13**(4), 611–630.
- THOME, H. (2005): *Zeitreihenanalyse: eine Einführung für Sozialwissenschaftler und Historiker*. Munich, Germany: Oldenbourg Verlag. 400 pp.
- TUCKER, C. J. (1979): Red and photographic infrared linear combinations for monitoring vegetation. In: *Remote Sensing of Environment* **8**(2), 127–150.
- UNITED STATES GEOLOGICAL SURVEY (USGS) (2012): Shuttle Radar Topography Mission, 3 Arc Second scene SRTM3N03E011V2, Filled Finished-B, aquisition date: 2010-02-11. Ed. by GLOBAL LAND COVER FACILITY, UNIVERSITY OF MARYLAND. College Park, MD, USA.
- US GEOLOGICAL SURVEY (2013): Using the USGS Landsat 8 Product. URL: http://landsat.usgs.gov/Landsat8_Using_Product.php (visited on 10/30/2014).
- USDA (1951): Soil Survey Manual. U.S. Government Printing Office. 538 pp.
- USDA (1983): National Soil Survey Handbook (NSSH) No. 430.

- USDA AGRICULTURAL RESEARCH SERVICE (2013): Science Documentation Revised universal Soil Loss Equation Version 2 (RUSLE2) (for the model with release date of May 20, 2008). Washington, D.C., USA. 330 pp.
- VAN DER KNIJFF, J. M.; JONES, R. J. A. & MONTANARELLA, L. (2000): Soil erosion risk assessment in Europe. n. p.: European Soil Bureau, European Commission.
- VAN DIJK, A. I. J. M; BRUIJNZEEL, L. A & ROSEWELL, C. J (2002): Rainfall intensity–kinetic energy relationships: a critical literature appraisal. In: *Journal of Hydrology* **261**(1), 1–23.
- VAN GENUCHTEN, M. T. (1980): A closed-form equation for predicting the hydraulic conductivity of unsaturated soils. In: *Soil Science Society of America Journal* **44**(5), 892–898.
- VAN ROMPAEY, A. J. J.; GOVERS, G.; VAN HECKE, E. & JACOBS, K. (2001): The impacts of land use policy on the soil erosion risk: a case study in central Belgium. In: *Agriculture, Ecosystems & Environment* **83**(1), 83–94.
- VAN SOEST, D. P. (1998): *Tropical Deforestation: An Economic Perspective*. Dissertation. Tilburg University. 268 pp.
- VANELSLANDE, A.; ROUSSEAU, P.; LAL, R.; GABRIELS, D. & GHUMAN, B. S. (1984): Testing the applicability of a soil erodibility nomogram for some tropical soils. In: *IAHS Publications* **144**, 463–473.
- VANELSLANDE, A.; LAL, R. & GABRIELS, D. (1987): The erodibility of some Nigerian soils: A comparison of rainfall simulator results with estimates obtained from the Wischmeier nomogram. In: *Hydrological Processes* **1**(3), 255–265.
- VERSTRAETEN, G. & POESEN, J. (2000): Estimating trap efficiency of small reservoirs and ponds: methods and implications for the assessment of sediment yield. In: *Progress in Physical Geography* **24**(2), 219–251.
- VERSTRAETEN, G. & POESEN, J. (2001): Variability of dry sediment bulk density between and within retention ponds and its impact on the calculation of sediment yields. In: *Earth Surface Processes and Landforms* **26**(4), 375–394.
- VERSTRAETEN, G. & POESEN, J. (2002): Using sediment deposits in small ponds to quantify sediment yield from small catchments: possibilities and limitations. In: *Earth Surface Processes and Landforms* **27**(13), 1425–1439.
- VOGLER, J. B. & BUTLER, D. R. (1996): Pedestrian- and Bicycle-Induced Path Erosion on a University Campus. In: *Physical Geography* **17**(5), 485–494.
- VOLK, M.; MÖLLER, M. & WURBS, D. (2010): A pragmatic approach for soil erosion risk assessment within policy hierarchies. In: *Land Use Policy* **27**(4), 997–1009.
- VRIELING, A.; STERK, G. & VIGIAK, O. (2006): Spatial evaluation of soil erosion risk in the West Usambara Mountains, Tanzania. In: *Land Degradation & Development* **17**(3). WOS:000238455400005, 301–319.
- VRIELING, A.; JONG, St. M. DE; STERK, G. & RODRIGUES, S. C. (2008): Timing of erosion and satellite data: A multi-resolution approach to soil erosion risk mapping. In: *International Journal of Applied Earth Observation and Geoinformation* **10**(3), 267–281.
- VRIELING, A.; STERK, G. & JONG, S. M. DE (2010): Satellite-based estimation of rainfall erosivity for Africa. In: *Journal of Hydrology* **395**(3), 235–241.

- VRIELING, Anton; HOEDJES, Joost C. B. & VELDE, Marijn VAN DER (2014): Towards large-scale monitoring of soil erosion in Africa: Accounting for the dynamics of rainfall erosivity. In: *Global and Planetary Change* **115**, 33–43.
- WALLING, D. E. (1983): The sediment delivery problem. In: *Journal of Hydrology* **65**(1), 209–237.
- WALLING, D. E. (1984): The sediment yields of African rivers. In: WALLING, D. E.; FOSTER, S. S. D. & WURZEL, P. (eds.): *Challenges in African hydrology and water resources (Proceedings of the Harare Symposium, July 1984, convened and organized by the Ministry of Water Resources and Development and the Department of Civil Engineering, University of Zimbabwe, in cooperation with UNEP, UNESCO, WMO, IAH and IAHS)*. **144**. IAHS publications. Wallingford, U.K.: IAHS Press, 265–284
- WALLING, D. E. & WEBB, B. W. (1996): Erosion and sediment yield: A global overview. In: WALLING, D. E. & WEBB, B. W. (eds.): *Erosion and Sediment Yield: Global and Regional Perspectives : Proceedings of an International Symposium Held at Exeter, UK, from 15 to 19 July 1996*. IAHS publications 236. Wallingford, U.K.: IAHS Press
- WANG, L. & LIU, H. (2006): An efficient method for identifying and filling surface depressions in digital elevation models for hydrologic analysis and modelling. In: *International Journal of Geographical Information Science* **20**(2), 193–213.
- WARREN, St. D.; MITASOVA, H.; HOHMANN, M. G.; LANDSBERGER, Sh.; ISKANDER, F. Y.; RUZYCKI, Th. S. & SENSEMAN, G. M. (2005): Validation of a 3-D enhancement of the Universal Soil Loss Equation for prediction of soil erosion and sediment deposition. In: *CATENA. 25 Years of Assessment of Erosion* **64**(2), 281–296.
- WATERLOO, M. J.; NTONGA, J. C.; DOLMAN, A. J. & AYANGMA, A. B. (2000): Impact of shifting cultivation and selective logging on the hydrology and erosion of rain forest land in south Cameroon. In: *Tropenbos-Cameroon Documents*(3), 84.
- WICKHAM, H. (2012): stringr: Make it easier to work with strings. R package version 0.6.2.
- WILCOXON, F. (1945): Individual Comparisons by Ranking Methods. In: *Biometrics Bulletin* **1**(6), 80–83.
- WILLIAMS, J. R. (1977): Sediment delivery ratios determined with sediment and runoff models. In: *IAHS Publications* **122**, 168–179.
- WISCHMEIER, W. H. & SMITH, D. D. (1958): Rainfall energy and its relationship to soil loss. In: *Eos, Transactions American Geophysical Union* **39**(2), 285–291.
- WISCHMEIER, W. H. & SMITH, D. D. (1978): Predicting rainfall erosion losses - a guide to conservation planning. In: *Agriculture Handbooks (USA)*, No. 537, 62 pp.
- WISCHMEIER, W. H.; JOHNSON, C. B. & CROSS, B. V. (1971): Soil erodibility nomograph for farmland and construction sites. In: *Journal of Soil and Water Conservation* **26**(5), 189–192.
- WU, S.; LI, J. & HUANG, G. (2005): An evaluation of grid size uncertainty in empirical soil loss modeling with digital elevation models. In: *Environmental Modeling & Assessment* **10**(1), 33–42.
- YALE CENTER FOR EARTH OBSERVATION (2013): *Yale Guide to Landsat 8 Image Processing*. In: *Understanding Landsat 8*. New Haven, CT, USA; (<http://www.yale.edu/ceo/Documentation/Landsat%20image%20processing.pdf> [2014-11-01]): Yale University

- YEMEFACK, M. (2005): Modelling and Monitoring Soil and Land Use Dynamics within Shifting Agricultural Landscape Mosaic Systems in Southern Cameroon. Dissertation. The Netherlands: ITC Enschede and Utrecht University.
- YEMEFACK, M.; BLJKER, W. & DE JONG, St. M. (2006): Investigating relationships between Landsat-7 ETM+ data and spatial segregation of LULC types under shifting agriculture in southern Cameroon. In: International Journal of Applied Earth Observation and Geoinformation. Perspectives on modelling and managing geospatial Data **8**(2), 96–112.
- YU, B. (1998): Rainfall erosivity and its estimation for Australia's tropics. In: Soil Research **36**(1), 143–166.
- ZEVENBERGEN, L. W. & THORNE, C. R. (1987): Quantitative analysis of land surface topography. In: Earth Surface Processes and Landforms **12**(1), 47–56.
- ZHANG, H.; YANG, Q.; LI, R.; LIU, Q.; MOORE, D.; HE, P.; RITSEMA, C. J. & GEISSEN, V. (2013): Extension of a GIS procedure for calculating the RUSLE equation LS factor. In: Computers & Geosciences **52**, 177–188.
- ZHANG, J. X.; CHANG, K.-T. & WU, J. Q. (2008): Effects of DEM resolution and source on soil erosion modelling: A case study using the WEPP model. In: International Journal of Geographical Information Science **22**(8), 925–942.
- ZHANG, R. (1997): Determination of Soil Sorptivity and Hydraulic Conductivity from the Disk Infiltrometer. In: Soil Science Society of America Journal **61**, 1024–1030.
- ZHANG, X.; WU, B.; LING, F.; ZENG, Y.; YAN, N. & YUAN, Ch. (2010): Identification of priority areas for controlling soil erosion. In: CATENA **83**(1), 76–86.

Appendix

DVD

A DVD is attached to the thesis, which contains all raw data as well as all R-scripts for preprocessing, data preparation, calculation and modeling.

Explanations for all files on the DVD are given in README.txt-files in the folders.

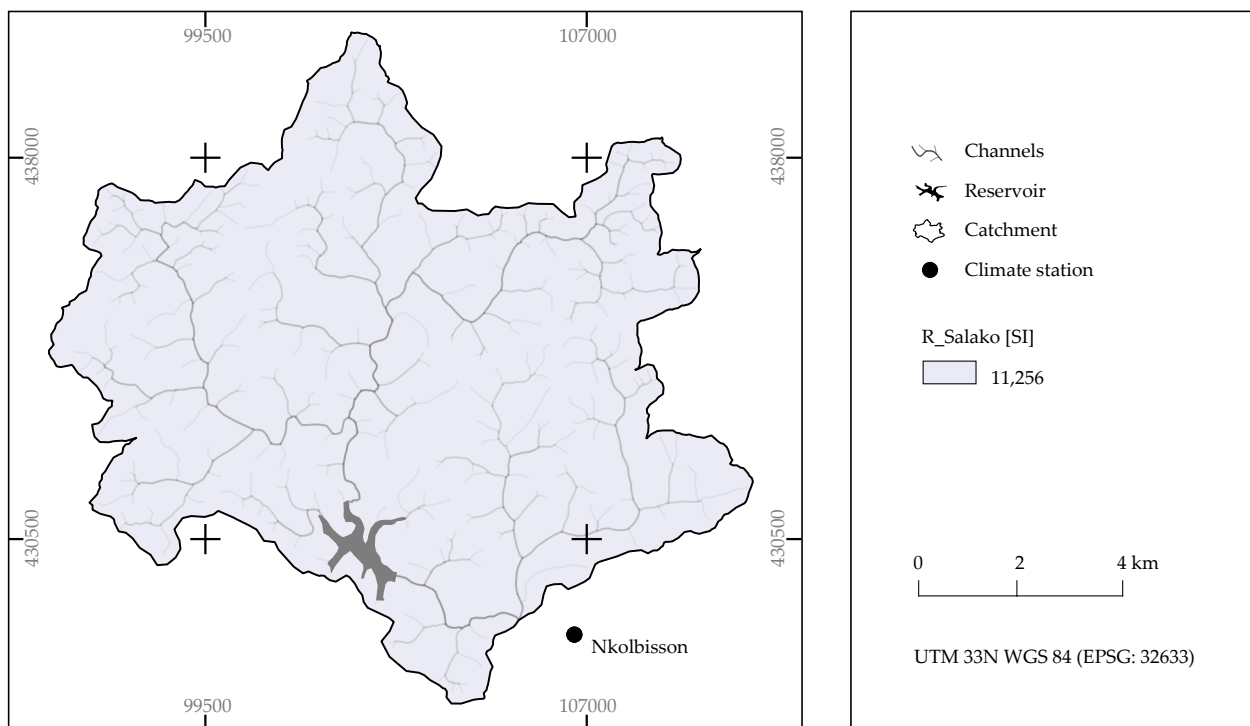


Figure 7.1: Map of the R-factor, which is kept constant over the entire catchment. The location of the meteorological station in Nkolbisson is marked with a bullet (●).

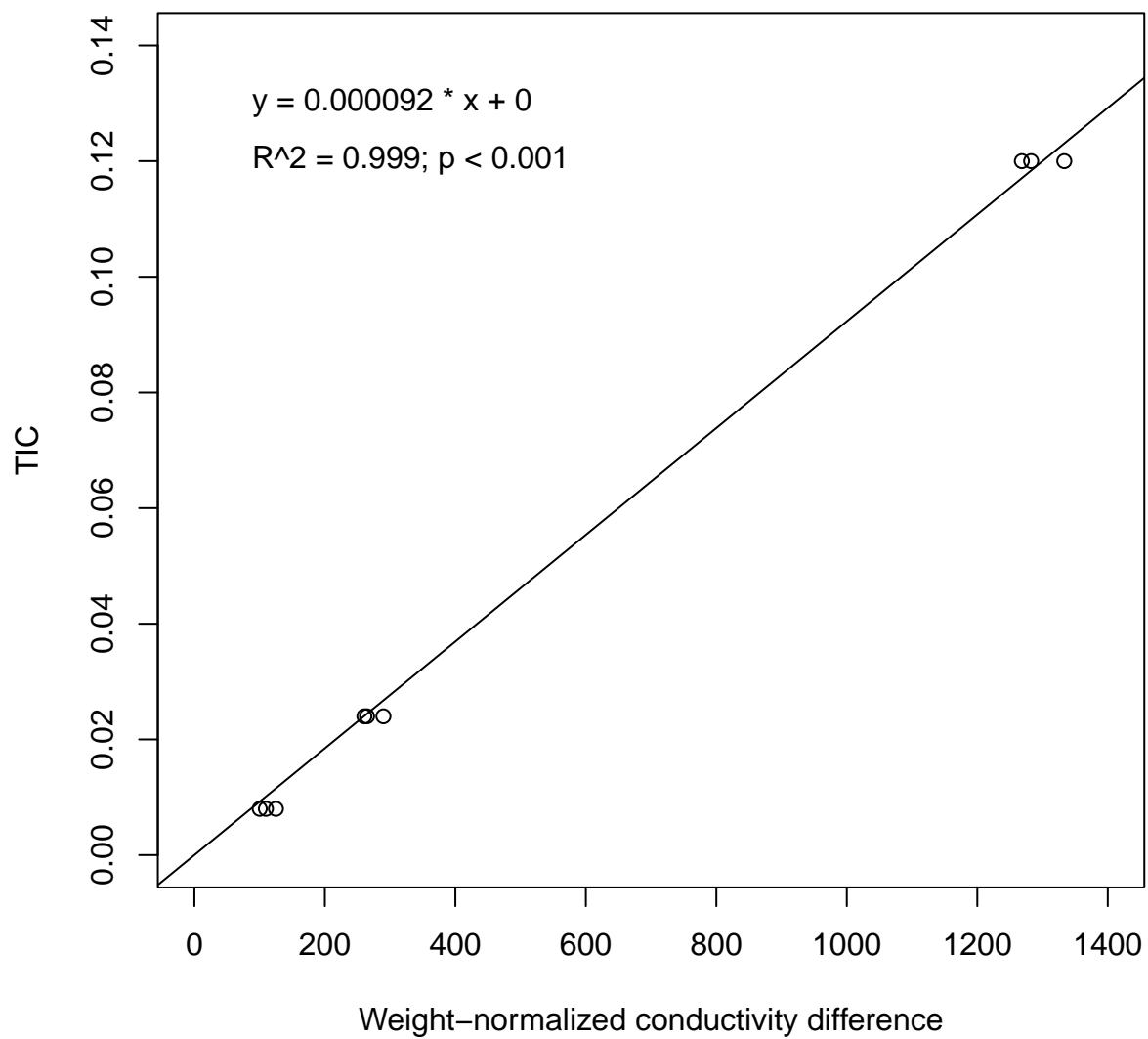


Figure 7.2: Linear model of total organic carbon (TOC) calibration. Conductivity differences (Woesthoff carmhograph) of standards were measured and weight-normalized; the relationship between the differences and the known TIC was than used to calculate the TIC from measured conductivity differences of the soil samples.

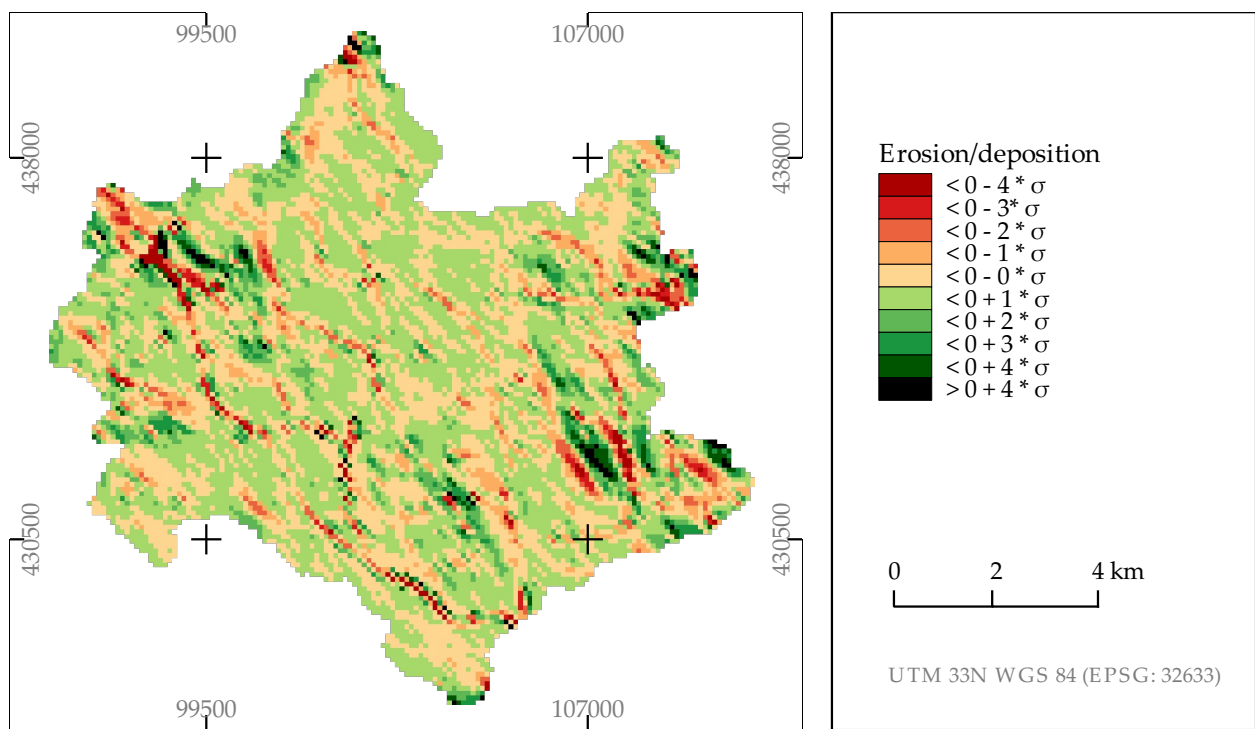
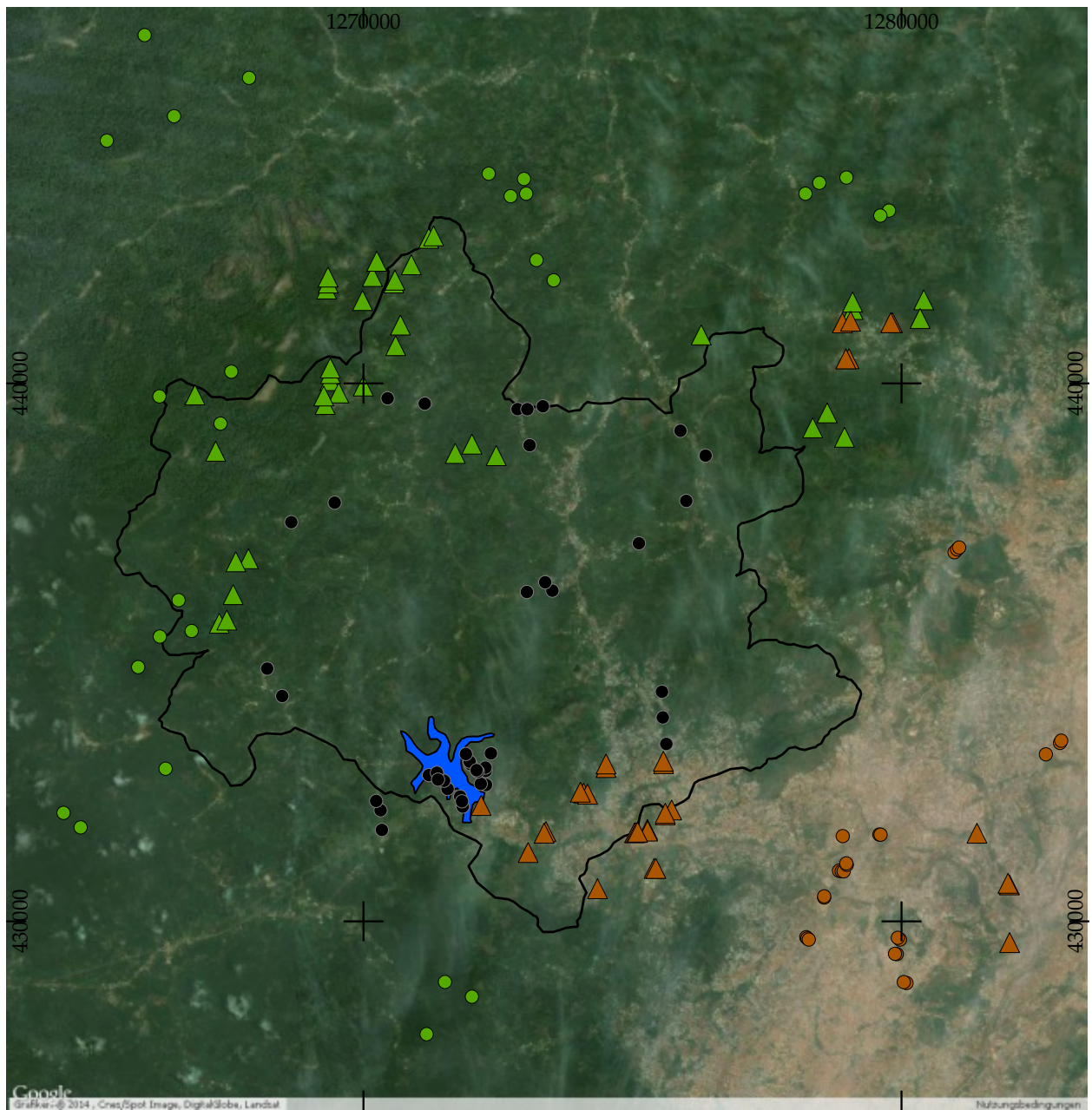


Figure 7.3: Erosion/deposition areas calculated with the Topographic erosion potential index. For calculating erosion risk, all areas with net deposition were excluded from erosion modeled with RUSLE3D.



Calibration

- ▲ C=0
- ▲ C=1

Validation

- C=0
- C=1
- C=0-1

- Mefou Reservoir
- Catchment

Google Satellite



Figure 7.4: Point samples of ground-truthing (training and validation data set) based on the GoogleEarth image (green and orange bullets and triangles) and field observation (black bullets).

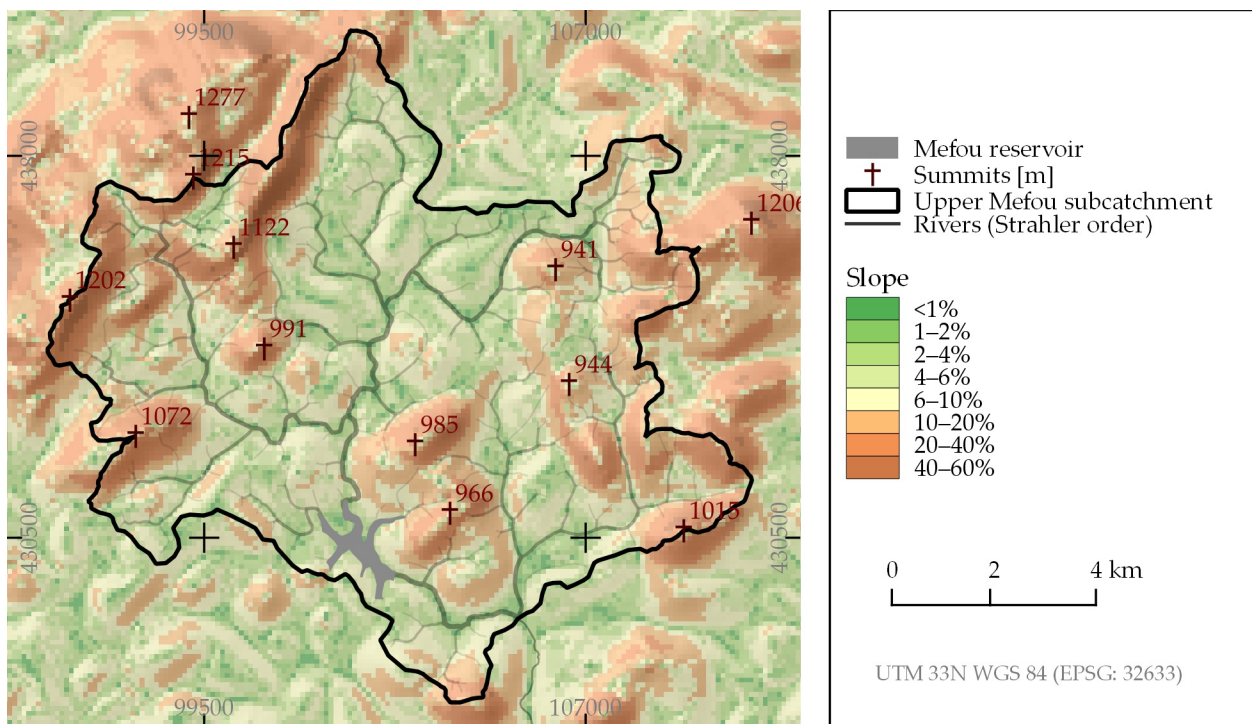


Figure 7.5: Slope map of the Upper Mefou subcatchment. Classification of slope according to the system of WISCHMEIER & SMITH (1978).

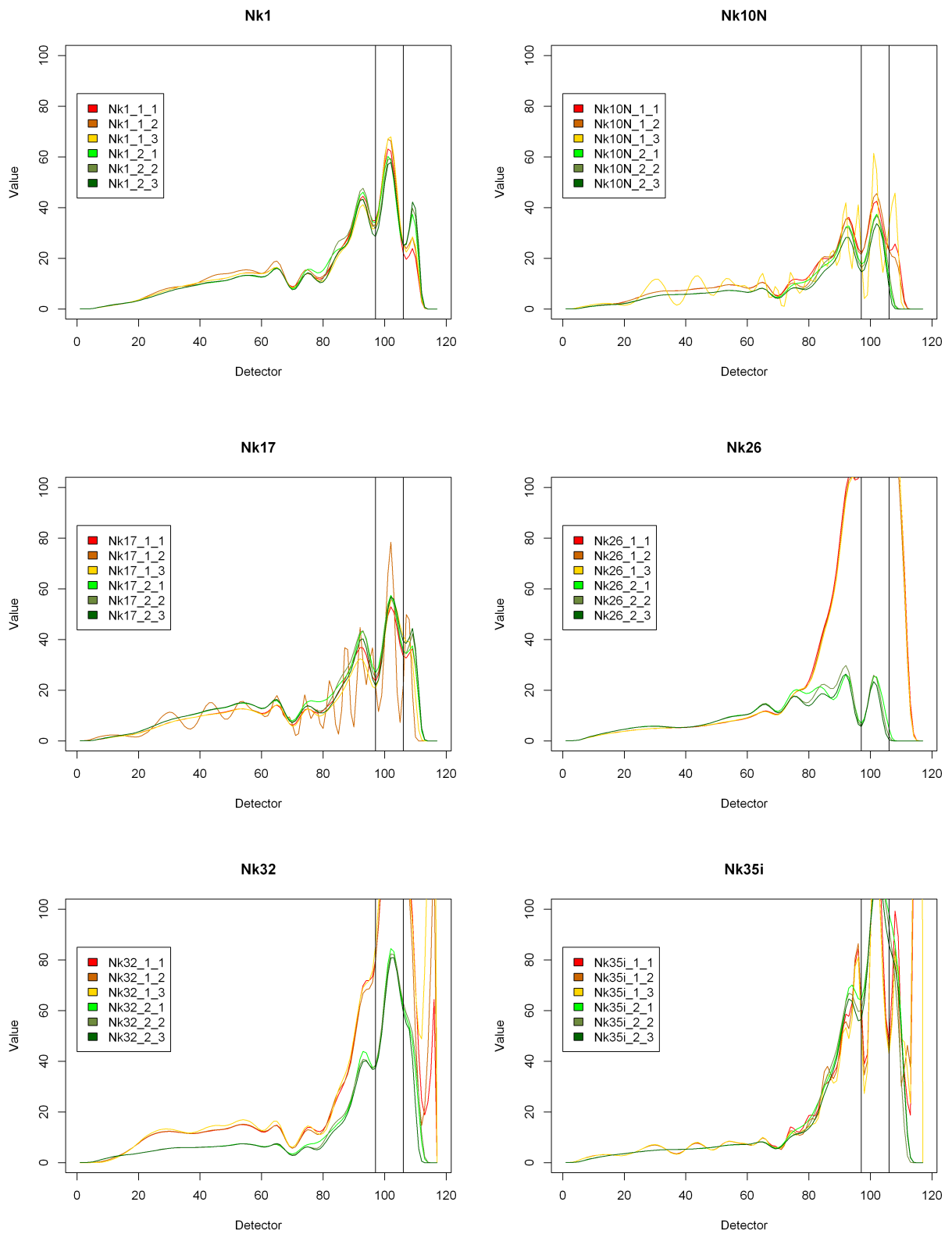


Figure 7.6: Selection of laser diffraction results of an unproblematic sample (Nk1) and some erroneous samples.

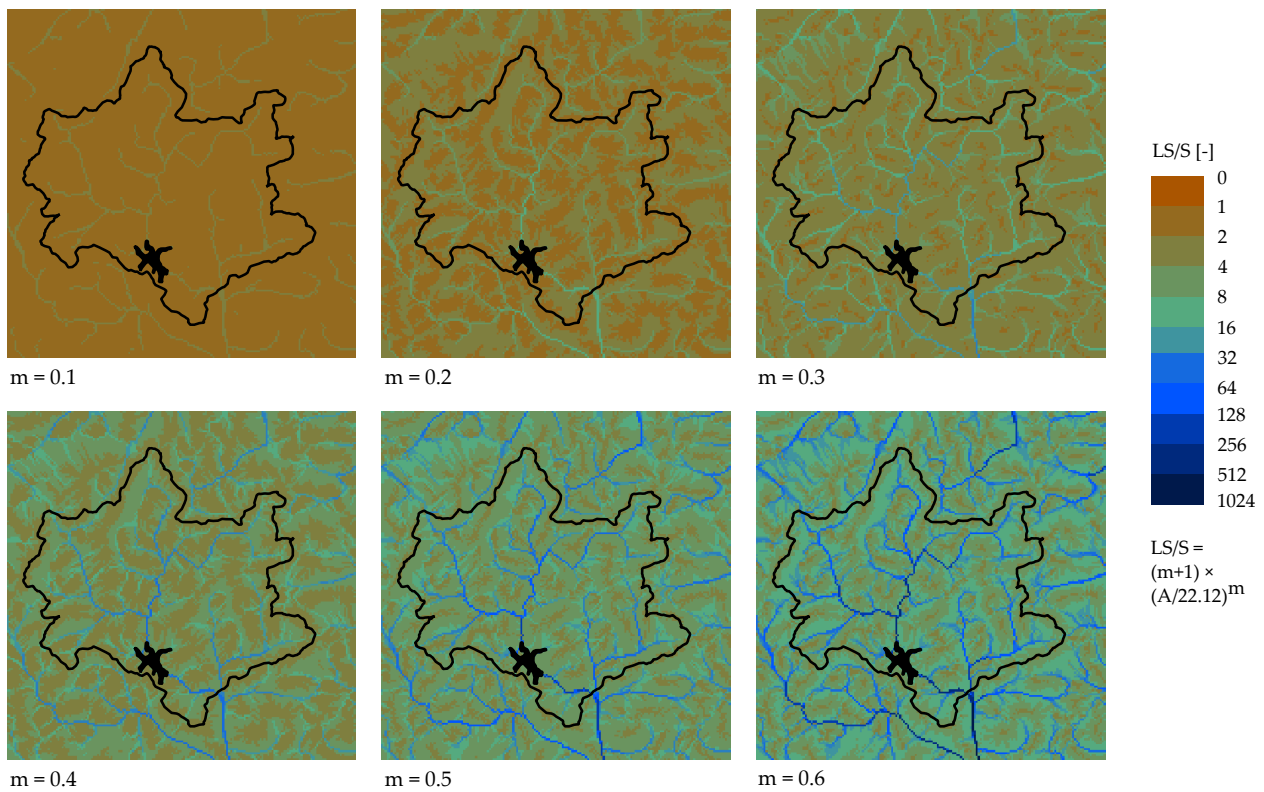


Figure 7.7: Graphical representation of the influence of the rill-to-interill ratio m on LS/S —the slope length component of the RUSLE's topographic factor.

Erklärung

Hiermit versichere ich, dass ich die vorliegende Arbeit mit dem Titel *Soil Erosion Risk Assessment in the Upper Mefou Subcatchment, Southern Cameroon Plateau* eigenständig und nur mit den angegebenen Hilfsmitteln verfasst habe.

Die Arbeit hat in dieser oder anderer Form in keinem anderen Prüfungsverfahren vorgelegen.

Fabian Becker, Berlin